

DISCLAIMER

This report was prepared as an account of work sponsored by an agency of the United States Government. Neither the United States Government nor any agency thereof, nor any of their employees, makes any warranty, expressed or implied, or assumes any legal liability or responsibility for the accuracy, completeness, or usefulness of any information, apparatus, product, or process disclosed, or represents that its use would not infringe privately owned rights. Reference herein to any specific commercial product, process, or service by trade name, trademark, manufacturer, or otherwise does not necessarily constitute or imply its endorsement, recommendation, or favoring by the United States Government or any agency thereof. The views and opinions of authors expressed herein do not necessarily state or reflect those of the United States Government.

This report has been reproduced directly from the best available copy.

Available to DOE and DOE contractors from the Office of Scientific and Technical Information, P.O. Box 62, Oak Ridge, TN 37831; prices available from (615) 576-8401.

Available to the public from the National Technical Information Service, U.S. Department of Commerce, 5285 Port Royal Rd., Springfield VA 22161

DOE/BC/14953-10
Distribution Category UC-122

Increased Oil Production and Reserves From
Improved Completion Techniques in the Bluebell
Field, Uinta Basin, Utah

Annual Report for the Period
September 30, 1993 to September 30, 1994

By
M. Allison

July 1995

Work Performed Under Contract No. DE-FC22-92BC14953

Prepared for
U.S. Department of Energy
Assistant Secretary for Fossil Energy

Edith Allison, Project Manager
Bartlesville Project Office
P.O. Box 1398
Bartlesville, OK 74005

Prepared by
Utah Geological Survey
Salt Lake City, UT 84109

CONTENTS

ABSTRACT	1
EXECUTIVE SUMMARY	2
INTRODUCTION	4
GENERAL GEOLOGY AND RESERVOIR CHARACTERISTICS	7
Geology	7
Production Characteristics	13
Study Sites	14
OUTCROP STRATIGRAPHY AND PETROPHYSICS	33
Petrology	33
Porosity and Permeability	35
Clay Analysis	36
CORE DESCRIPTION AND PETROPHYSICS	36
SURFACE FRACTURING PATTERNS	45
Bluebell Field Area	45
Indian Canyon Area	47
RESERVOIR DATA AND FLUID PROPERTIES	47
Reservoir Data	47
Reservoir Characterization and Geologic Data	48
Production Information	48
Decline Curve Analysis	50
Reservoir Geologic Information	50
Reservoir Fluid Properties	54
Thermodynamic Properties	57
RESERVOIR SIMULATIONS	59
Preliminary Single-Well Models	60
Comprehensive Single-Well Models	61
East Study-Site Model	64
West Study-Site Model	67
REFERENCES	73
APPENDIX A	76
APPENDIX B	88

ILLUSTRATIONS

Figure 1. Structure contour map of the Bluebell field.	6
Figure 2. The Uinta Basin with Bluebell, Altamont, and Cedar Rim fields shown.	8
Figure 3. Major structural features, surface faults, and fracture zones in and around the Uinta Basin.	9
Figure 4. Generalized southwest to northeast cross section of Tertiary rocks in the Uinta Basin.	9
Figure 5. Conceptual block diagram with distribution and interpretation of depositional environments associated with the early Eocene Lake Uinta.	10
Figure 6. Cumulative oil production of the wells in Bluebell field.	11
Figure 7. Cross section through the Michelle Ute and Malnar Pike wells.	12
Figure 8. Initial oil potential of the first well completed in a section versus the second.	15
Figure 9. Cumulative oil production after five years of production of the first well completed in a section versus the second.	15
Figure 10. Histogram of gross perforations.	16
Figure 11. Well location map of the east study-site.	17
Figure 12. Cross section QEL 1 & 2.	18
Figure 13. Cross section QEL 3,4, & 5.	19
Figure 14. Isopach QEL-1.	20
Figure 15. Isopach QEL-2.	21
Figure 16. Isopach QEL-3.	22
Figure 17. Isopach QEL-4.	23
Figure 18. Isopach QEL-5.	24
Figure 19. Structure QEL-1.	25
Figure 20. Structure QEL-3.	26
Figure 21. Well location map of the west study-site.	27
Figure 22. Cross section of lower Green River, west study-site.	28
Figure 23. Lower Green River cumulative production.	29
Figure 24. Total thickness lower Green River productive beds.	30
Figure 25. Lower Green River structure.	31
Figure 26. Wasatch cumulative production.	32
Figure 27. Green River Formation measured section, Willow Creek Canyon, Carbon and Uintah Counties, Utah.	34
Figure 28. Core-plug porosity of carbonate and clastic outcrop samples.	37
Figure 29. Porosity of clastic core-plug samples taken from the outcrop compared to the horizontal permeability.	37
Figure 30. Porosity versus horizontal permeability of core-plug samples classified as arenites.	38
Figure 31. Vertical permeability of carbonate versus clastic core-plug samples taken from the outcrop.	39
Figure 32. Horizontal permeability of carbonate compared to clastic core-plug samples taken from the outcrop.	39

Figure 33. Description of the core taken in the Wasatch Formation from the 2-22A1E well.	41
Figure 34. Structure contour map of the Bluebell field with azimuth orientations of surface fractures shown.	46
Figure 35. Decline curve analysis of the Michelle Ute well.	52
Figure 36. Decline curve analysis of the Malnar Pike well.	52
Figure 37. Cumulative oil production and projection for the Michelle Ute well.	53
Figure 38. Cumulative oil production and projection for the Malnar Pike well.	53
Figure 39. Original oil-in-place calculations for all perforated zones in the Michelle Ute well.	54
Figure 40. Original oil-in-place calculations for all perforated zones in the Malnar Pike well.	55
Figure 41. Long column gas chromatography analyses of the yellow and black wax crudes.	58
Figure 42. Actual versus preliminary single-well model simulated cumulative oil production for the Michelle Ute well.	62
Figure 43. Actual versus preliminary single-well model simulated cumulative gas production for the Michelle Ute well.	62
Figure 44. Actual versus preliminary single-well model simulated cumulative oil production for the Malnar Pike well.	63
Figure 45. Actual versus preliminary single-well model simulated cumulative gas production for the Malnar Pike well.	63
Figure 46. Actual versus comprehensive single-well model simulated cumulative oil production for the Michelle Ute well.	65
Figure 47. Actual versus comprehensive single-well model simulated cumulative gas production for the Michelle Ute well.	65
Figure 48. Actual versus simulated cumulative oil production from five zones in five wells in the four-square mile area east study-site.	66
Figure 49. Actual versus simulated cumulative gas production from five zones in five wells in the four-square mile area east study-site.	66
Figure 50. Actual versus simulated cumulative oil production for the Michelle Ute well.	68
Figure 51. Actual versus simulated cumulative gas production for the Michelle Ute well.	68
Figure 52. Actual versus simulated cumulative oil production for the Malnar Pike well.	69
Figure 53. Actual versus simulated cumulative gas production for the Malnar Pike well.	69
Figure 54. Actual versus simulated cumulative oil production of the lower Green River Formation.	70
Figure 55. Actual versus simulated cumulative gas production of the lower Green River Formation.	70
Figure 56. Actual versus simulated cumulative oil production for the State 3-10C well.	71

Figure 57. Actual versus simulated cumulative gas production for the
State 3-10C well. 71

TABLES

Table 1. Point counts of sand-dominated clastic samples from the Willow Creek
Canyon section of the Green River Formation. 35
Table 2. Core from wells drilled in the Bluebell field that are being examined. . 40
Table 3. Compilation of gas-oil ratios (GOR) for a few selected wells. 50
Table 4. Table of thermodynamic properties. 57

ACKNOWLEDGEMENTS

This research is performed under the Class I Oil Program of the U.S. Department of Energy (DOE), Pittsburgh Energy Technology Center contract number DE-FC22-92BC14953. The Contracting Officer's Representative is Edith Allison with the DOE Bartlesville Project Office.

Project Contributors:

Principal Investigator: M. Lee Allison, Utah Geological Survey
Program Manager: Craig D. Morgan, Utah Geological Survey
Contributing Scientists: Milind D. Deo, University of Utah,
Dept. of Chemical and Fuels Engineering
and under his direction Rajesh J. Pawar, student
Thomas H. Morris, Brigham Young University, Dept. of
Geology, and students under his direction;
Ann Garner and MaryBeth Wegner
Bart J. Kowallis, Brigham Young University,
Dept. of Geology
Carol N. Tripp, Consulting Geologist
Richard Jarrard, University of Utah,
Dept. of Geology and Geophysics
DeForrest Smouse, Quinex Energy Corp.
Lewis F. Wells, Quinex Energy Corp.
Richard Curtice, Halliburton Energy Services

ABSTRACT

The Bluebell field produces from the Tertiary lower Green River and Wasatch Formations of the Uinta Basin, Utah. The productive interval consists of thousands of feet of interbedded fractured clastic and carbonate beds deposited in a fluvial-dominated deltaic lacustrine environment. Although some wells have produced over 1 million barrels (159,000 m³) of oil, many have produced only 100,000 to 250,000 barrels (15,000-31,000 m³), or less, of oil.

The lower portion of the productive interval is overpressured, requiring that approximately 10,000 feet (3,050 m) of intermediate casing be set. The final 2,000 to 4,000 feet (610-1,220 m) of drilling is slow and difficult requiring weighted mud. Wells are typically completed by perforating 40 or more beds over 1,000 to 3,000 vertical feet (305-915 m), then applying an acid-frac treatment to the entire interval. This completion technique is believed to leave many potentially productive beds damaged and/or untreated, while opening up some water and thief zones.

Bluebell project personnel are studying ways to improve completion techniques used in the field to increase primary production in both new wells and recompletions. The study includes detailed petrographic examination of the different lithologic reservoir types in both the outcrop and core. Outcrop, core, and geophysical logs are being used to identify and map important depositional cycles. Petrographic detail will be used to improve log calculation methods which are currently highly questionable due to varying water chemistry and clay content in the Green River and Wasatch Formations. Field mapping of fractures and their relationship to basin tectonics helps predict the orientation of open fractures in the subsurface. The project includes acquiring bore-hole imaging logs from new wells in the Bluebell field thereby obtaining detailed subsurface fracture data previously not available. Reservoir simulation models are being constructed to improve the understanding of pressure and fluid flow within the reservoir. A detailed database of well completion histories has been compiled and will be studied to determine which were the most and the least effective methods used in the past.

The reservoir characterization study will identify specific beds and/or facies that have the greatest production potential. Improved reservoir characterization and a better understanding of the reservoir production characteristics will hopefully help identify damaged intervals that still contain significant volumes of moveable oil. Completion techniques will then be designed that are best suited for the specific lithologic type.

The project is in the first year of the two year characterization study. The first year has been spent primarily gathering and compiling both surface and subsurface data. The second year will be one of evaluating and interpreting all the various components resulting in specific demonstratable recommendations to be carried out in phase II of the project.

EXECUTIVE SUMMARY

The objective of the project is to increase oil production and reserves from improved completion techniques in the Uinta Basin, Utah. To accomplish this objective a two year geologic and engineering characterization of the Bluebell field is being conducted. The study is evaluating surface and subsurface data, current completion techniques, and common production problems.

A 2,786-foot (849.2-m) stratigraphic section in the Willow Creek Canyon area of Carbon and Duchesne Counties, Utah, was examined and described. The section included a portion of the upper and all of the lower Green River Formation, and the Green River/Wasatch (Colton) transition. Depositional environments range from paralic fluvial to open lacustrine. Petrographic classification and textural analysis were completed on 33 thin sections. All thin sections of clastic rocks were point counted. Porosity and permeability were cross-plotted for the 32 core-plug analyses from outcrop samples. The data indicates that the feldspathic arenites tend to have the best porosity and permeability. Porosity values for all samples analyzed range from 0.2 to 27.2 percent and permeabilities range from less than 0.01 to 1,342 millidarcies.

Fractures play an important role in oil production in the Bluebell field and throughout the Uinta Basin. Surface fracture orientations have been mapped throughout the field and in the Green River Formation in other areas of the basin. All of the surface fracture measurements show two major joint sets. In general, one fracture set tends to follow the regional structural trend (which bends) of the north margin of the basin and the other set is nearly orthogonal to the first. There is no consistent pattern of cross-cutting of the fractures. Bore-hole imaging logs have been obtained in recently drilled wells to evaluate orientation, density, aperture, and facies control of fractures in the reservoir.

Over 1,600 feet (488 m) of core from 10 different wells are being described. Thin sections will be made and described and X-ray diffraction will be conducted on several samples for clay identification. Core data will be used to identify facies and depositional environments, improve geophysical log calculations, and improve understanding of the reservoir properties of differing facies.

Stratigraphic cross sections were constructed for the east and west study-sites. Porosity, oil, and water saturations were determined at 2-foot (0.6-m) intervals through the productive zones for many of the wells in both study-sites. The data is being used to construct both single-well and multi-well reservoir simulation models. Structure and thickness maps were prepared for many of the individual beds.

Productive intervals can be divided into three primary zones. The first zone consists of the upper Wasatch transition (which may include part of the lower Green River Formation) and occurs at an average depth of 9,000 to 10,000 feet (2,745-3,050 m), which is usually normally pressured. The zone consists of interbedded limestone, dolomite, sandstone, and shale that were deposited in a transitional shoreline to nearshore lacustrine environment. The zone was the original drilling objective when the Roosevelt field was first discovered in 1948. The Roosevelt field

is now the Roosevelt unit, a federal unit within the Bluebell field.

The second and third zones consist of the Wasatch and underlying lower Wasatch transition zone (Flagstaff equivalent?). These two zones are typically overpressured in part and occur at an average depth of 11,000 to 14,000 feet (3,355-4,270 m). The Wasatch typically consist of shallow lacustrine to fluvial deltaic sandstone, siltstone, and shale. The lower Wasatch transition consists of mud flat to shallow lacustrine argillaceous limestone, dolomite, and some sandstone. The overpressured Wasatch and lower Wasatch transition became the primary drilling objectives beginning in 1970 (Smouse, 1993). The Wasatch clastics and lower Wasatch transition carbonates are usually perforated and completed together. In some wells the upper Wasatch transition, Wasatch, and lower Wasatch transition are all perforated and completed together.

Digitizing of geophysical well logs in and around the Bluebell field has been completed. The database consists of 240 logs from 80 wells. The digital data will be used for field-wide correlation, detailed porosity, clay content, and fluid saturation calculations.

Average reservoir and hydrocarbon parameters have been determined. The oil formation factor is 1.45 to 1.50 at a gas-to-oil ratio of 800 to 900 cubic feet of gas to a barrel of oil. The initial reservoir pressure was estimated to have been approximately 4,000 pounds per square inch (27,000 KPa) at an average depth range of 10,000 to 12,000 feet (3,000-3,700 m). Bubble point was calculated to be 3,200 pounds per square inch (22,000 KPa).

Preliminary modeling in the east study-site indicates a possible 3 to 6 million barrels (0.9-1.8 million m³) of oil-in-place in 40 acres (16.2 ha), with only 2 to 4 percent recovery. Single and multi-well reservoir simulation models have been constructed for both study-sites. Revisions to the model are continually being made to determine the best methods for scaling up from single to multi-well representations.

A digital geological database was established for the Bluebell field. Location information and monthly oil, gas, and water production (from 1984 through 1993) for every well in the field has been entered. Formation and marker bed tops, oil and gas analyses, open-hole and completion test data, and original and recompletion treatments, have been entered for over 90 wells to date. The well completion histories will be used to determine which previous and currently used methods and chemical additives are the most and least effective completion treatment.

INTRODUCTION

The Bluebell field in the Uinta Basin of northeast Utah has produced over 127 million barrels (38.7 million m³) of oil (MMBO) from fluvial-dominated deltaic reservoirs in the Tertiary Green River and Wasatch Formations. Three contiguous fields, Bluebell, Altamont, and Cedar Rim, have produced over 243 MMBO (741.2 million m³) and currently represent 31 percent of the total annual production for the state of Utah. More than one quarter of the wells drilled in the Bluebell field have been abandoned and as water production increases the abandonment rate is expected to increase. Well spacing is two wells per 640 acres (259.2 ha) but much of the field is still produced at one well per 640 acres (259.2 ha).

In the Bluebell, Altamont, and Cedar Rim field complex the Green River and Wasatch Formations contain an oil-bearing section up to 8,000 feet (2,440 m) thick of which as much as 2,500 feet (762 m) was originally overpressured. Most of the production comes from (top to bottom): (1) carbonates of the lower Green River Formation/upper Wasatch transition that were deposited in a near to offshore lacustrine environment, (2) generally thin bedded sandstones of the Wasatch Formation deposited in fluvial-dominated deltas, and (3) carbonates and some interbedded sandstones of the lower Wasatch transition deposited in mud flats to offshore lacustrine environments. Almost all of the beds have low matrix permeability which is often enhanced by naturally occurring vertical fractures.

Although the Uinta Basin is extremely rich in hydrocarbons, producing them is often a marginal economic success. Drilling costs are very high. The lower overpressured zone makes it necessary to set approximately 10,000 feet (3,050 m) of intermediate casing before drilling the rest of the hole with weighted (12 to 14 lb/gal [1.44-1.68 Kg/L]) mud. Multiple, thin, often low porosity and permeability beds that are often fractured and contain differing water compositions, make conventional log analysis extremely difficult. Most perforations are selected primarily based upon drilling shows.

Since it is unknown which beds could produce large volumes and which will produce only small volumes of oil, operators perforate a large number of beds over a 1,000 to 3,000 vertical-foot (305-915-m) interval. The typical treatment for such a large gross perforated interval is to pump about 20,000 gallons (75,700 l) of hydrochloric acid (HCL) with some diverters. The treatment, being applied to carbonates and sandstones, overpressured and normally pressured beds, low and high porosity beds, some naturally fractured beds, oil and water saturated beds, is a very hit or miss process. Undoubtedly, some thief and water-producing beds are opened while potentially productive oil beds are left untreated.

When production logs are run, they typically show that the majority of the perforations are not producing. It is unknown if the non-producing beds are already depleted or if they are damaged and were never properly treated. In many cases the non-producing beds may still contain significant amounts of recoverable hydrocarbons. Unable to accurately evaluate the formation, recompletions consist of applying more

acid to the entire gross perforated interval. Occasionally, more perforations will be added before applying additional acid.

This project intends to demonstrate ways to increase production and reserves in the Bluebell field through improved completion techniques for new and recompleted wells. The first year of a two year detailed geological and engineering reservoir characterization of the Green River and Wasatch Formations has been completed. Work is continuing on: (a) log analysis and petrophysics evaluation, (b) examination of outcrops, well cuttings, and cores in order to understand reservoir heterogeneity and capacity, (c) detailed correlation of geophysical logs and construction of various subsurface maps to define lithofacies, fracture trends, and paleodepositional setting of the primary producing horizons, (d) determination of the location of fractures throughout the producing section, their orientation, nature and relation to lithology or facies, (e) statistical analysis of the completion techniques and production histories of wells in the field to identify those practices which are most economical and result in the most productive wells, and (f) determination of in-place and mobile reserves.

Although much of the work is field-wide, the project is concentrating on two study-sites. The east study-site is in the eastern portion of the Bluebell field (figure 1) and includes the Roosevelt unit. The area has both lower Green River/upper Wasatch transition, Wasatch, and lower Wasatch transition. Some wells commingle lower Wasatch, Wasatch, and lower Green River/upper Wasatch production. This part of the field typically has the poorest producers, generally less than 200,000 BO (31,800 m³) per well and many, less than 100,000 BO (15,900 m³) per well.

The west study-site is in the west-central portion of the field. It includes some of the best producing wells with cumulative production of over 3 MMBO (0.47 million m³) per well. Many of the wells were originally drilled and completed in the lower Green River/upper Wasatch transition. These wells were later deepened and completed in the Wasatch and lower Wasatch transition. Geophysical logs, test and production data is more complete in the west study-site than the east study-site. Hopefully, detailed modeling of the west study-site will not only tell us about that part of the field but will provide a basis for many of the assumptions that have to be made to model the east study-site.

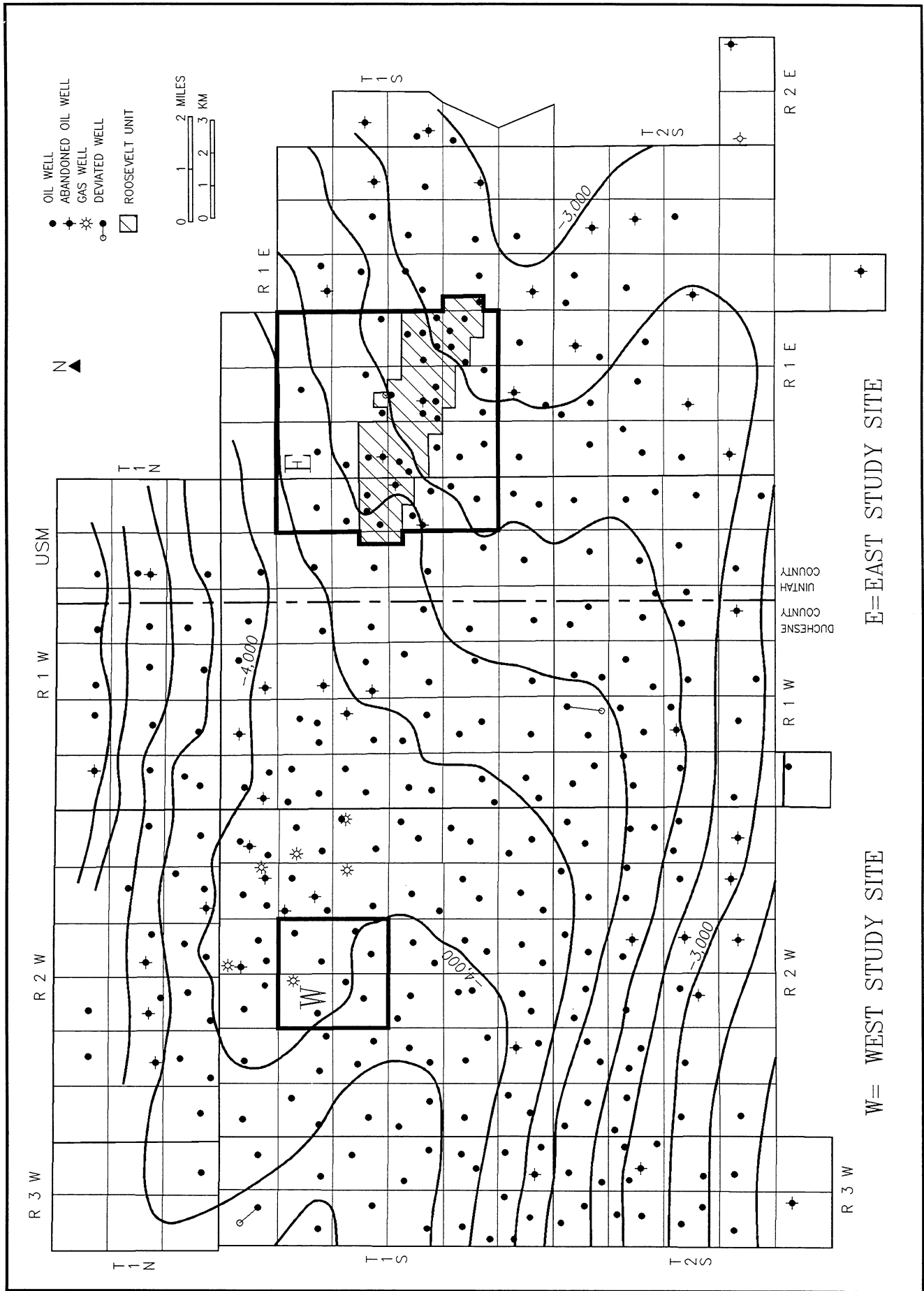


Figure 1. Structure contour map of the Bluebell field. Contours drawn on the top of the middle marker of the Green River Formation. Contour interval is 200 feet. East and west study-sites and the Roosevelt Unit are shown (modified from Morgan, 1994).

GENERAL GEOLOGY AND RESERVOIR CHARACTERISTICS

The Bluebell field is the largest oil producing field in the Uinta Basin. Bluebell is one of three contiguous oil fields; Bluebell, Altamont, and Cedar Rim (figure 2). The basin is an asymmetrical syncline deepest in the north-central area near the basin boundary fault (figure 3). The Bluebell field produces oil from the Eocene-Paleocene Green River and Wasatch Formations near the basin center (figure 4).

The Bluebell field is 251 square miles (650 km²) in size and covers all or parts of Townships 1 North, 1 and 2 South, Ranges 1 East and 1 through 3 West, Uintah Base Meridian (figure 1). Over 127 MMBO (20.2 million m³) and 155 billion cubic feet (BCF) (4.4 billion m³) of associated gas have been produced (December 31, 1993). The spacing is two wells per section, but much of the field is still produced at one well per section. The Roosevelt Unit within the Bluebell field operates under the unit agreement. Although some wells have produced over 3 MMBO (0.47 million m³), most produce less than 0.5 MMBO (79,500 m³) (figure 6).

Geology

The Green River and Wasatch Formations were deposited in intertonguing relationship in and around ancestral Lake Flagstaff and Lake Uinta. Depositional cycles show rapid lake level fluctuations and changes in water chemistry (Fouch and Pitman, 1991, 1992; Fouch and others, 1992). The Green River and Wasatch Formations were deposited in alluvial-fluvial, marginal lacustrine, and open lacustrine environments (figure 5). The depositional environments are described in detail by Fouch (1975, 1976, 1981), Ryder and others (1976), Pitman and others (1986), Pitman and others (1982), Bruhn and others (1983), Stokes (1986), Castle (1991), Fouch and Pitman (1991, 1992), Fouch and others (1990) and Franczyk and others (1992).

The production at Bluebell comes from three primary intervals: (1) lower Green River Formation/upper Wasatch transition, (2) Wasatch Formation, and (3) lower Wasatch transition (possible Flagstaff equivalent) (figure 7). The lower Green River/upper Wasatch transition is informally defined as from the middle marker to the top of the Wasatch (redbeds). The lower Green River/upper transition, upper transition/Wasatch, and Wasatch/lower transition contacts are transitional and intertonguing, as a result they are difficult to identify accurately.

Production from the Bluebell field was first established in the Roosevelt Unit from the lower Green River/upper Wasatch transition at depths less than 11,000 feet. Production is both stratigraphically and structurally controlled. Of the 17 wells completed in the lower Green River/upper Wasatch transition, eight have produced over 100,000 BO, and four of the eight have produced over 350,000 BO. Productive beds are interbedded calcareous sandstones, limestones, marlstones, and ostracodal limestones, deposited in fluvial-deltaic and carbonate mud flat environments. Many of the lower Green River beds are laterally extensive and highly fractured. As a result,

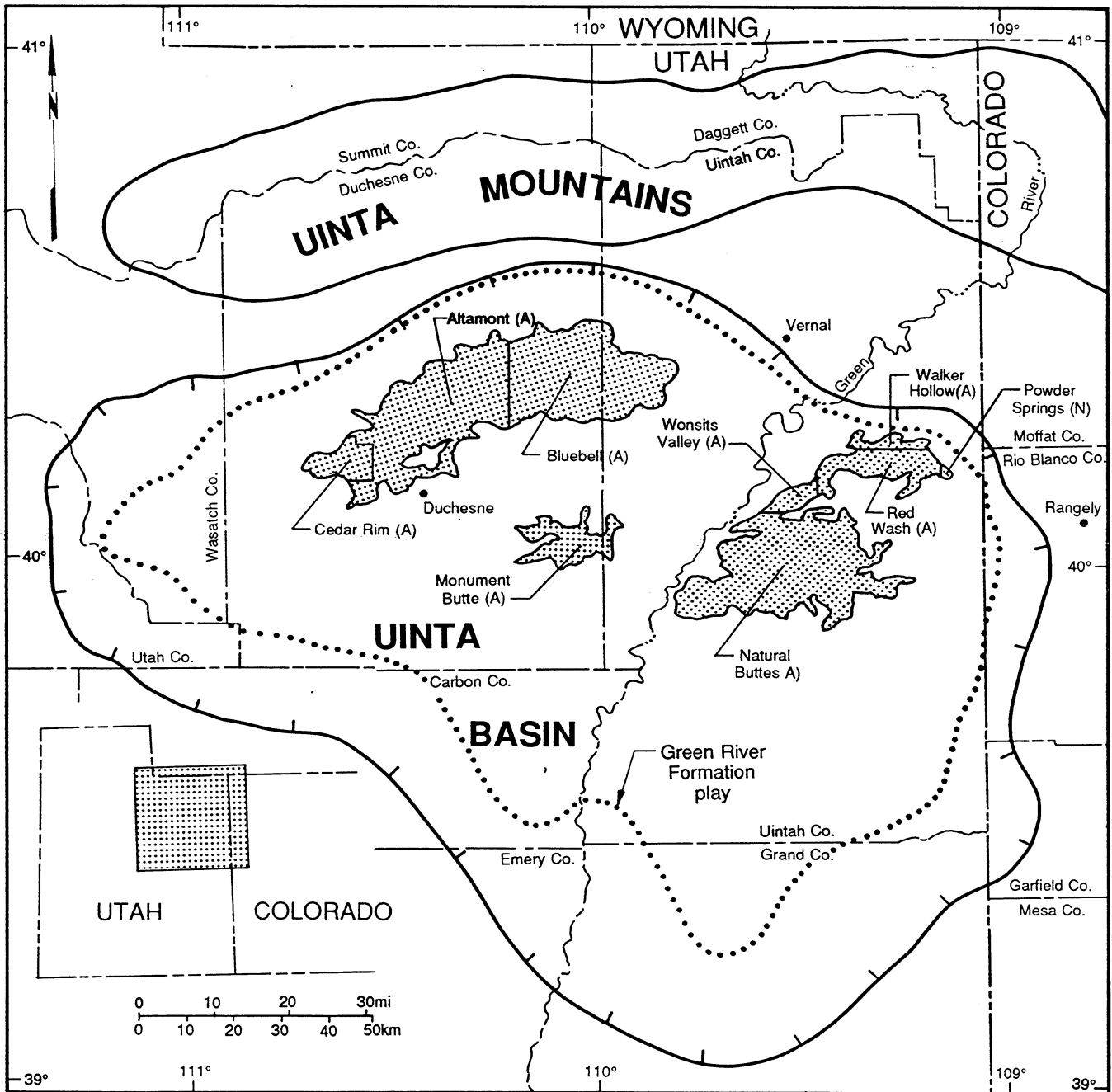


Figure 2. The Uinta Basin with Bluebell, Altamont, Cedar Rim and other fields shown. Reservoirs are labeled: 1, Uinta Formation; 2, Green River Formation; 3, Wasatch Formation. Hachured lines indicates approximate limits of Tertiary units in the Uinta Basin (from Chidsey, 1993).

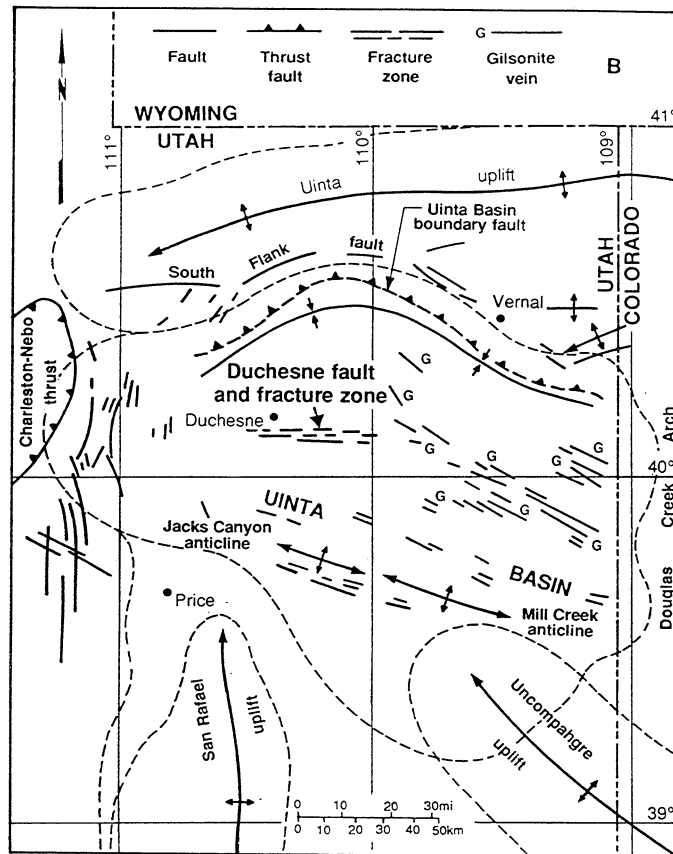


Figure 3. Major structural features, surface faults, and fracture zones in and around the Uinta Basin (from Chidsey, 1993).

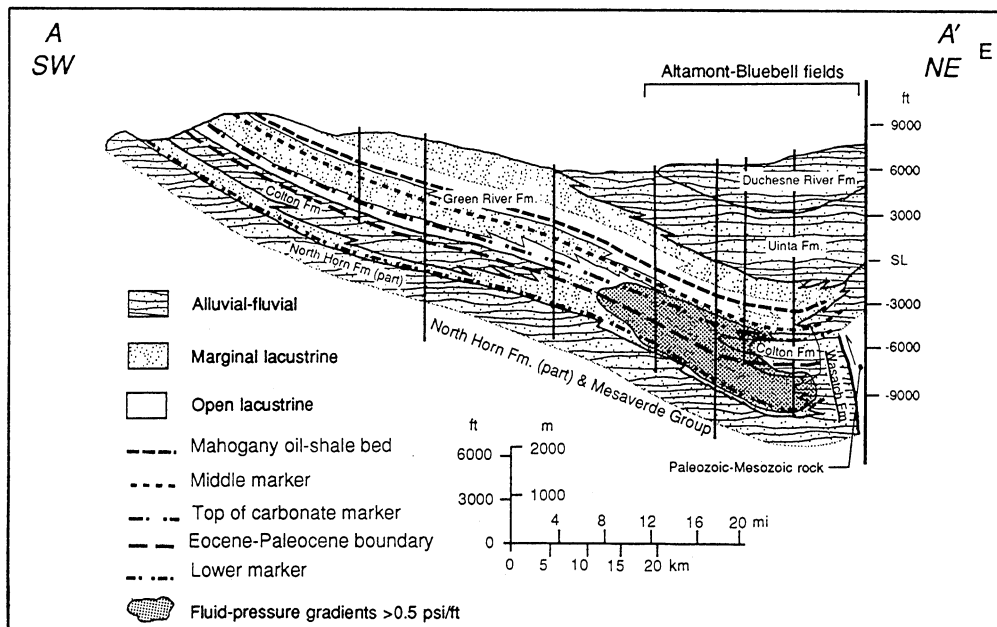


Figure 4. Generalized southwest to northeast cross section of Tertiary rocks in the Uinta Basin showing major facies and intertonguing relationships. Area of fluid-pressure gradients >0.5 psi/ft (11.3 KPa/m) are shown (from Fouch and others, 1992).

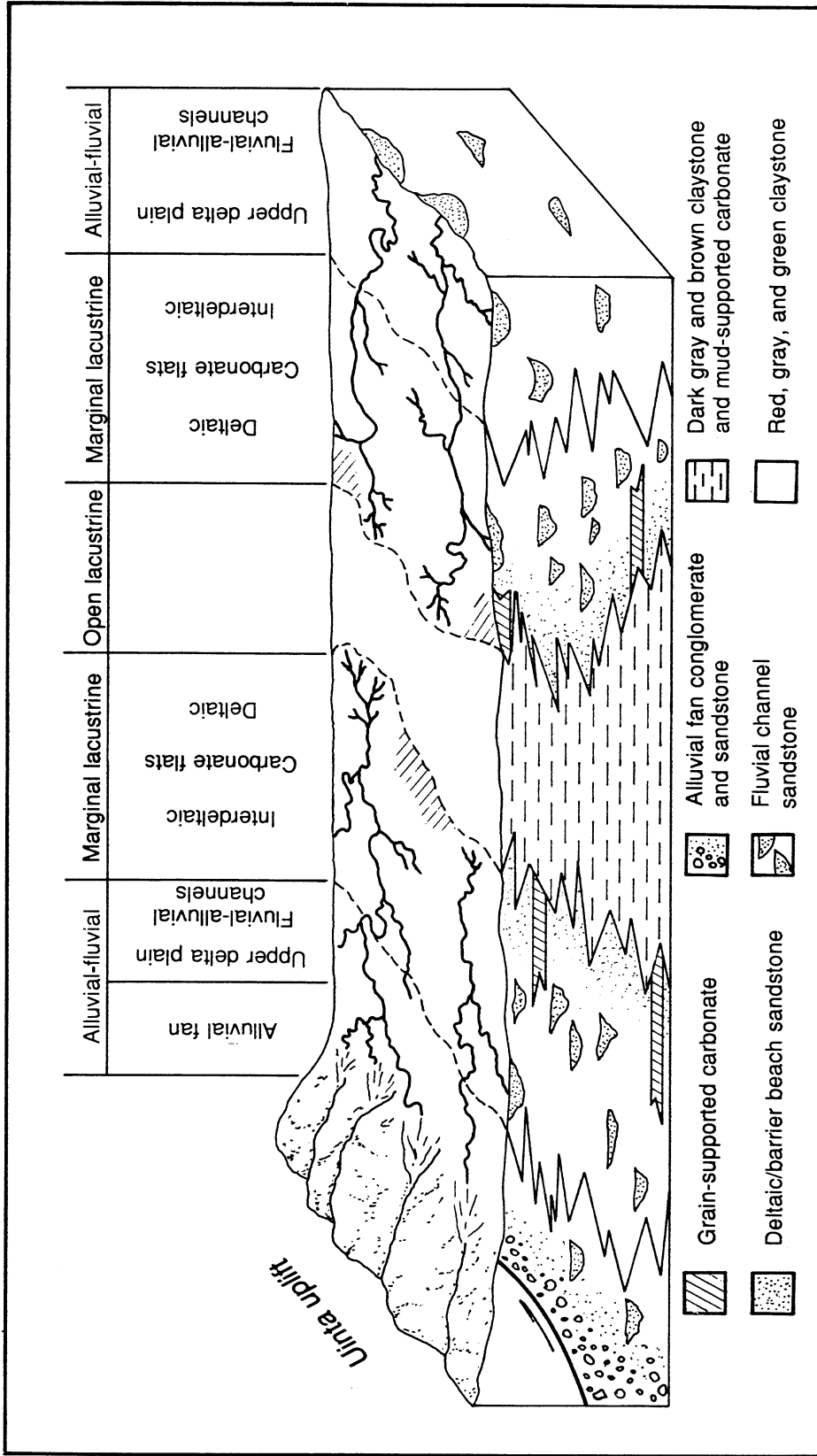


Figure 5. Conceptual block diagram with distribution and interpretation of depositional environments and lithology of alluvial-fluvial, marginal lacustrine, and open lacustrine facies associated with the early Eocene Lake Uinta. Width of the lake in diagram is approximately 25 miles (40.2 km) (from Chidsey, 1993).

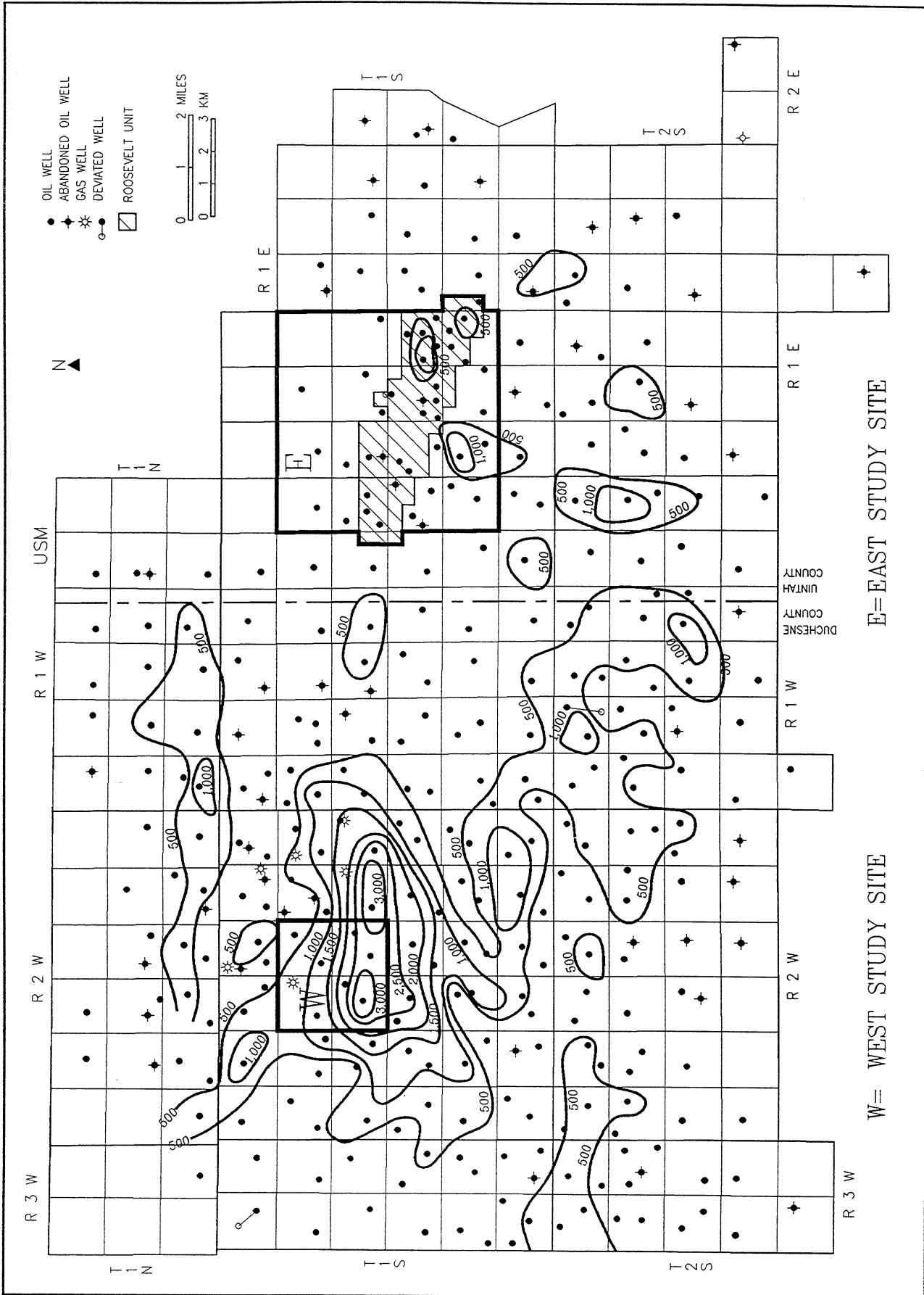


Figure 6. Cumulative oil production of the wells (as of December 31, 1992) is given in thousands of barrels of oil. The contour interval is 500 thousand barrels of oil (modified from Morgan, 1994).

Michelle Ute 1-7AIE
 T1S R1E sec.7
 KB 5,643'

Malnar Pike 1-17
 T1S R1E sec.17'
 KB 5,522'

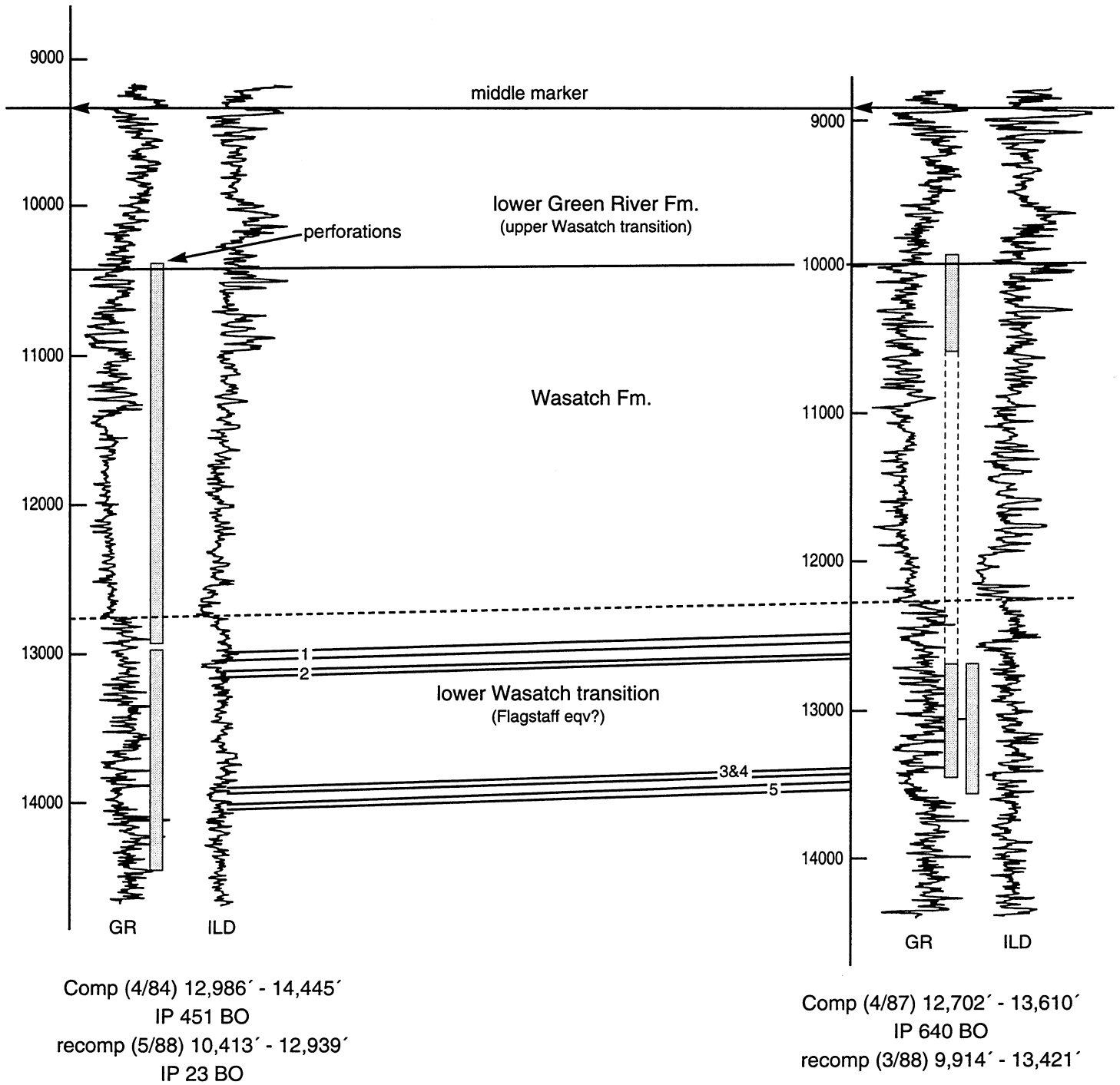


Figure 7. Cross section from the Michelle Ute to Malnar Pike wells using gamma ray (GR) and resistivity (ILD) curves. Datum is the middle marker of the Green River Formation. Correlated zones 1 through 5 are the zones of interest discussed in the demonstration phase of the project proposal.

many of these beds, which are currently not perforated in most of the deeper Wasatch producing wells, may be excellent targets to attempt new completions techniques and horizontal drilling completions.

The Wasatch production is primarily from sandstone and siltstones deposited in alluvial to fluvial-deltaic environments. The source for the Wasatch rebeds (sandstones, siltstones, and red shale) in Bluebell field was the Uinta Mountains to the north. The Wasatch rebeds thin rapidly from north to south through the field, with the best sandstone development occurring in the west portion of the field. The lower Wasatch transition (Flagstaff equivalent?), consists dominantly of carbonates with minor sandstone that were deposited in marginal to open lacustrine environments. The lower Wasatch is productive throughout most of the field. In the east portion of the field, lower Wasatch is a primary productive interval, while in the west portion both the Wasatch sandstones and lower Wasatch carbonates are productive.

Production Characteristics

The lower part of the Wasatch and lower Wasatch transition was originally overpressured. Drillstem tests (DST) and drilling kicks indicate pressure gradients of 0.65 psi/ft to 0.75 psi/ft (14.7-16.9 KPa/m) in parts of the field. The top of the overpressure zone cannot be accurately mapped due to limited test data. Mud data is unreliable because drillers often weighted the drilling mud before reaching the high pressure. Slope changes in geophysical log data caused by pressure changes are masked by the complex heterogeneity of the formation. Limited data does indicate that many of the lower Wasatch sandstones and the lower Wasatch carbonates were overpressured in the west-central portion of the field. In the east central portion of the field overpressuring generally does not occur until approximately the top of the lower Wasatch transition.

Pressure communication both vertical and horizontal, is greater than might be expected from a complex, heterogeneous reservoir. Where two wells per section are producing, the first well was usually tested for an initial potential from 1,000 to 3,000 BO (159-477 m³) per day. The second well in the section is often tested for an initial potential of 500 to 1,000 BO (79-159 m³) per day (figure 8). The second well appears to be above bubble point but much closer to it than the original well. As a result production decline is much more rapid in the second well. The first well commonly produces over 200,000 BO (31,800 m³), occasionally over 1,000,000 BO (159,000 m³) the first five years while the second well rarely produces over 200,000 BO (31,800 m³) the first five years (figure 9). Naturally occurring vertical fractures in the reservoir may be responsible for much of the pressure communication in the field. Fractures have been described in the limited core and bore-hole imaging logs that are available.

Individual beds in the lower Green River and Wasatch producing interval are difficult to evaluate. Fracturing and complex formation water chemistries make conventional geophysical log analysis highly questionable. Economics have discouraged open hole and/or production testing of individual beds. Therefore, it is

not clearly understood which beds in any particular well are potentially significant producers, limited producers, water producers, or thieves. As a result, the common practice is to perforate numerous beds over thousands of vertical feet and apply an acid-frac treatment, generally 20,000 gallons (75,700 l) of HCL. The typical well in the Bluebell field has between 1,500 to 2,000 feet (457-610 m) of gross perforations (figure 10). As a result, the treatment is being applied to both clastic and carbonates, fractured and unfractured beds, overpressured and normally pressured zones.

Study Sites

Although much of the work is field-wide, the project is concentrating on two study-sites. The east study-site is in the eastern portion of the Bluebell field (figures 1 and 11) and includes the Roosevelt unit. The area has lower Green River/upper Wasatch transition, Wasatch, and lower Wasatch transition zones. Some wells commingle lower Wasatch, Wasatch, and lower Green River/upper Wasatch production. This part of the field typically has the poorest producers, generally less than 200,000 BO (31,800 m³) per well and many, less than 100,000 BO (15,900 m³) per well.

The demonstration phase intends to recomplete two beds (QEL-1 and QEL-2) in the Michelle Ute (NW1/4SE1/4 section 7, T. 1 S., R. 1 E., Uinta Base Line) (figure 12) and horizontally redrill three beds (QEL-3, QEL-4, and QEL-5) in the Malnar Pike well (SW1/4SW1/4 section 17, T. 1 S., R. 1 E., Uinta Base Line) (figure 13). The beds range from 4 to 38 feet (1.2-11.6 m) with a thickness trend of northwest to southeast in the four section area (figures 14 through 18). Structural dip is approximately 280 feet/mile (53 m/km) to the north-northwest (figures 19 and 20).

The west study-site is in the west-central portion of the field (figures 1 and 21). It includes some of the best producing wells with cumulative production of over 3 MMBO (0.47 million m³) per well. Many of the wells were originally drilled and completed in the lower Green River/upper Wasatch transition (figure 22). Oil production ranged from 93,000 to 436,000 BO (14,800 to 69,300 m³) from nine beds with a cumulative thickness of 20 to 90 feet (6.1-27.4 m) (figures 23 and 24) dipping approximately 81 feet/mile (15 m/km) to the south-southwest (figure 25). These wells were later deepened and completed in the Wasatch and lower Wasatch transition and produced greater than 1,000,000 BO (159,000 m³) per well (figure 26). Geophysical logs, test and production data are more complete in the west study-site than the east study-site. Hopefully, detailed modeling of the west study-site will not only tell us about that part of the field but will provide a basis for many of the assumptions that have to be made to model the east study-site.

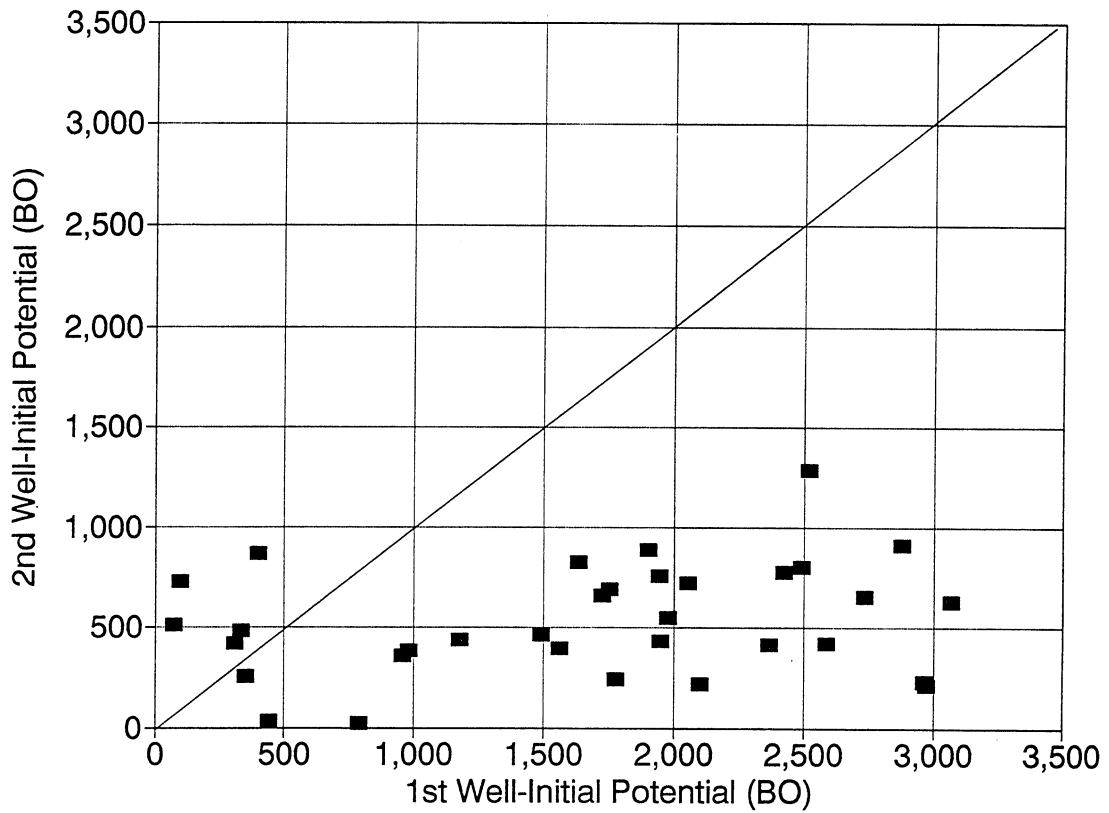


Figure 8. Initial potential in barrels of oil, of the first well completed in a section versus the second well.

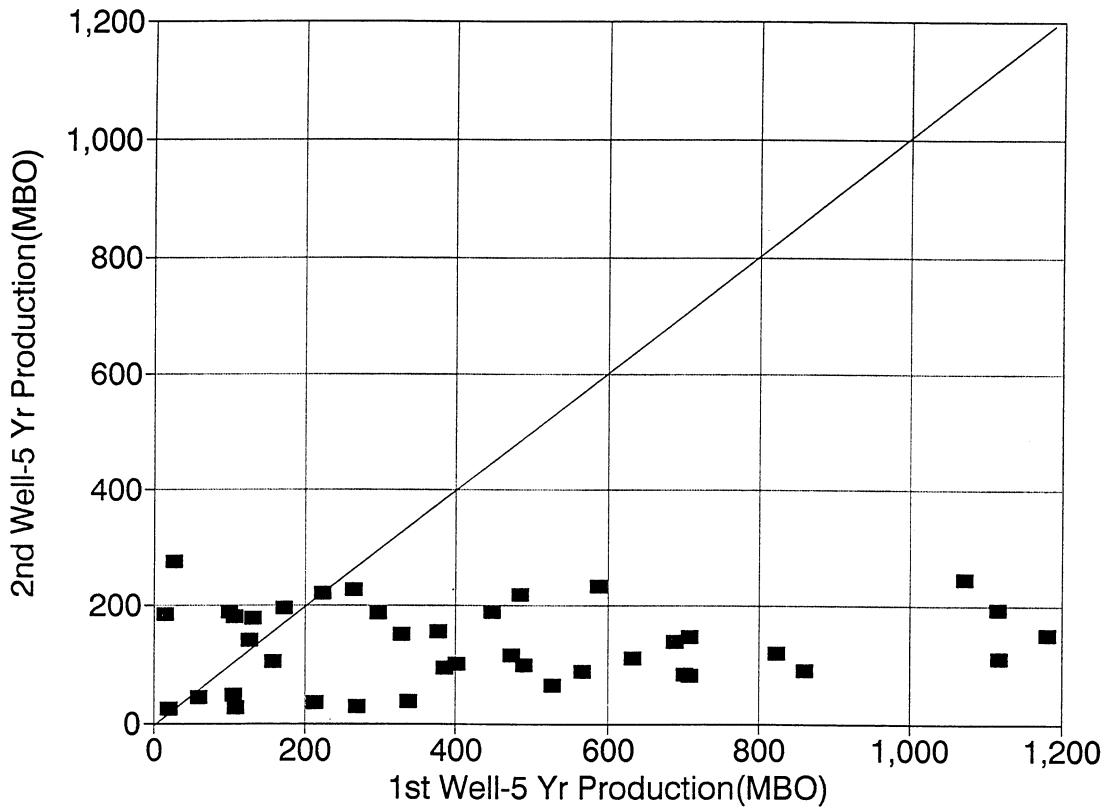


Figure 9. Cumulative production in thousands of barrels of oil, after five years of production, of the first well completed in a section versus the second well.

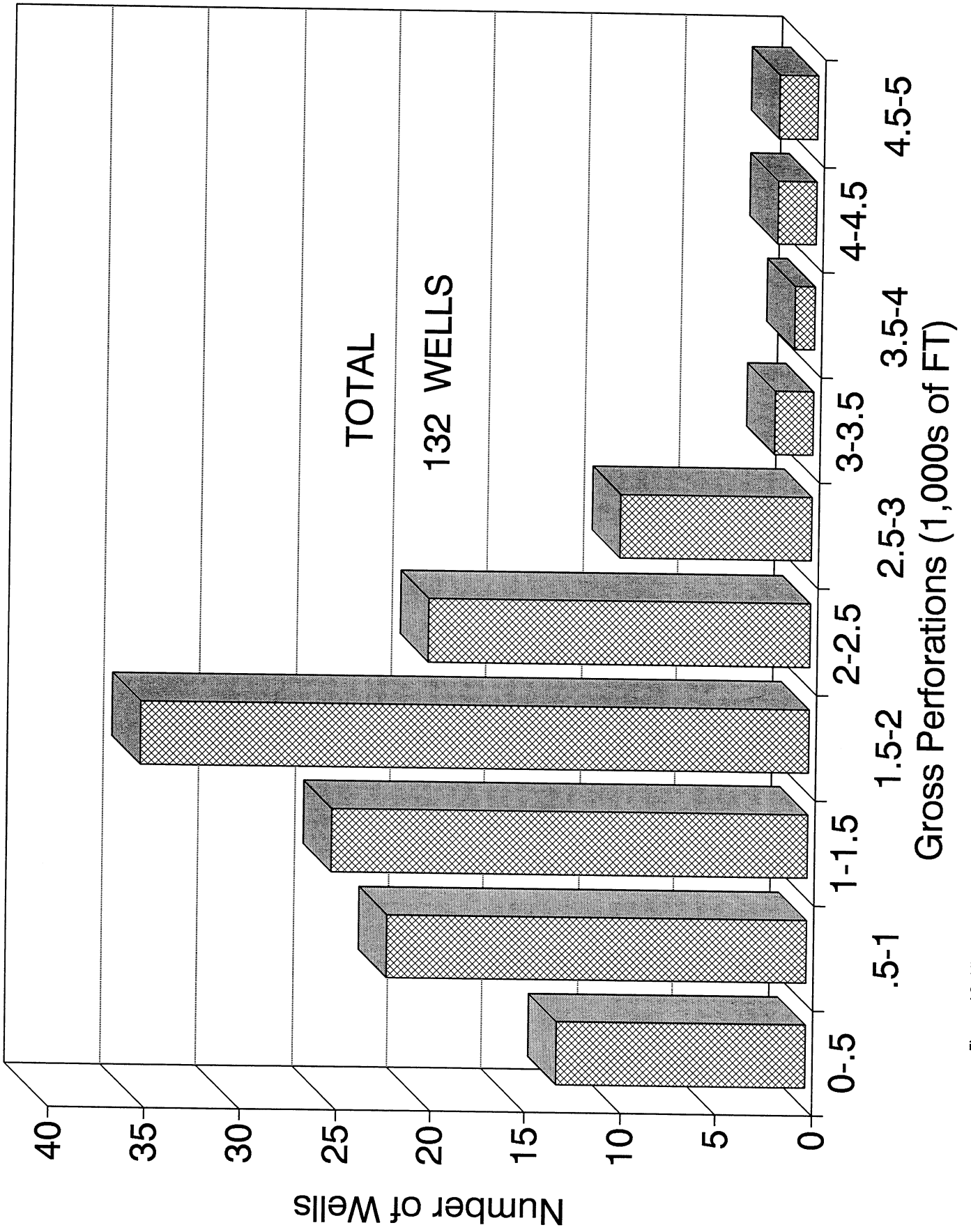


Figure 10. Histogram of gross perforations in thousands of feet, from a data set of 132 wells in the eastern portion of Bluebell field.

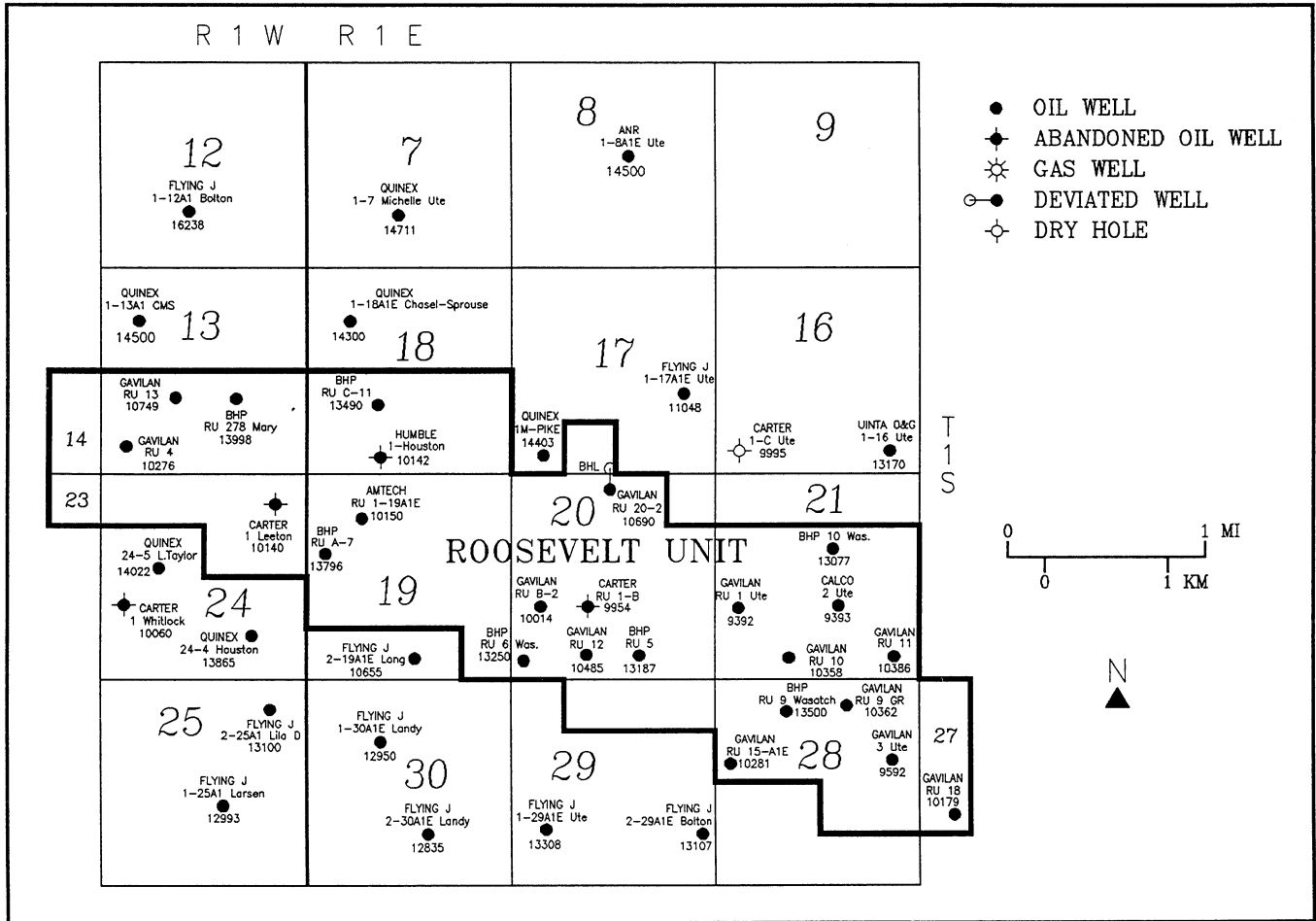


Figure 11. Well location map of the east study-site, Roosevelt Unit area. Michelle Ute is in section 7, and Malnar Pike (shown as 1M-Pike) is in section 17, T. 1 S., R. 1 E., Bluebell field, Uintah County, Utah.

Michelle Ute 1-7AIE
 T1S RIE sec. 7
 KB 5,643'
 comp (4/84) 12,986' - 14,445' (gross)
 IP 451 BOPD

Malnar Pike 1-17
 T1S RIE sec. 17
 KB 5,522'
 comp (4/87) 12,702' - 13,610' (gross) IP 640 BOPD
 recom (3/88) 9,914' - 13,421' (gross)

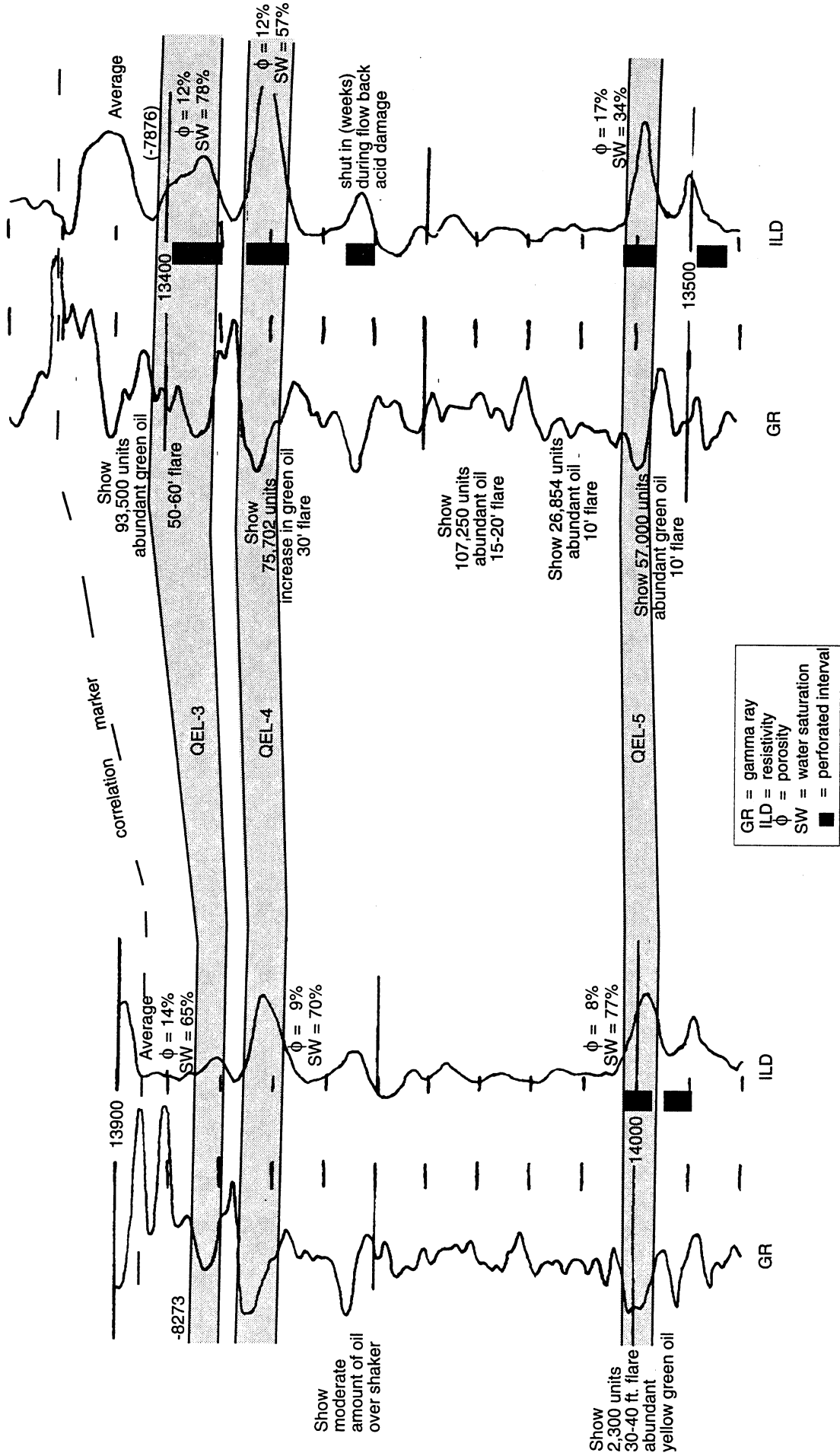


Figure 13. Cross section showing beds QEL-3, QEL-4, and QEL-5, which are being investigated for possible redrill in the Malnar Pike well. Refer to figure 11 for location of wells.

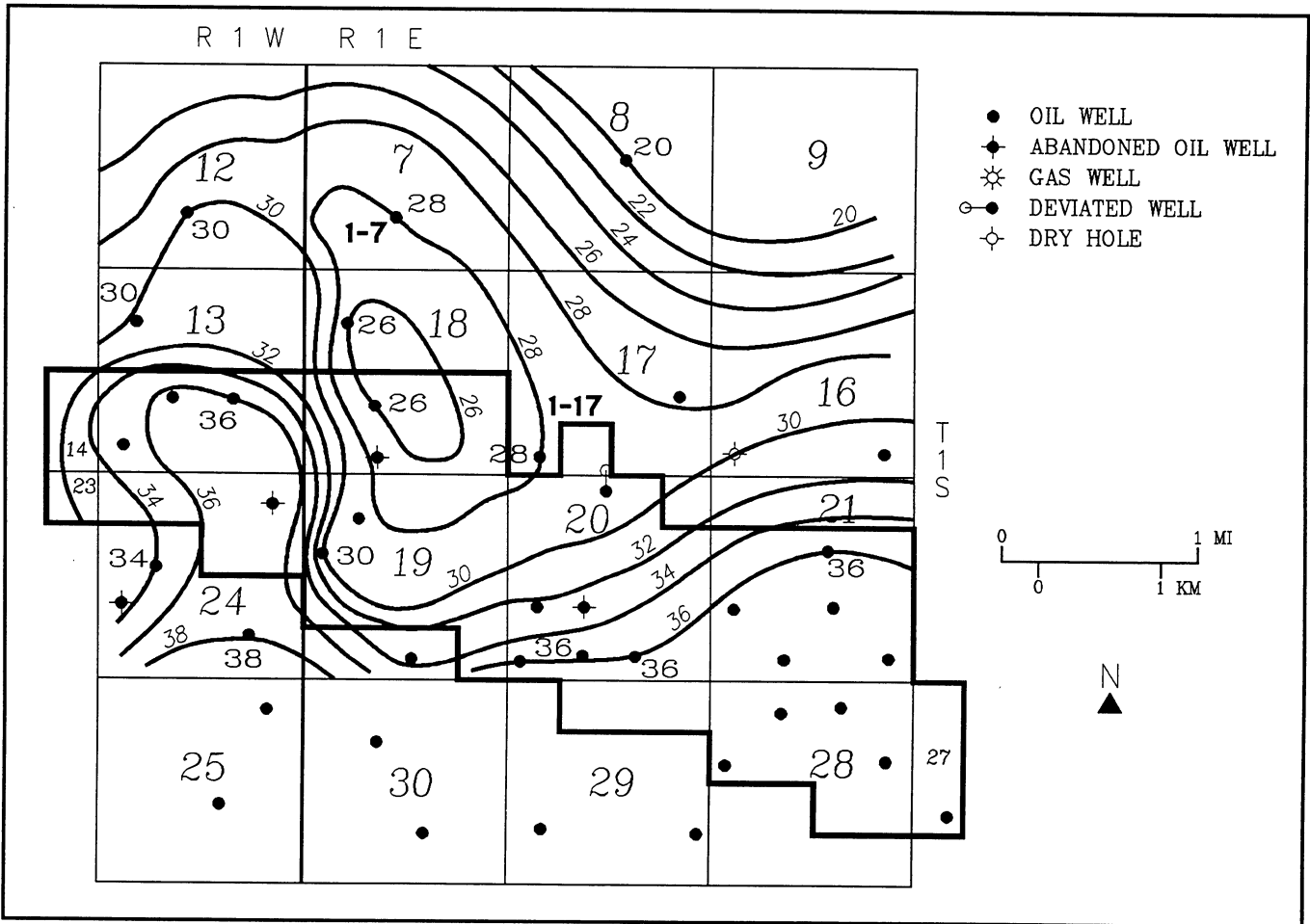


Figure 14. Thickness map of the QEL-1 bed. Contour interval is 2 feet.

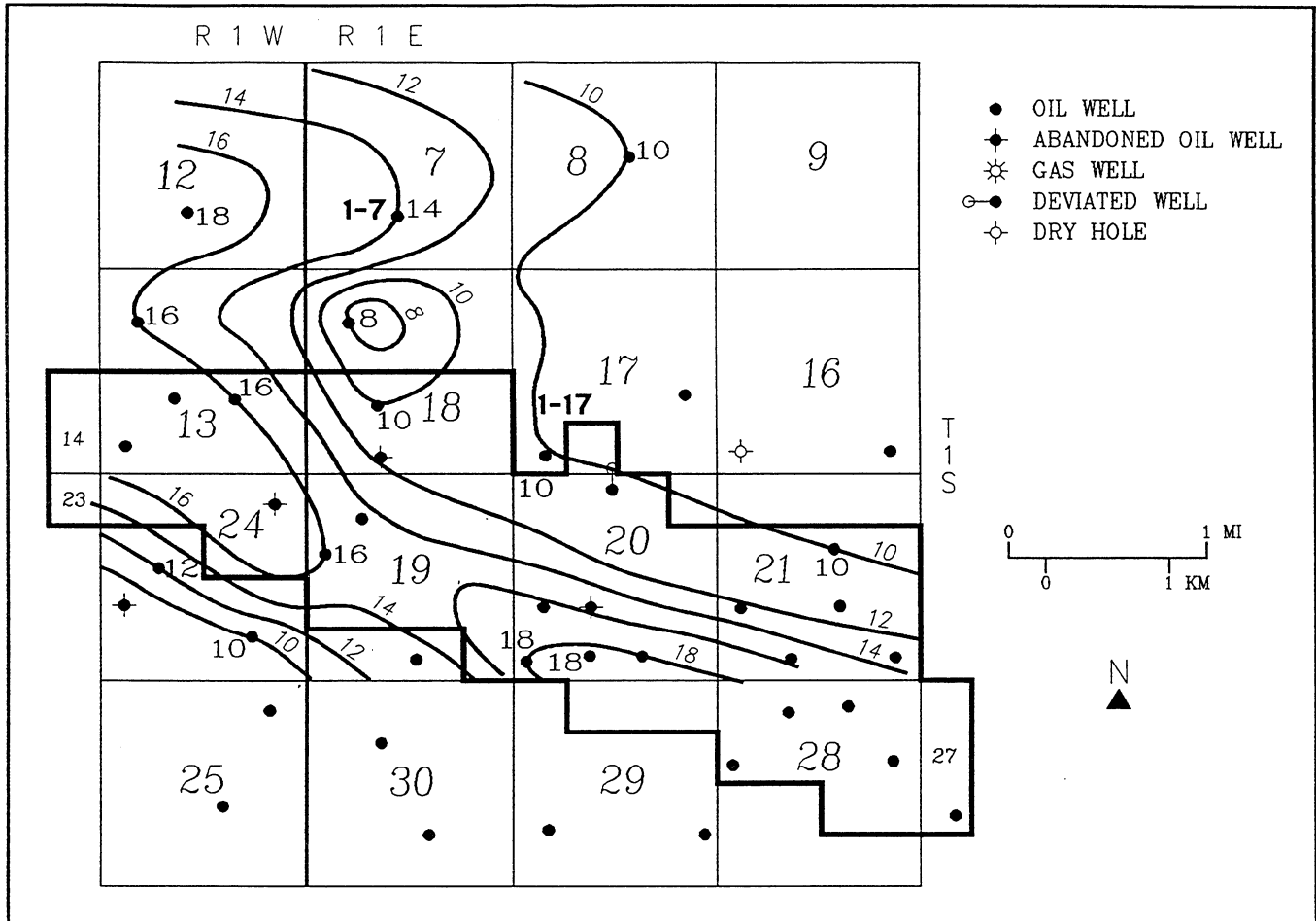


Figure 15. Thickness map of the QEL-2 bed. Contour interval is 2 feet.

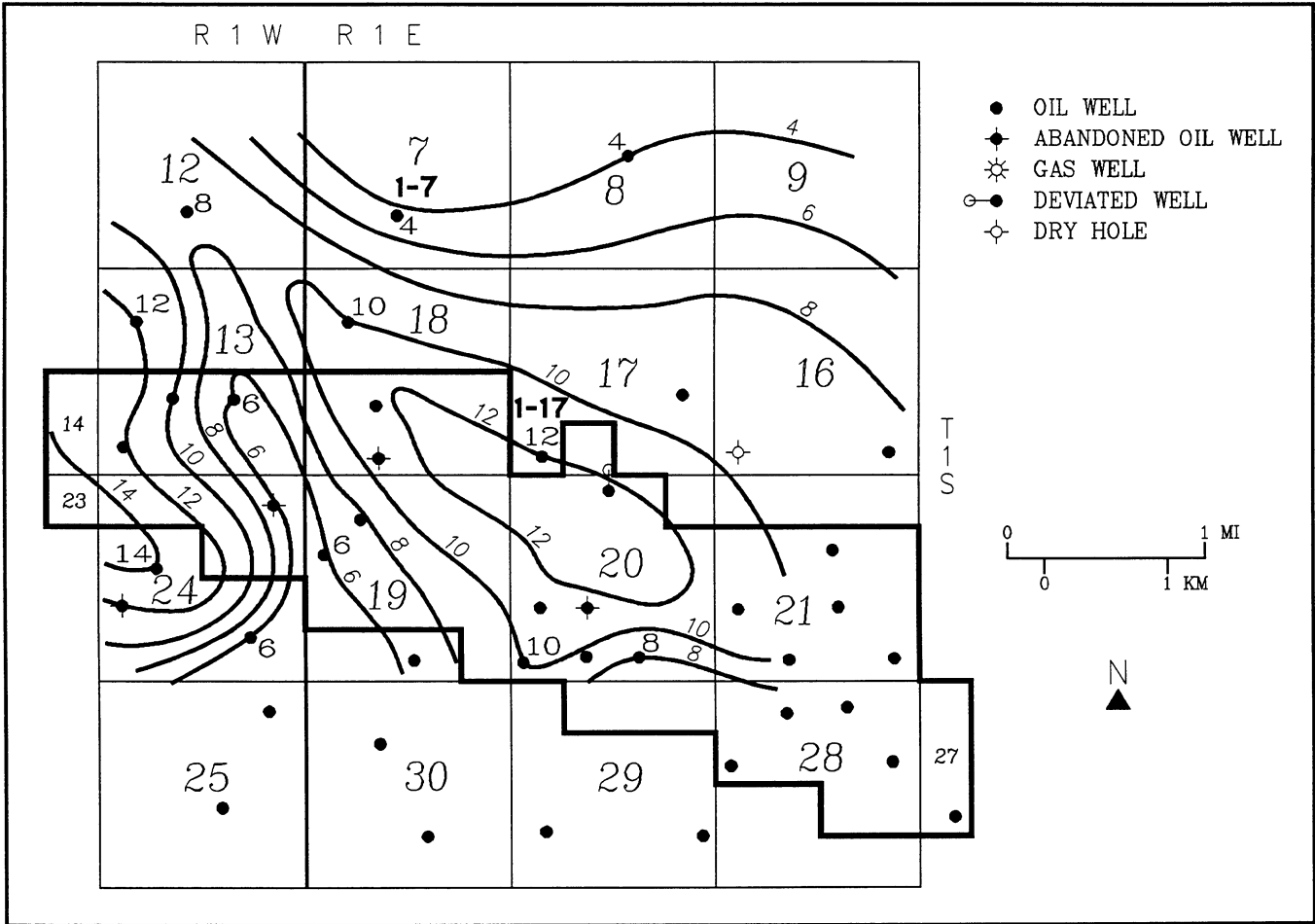


Figure 16. Thickness map of the QEL-3 bed. Contour interval is 2 feet.

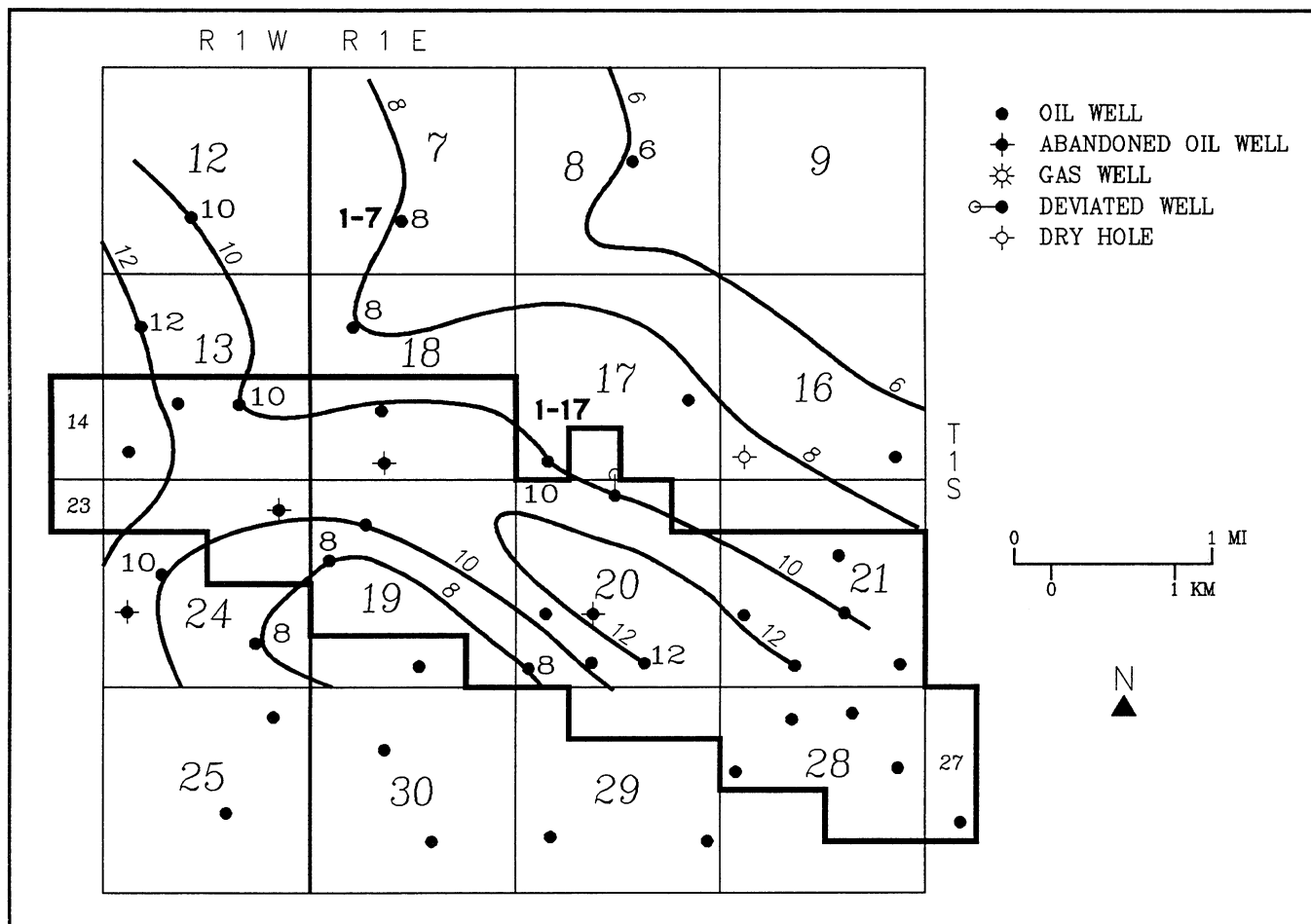


Figure 17. Thickness map of the QEL-4 bed. Contour interval is 2 feet.

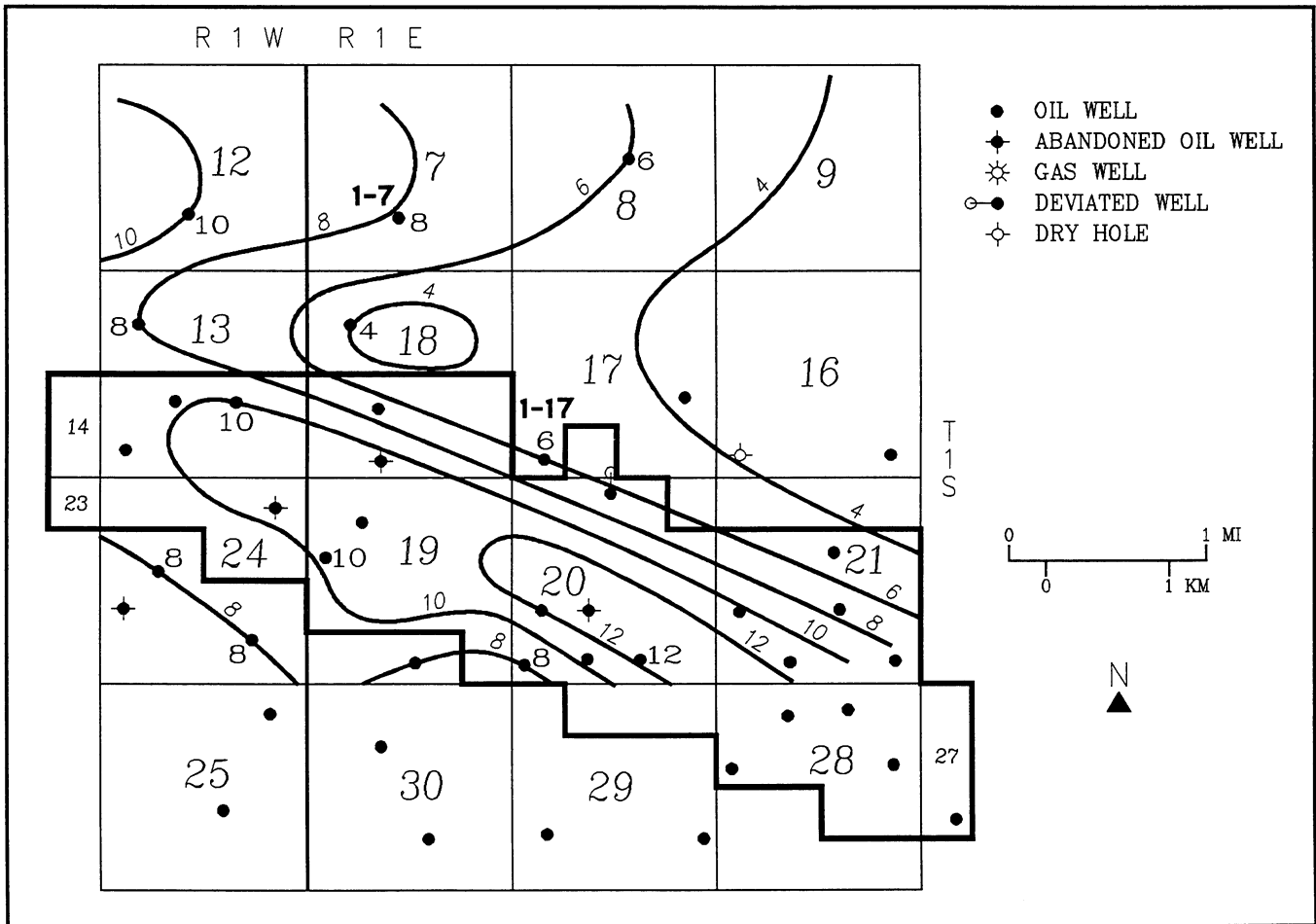


Figure 18. Thickness map of the QEL-5 bed. Contour interval is 2 feet.

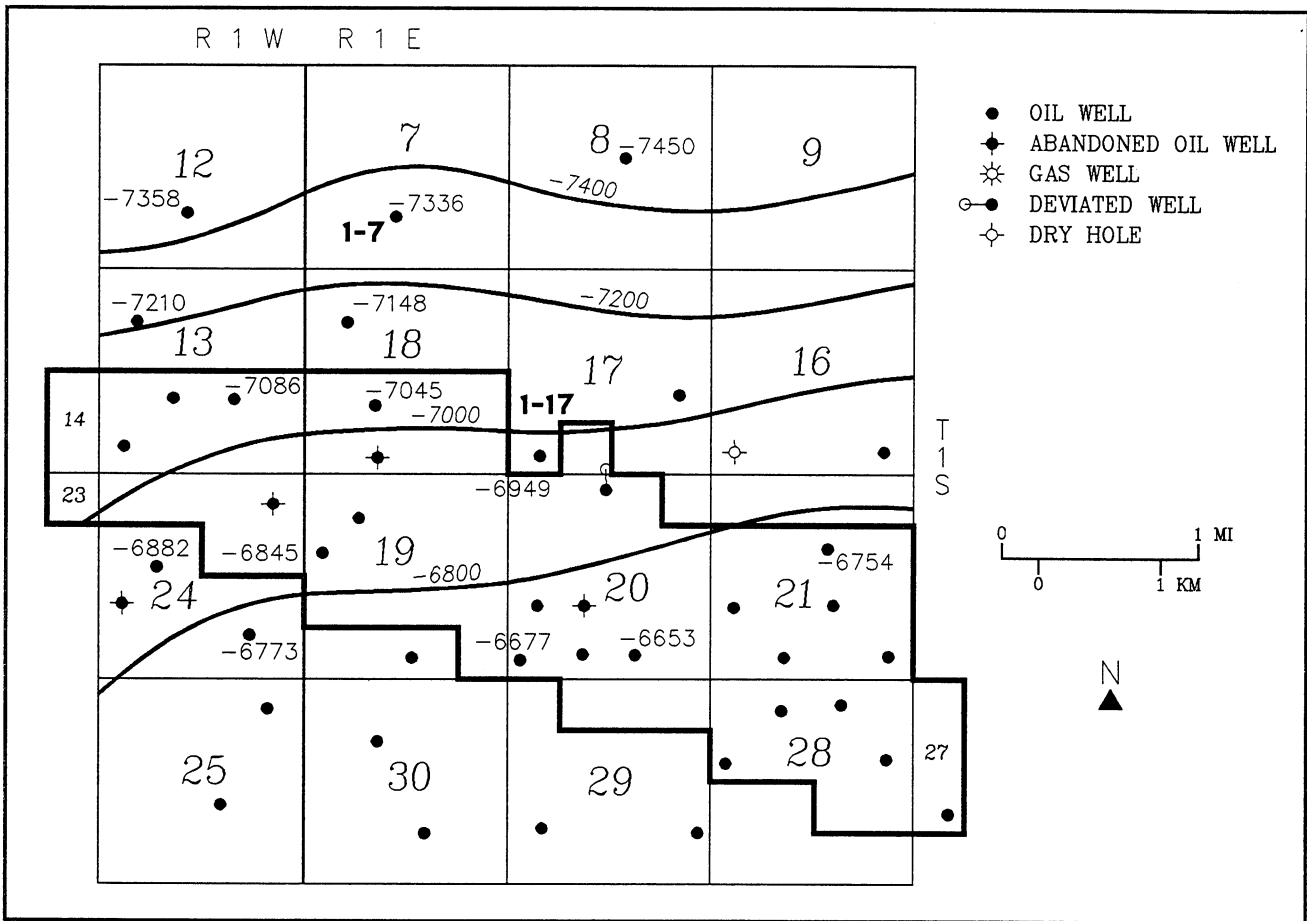


Figure 19. Structure contour map of the top of the QEL-1 bed. Contour interval is 200 feet.

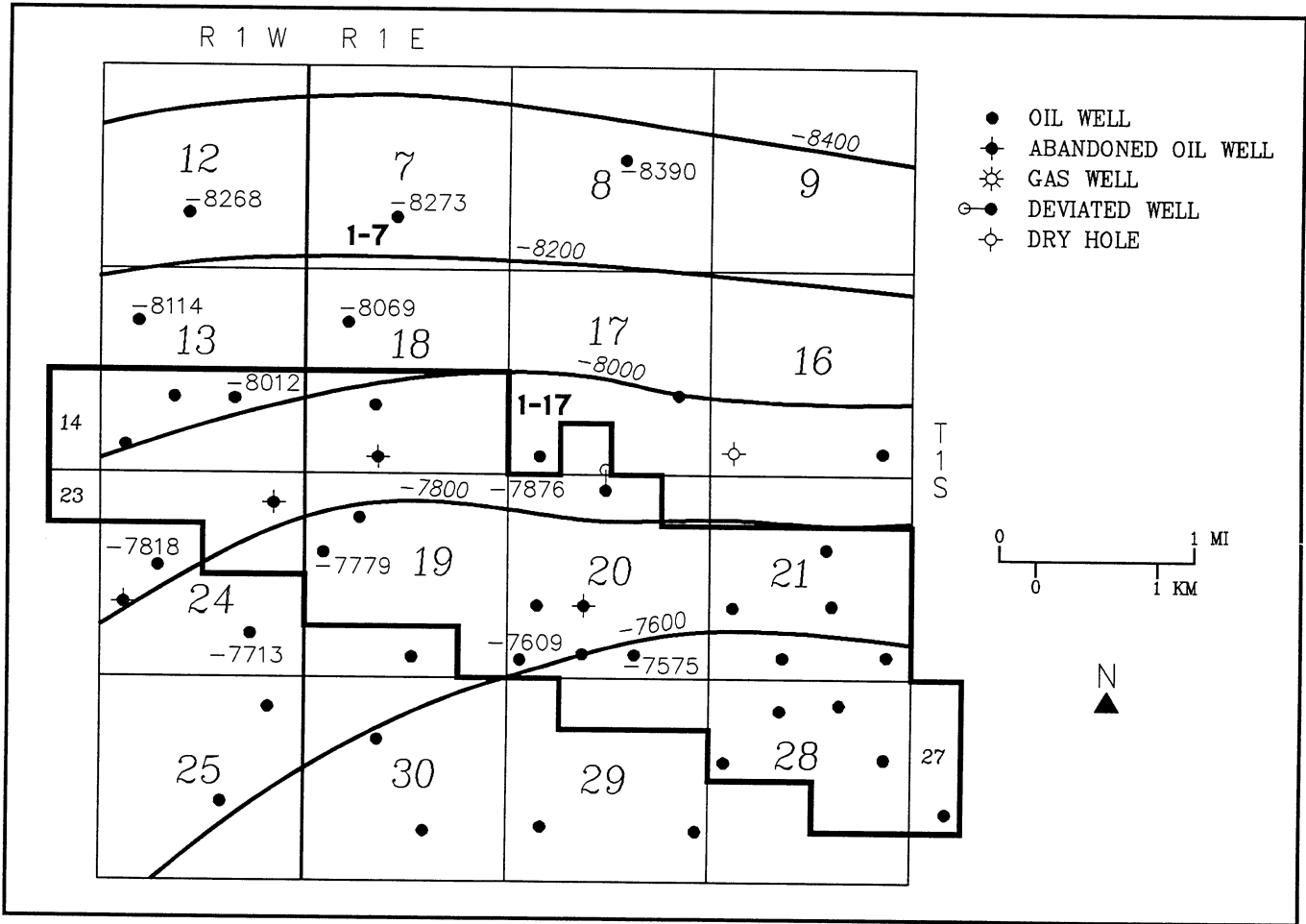


Figure 20. Structure contour map of the top of the QEL-3 bed. Contour interval is 200 feet.

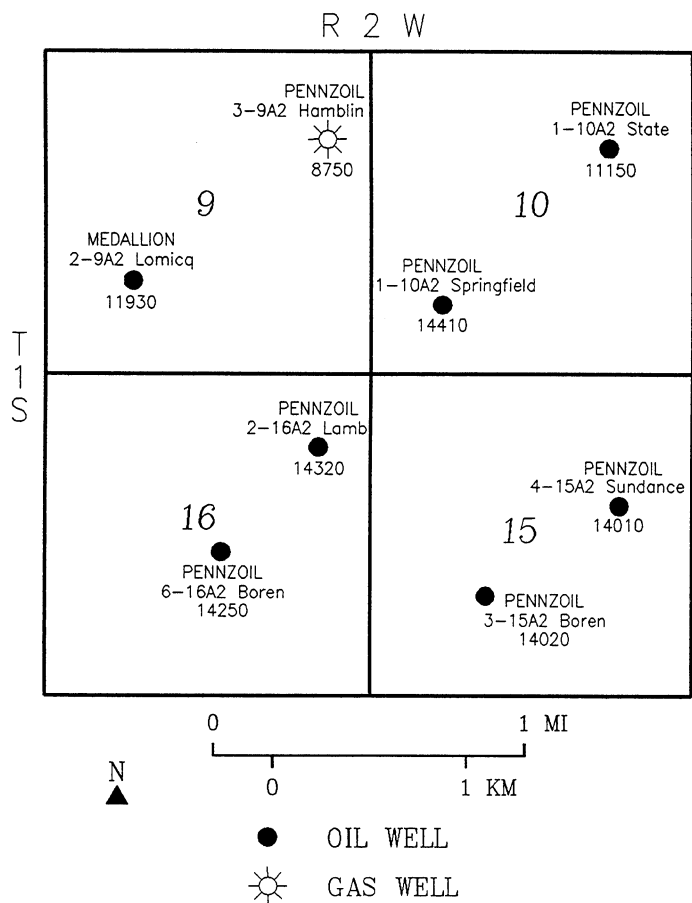


Figure 21. Well location map of the west study-site, sections 9, 10, 15, and 16, T. 1 S., R. 2 W., Bluebell field, Duchesne County, Utah.

2-9A2 Lamicoq
T1S R2W sec. 9

KB 5,921'
comp (11/70) 10,334' - 11,846' (gross) IP 401 BOPD
recomp (9/74) 13,535' - 14,854' (gross) IP 1,035 BOPD

1-10 A2 Springfield
T1S R2W sec. 10

KB 5,873'
comp (5/69) 10,370' - 10,516' (gross) IP 175 BOPD
recomp (8/72) 13,346' - 14,337' (gross) IP 1,191 BOPD

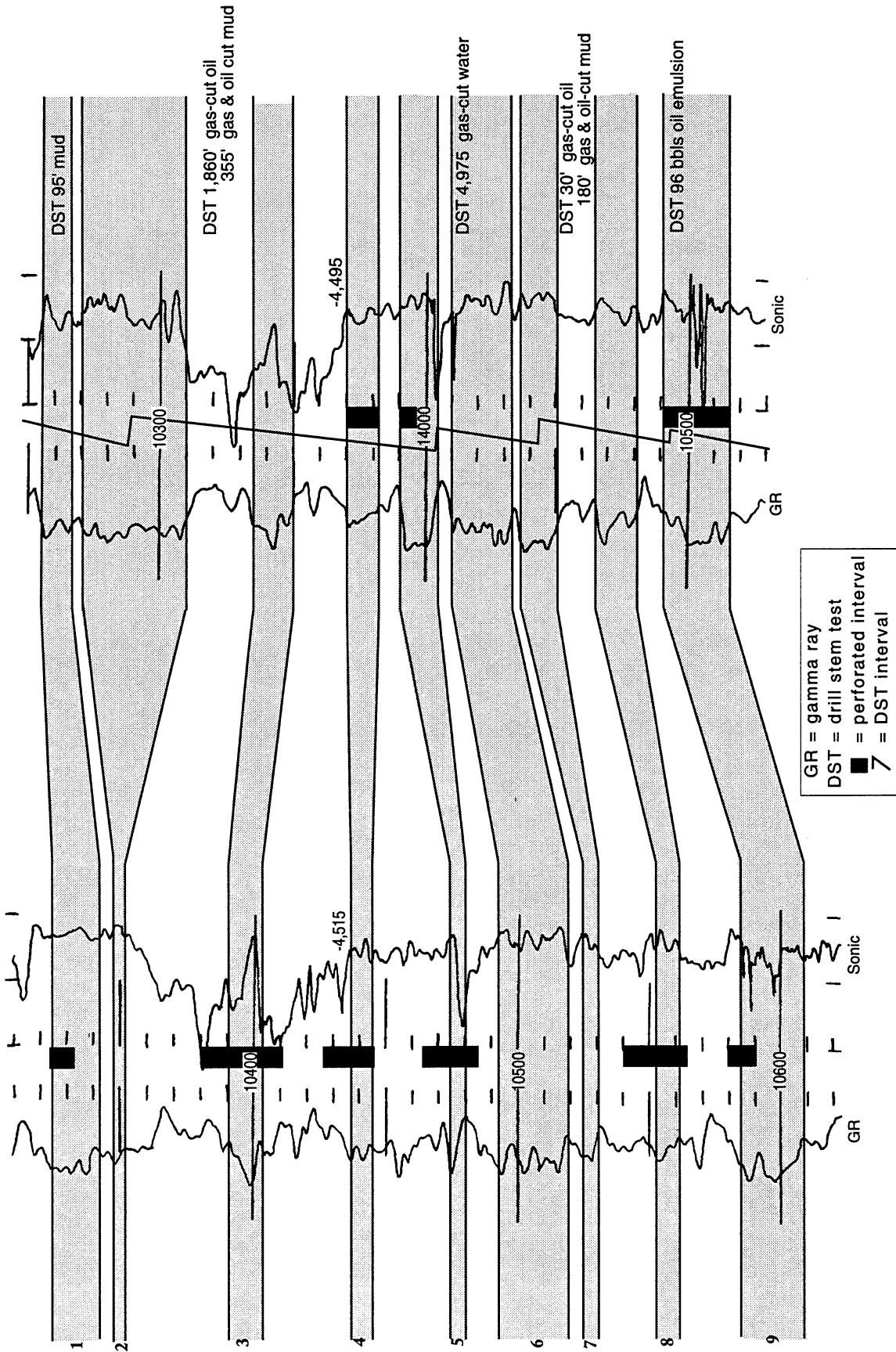


Figure 22. Cross section showing the oil productive beds in the lower Green River Formation, west study-site. Refer to figure 21 for location of wells.

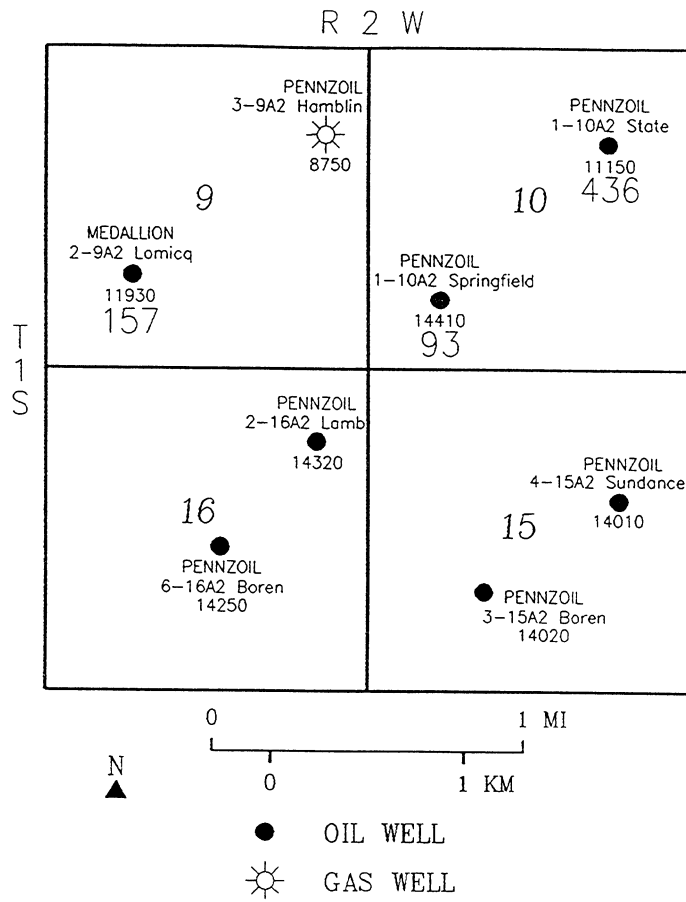


Figure 23. Cumulative oil production, in thousands of barrels, from the lower Green River Formation.

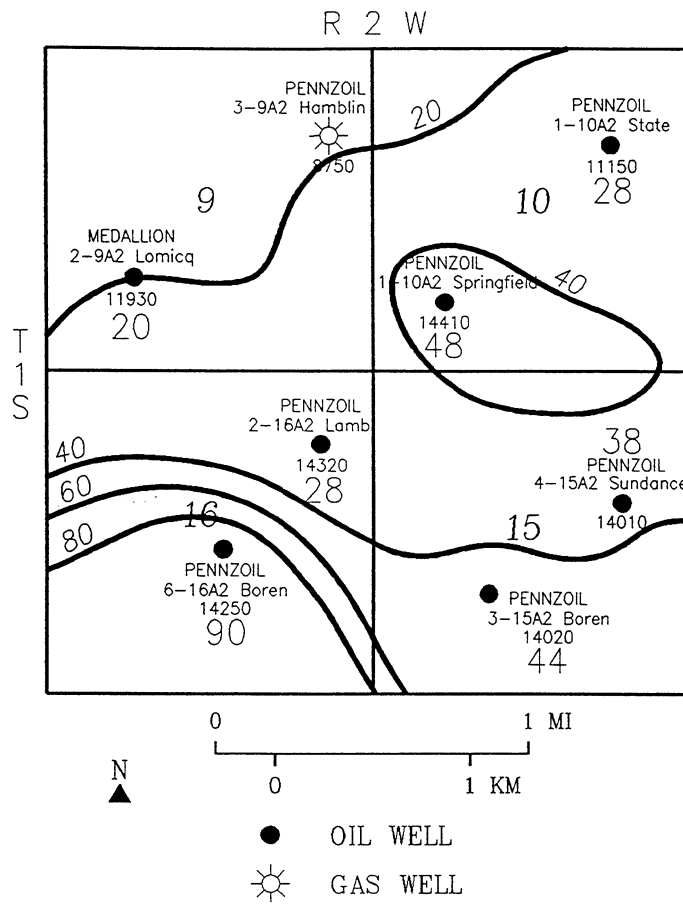


Figure 24. Total thickness of the nine oil productive beds in the lower Green River Formation. Contour interval is 20 feet.

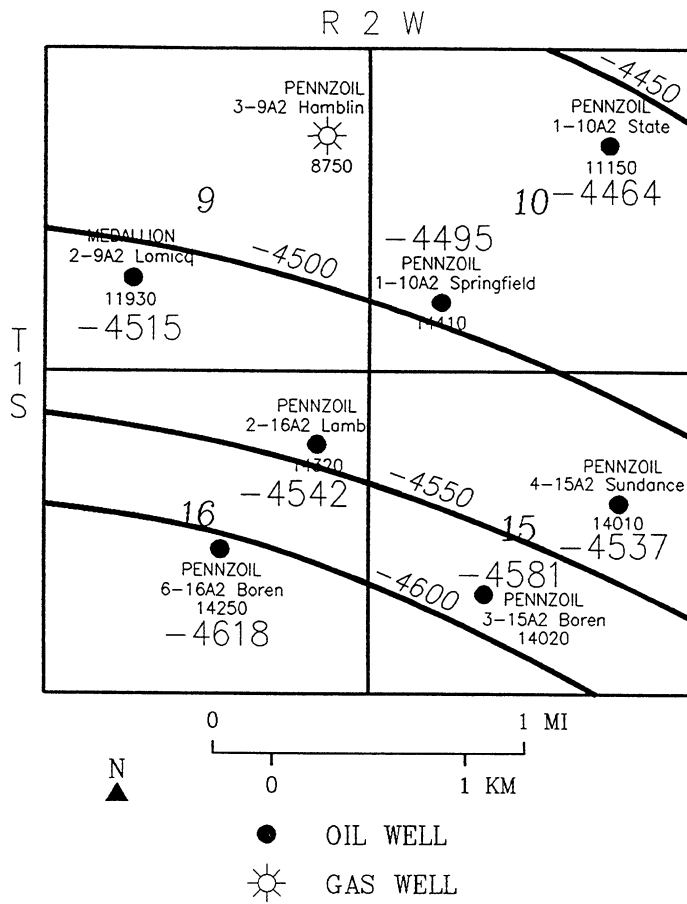


Figure 25. Structure contour map of the lower Green River Formation (bed 4). Contour interval is 50 feet.

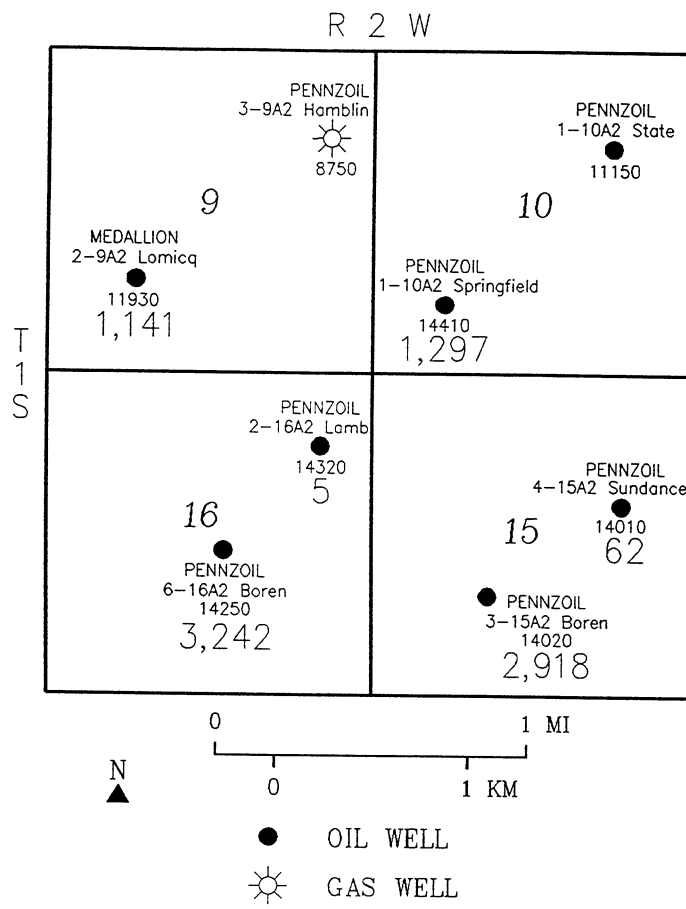


Figure 26. Cumulative oil production, in thousands of barrels, from the Wasatch Formation.

OUTCROP STRATIGRAPHY AND PETROPHYSICS

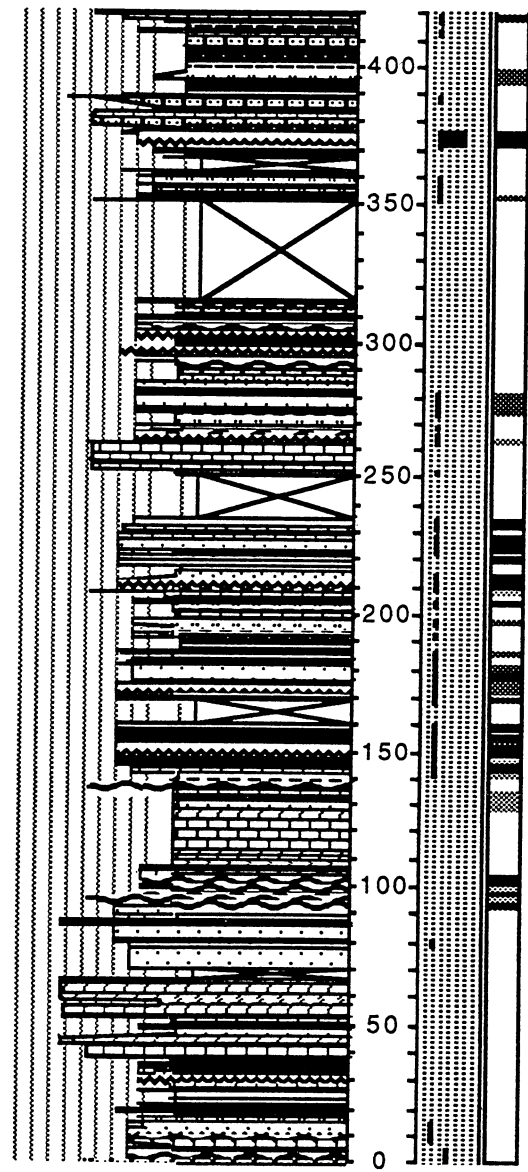
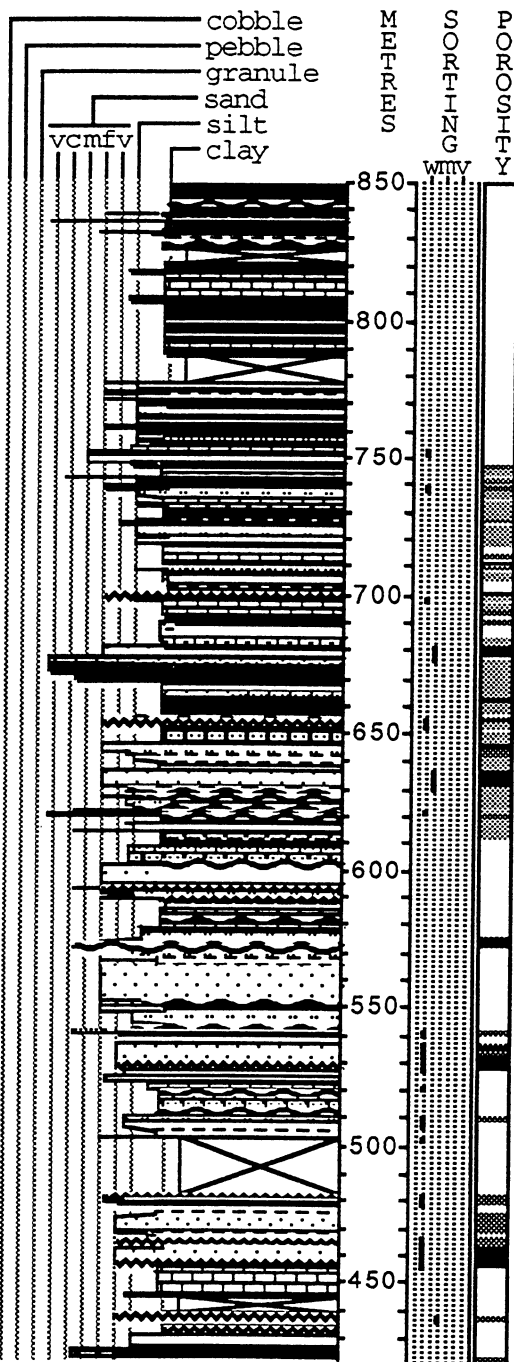
A 2,786-foot (849.2-m) section of the Green River/upper Wasatch transition (figure 27) was measured during the 1992 and 1993 summer field seasons from 1992 to 1993 by senior level undergraduate and graduate students under the direction of Thomas Morris and Ann Garner, Brigham Young University. The final total measured section will also include the upper part of the Flagstaff Limestone which was measured during the 1994 summer field season, and the Colton Formation (Wasatch equivalent) as measured by Smith (1986).

Inconsistencies in the lithologic naming were corrected after several outcrop samples were petrographically analyzed. The resulting lithologic classifications were then applied to all units that had the same properties as the analyzed samples. The section was recorded using commercial graphical software.

Petrology

Thirty-three thin sections were prepared from outcrop samples. Petrographic analyses of these samples is presented in Appendix A. The thin sections represent the volumetric majority of rock types in the measured section as well as a few less common but very interesting lithofacies. Sixteen of the thin sections were of sand-dominated clastic rocks and these were subjected to a 300 point count. The quartz fraction includes mono- and polycrystalline quartz as well as chert grains that could not be delineated as lithic fragments. Chert grains that could be identified as lithic fragments (they contained fossils, spicules, and so forth) were originally classified as such. Mica fragments were also included in the lithic count (table 1). Classification of the clastic rocks was from Carozzi (1993), which was modified from Dott, (1964). Carbonate rocks were classified according to Dunham (1962).

GRAIN SIZE



LITHOLOGY

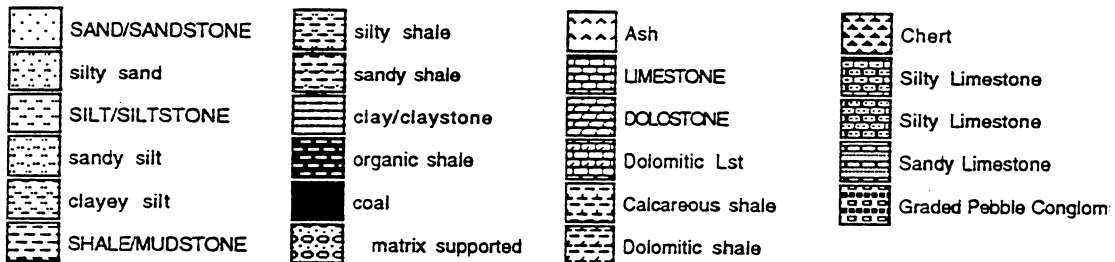


Figure 27. Green River Formation/upper Wasatch transition section measured along road cuts of highway 33, Willow Creek Canyon, Carbon and Uintah Counties Utah. Section begins in NW1/4SE1/4 section 23, T. 11 S., R. 8 W., Matts Summit 7 1/2' quadrangle, and ends in W1/2SE1/4 section 11, T. 7 S., R. 8 W., Jones Hole 7 1/2' quadrangle. Relative porosity is indicated by shaded bands in the porosity column with darker bands corresponding to higher porosity. Also, not all lithology indicators are present in this condensed section. However, they are all represented in the extended column (1" = 100 m). Larger scale section in the Appendix B for greater detail.

Table 1. Point counts of sand-dominated clastic samples from the Willow Creek Canyon section of the Green River Formation.

Sample Number	Quartz %	Feldspar %	Lithics %	Petrographic Classification
5-DN5	58.5	32.7	9.3	Feldspathic Wacke
140-EH85	63.6	34.8	1.6	Feldspathic Arenite
140-EH85A	63.2	36.4	0.4	Feldspathic Arenite
265-RP18	43.8	54.4	1.8	Feldspathic Wacke
282-RP35	55.8	37.8	6.4	Feldspathic Arenite
424-AA25	46.0	47.9	3.6	Feldspathic Arenite
608-RC2	44.2	49.6	3.6	Feldspathic Arenite
J3	47.0	38.6	14.4	Feldspathic Wacke
2nd J7	60.5	31.8	7.7	Feldspathic Arenite
4th J7 w/clasts	44.0	32.4	23.6	Feldspathic Arenite
11-10-12-1a	61.0	31.9	7.1	Feldspathic Arenite
11-10-12-2	54.2	31.1	14.7	Feldspathic Arenite
11-10-12-13a	45.1	48.3	6.6	Feldspathic Arenite
11-10-13-1b	43.0	41.1	16.0	Feldspathic Arenite
11-10-13-1c	49.3	23.9	17.2	Subfeldspathic Arenite
11-10-13-1f	45.2	43.9	10.8	Feldspathic Arenite

Porosity and Permeability

Core plugs were taken from every lithology that was petrologically analyzed. Permeabilities were analyzed using a pressure transducer in a Hassler sleeve. Porosities from the lab were compared to point count porosities. In general there was good agreement and where there is some disagreement an explanation is given in the petrologic description. It appears that arenite lithofacies have much greater interparticle porosity (figures 28 through 33). The plot in figure 28 of the porosity values of the arenites shows two distinct groupings; one being fairly open rocks and the other being relatively tight (very low porosity) rocks. Current research is being done to determine if the porosity differences between these groups is due to variations in general grain size, feldspar, and/or clay types, different encasing lithology, and perhaps unique diagenetic/burial histories.

This is important to the study because these arenites in general, are likely to have greater hydrocarbon storage capacity than do the carbonate rocks and it is vital to know which of the arenites make the best reservoirs. Porosity development in the deep subsurface of the Uinta Basin may be different from outcropping lithology. This will be investigated further during different phases of the project.

Clay Analysis

Clay analysis is being done on each of the samples that were analyzed for porosity and permeability. Initial results indicate that illite-smectite mixed layered clays and kaolinite are the most common clays found in the Green River Formation. Further analysis is being done to determine if other minor clays are present, what relative proportions each of the clays are found in the various lithology, and whether or not the presence of any given clay predisposes a rock to be tight (very low porosity) or not.

CORE DESCRIPTION AND PETROPHYSICS

Core from 10 wells in the Bluebell field, in or near the east and west study-sites, will be analyzed (table 2). To date, core from nine wells have been described and thin sections prepared and clay analysis is underway. Core descriptions include lithology, color, contact type, grain size and texture, sorting, relative porosity, sedimentary structures, bitumen staining, cement type, fossils, bioturbation (ichnofossils), qualitative fracture analysis (orientation, width, length, relative concentration, and any mineralization), and any anomalous or otherwise notable features. The core descriptions are being logged on commercial graphical software (figure 33).

Initial inspection indicates approximately 60 percent of the core consist of carbonates and 40 percent consist of clastics (predominantly sandstones). The carbonate rocks in general have good porosity and randomly oriented, interconnected fractures, whereas the fractures in the sandstones are more vertical and isolated. The sandstones, however, do have the best reservoir capacity due to inherent interparticle porosity. Preliminary analysis of clay types indicates swelling illite-smectite mixed layer clays as well as kaolinite in both the clastic and carbonate rocks. These swelling clay types have the potential to combine with the high pour point waxy oils to reduce production efficiency and total recovery.

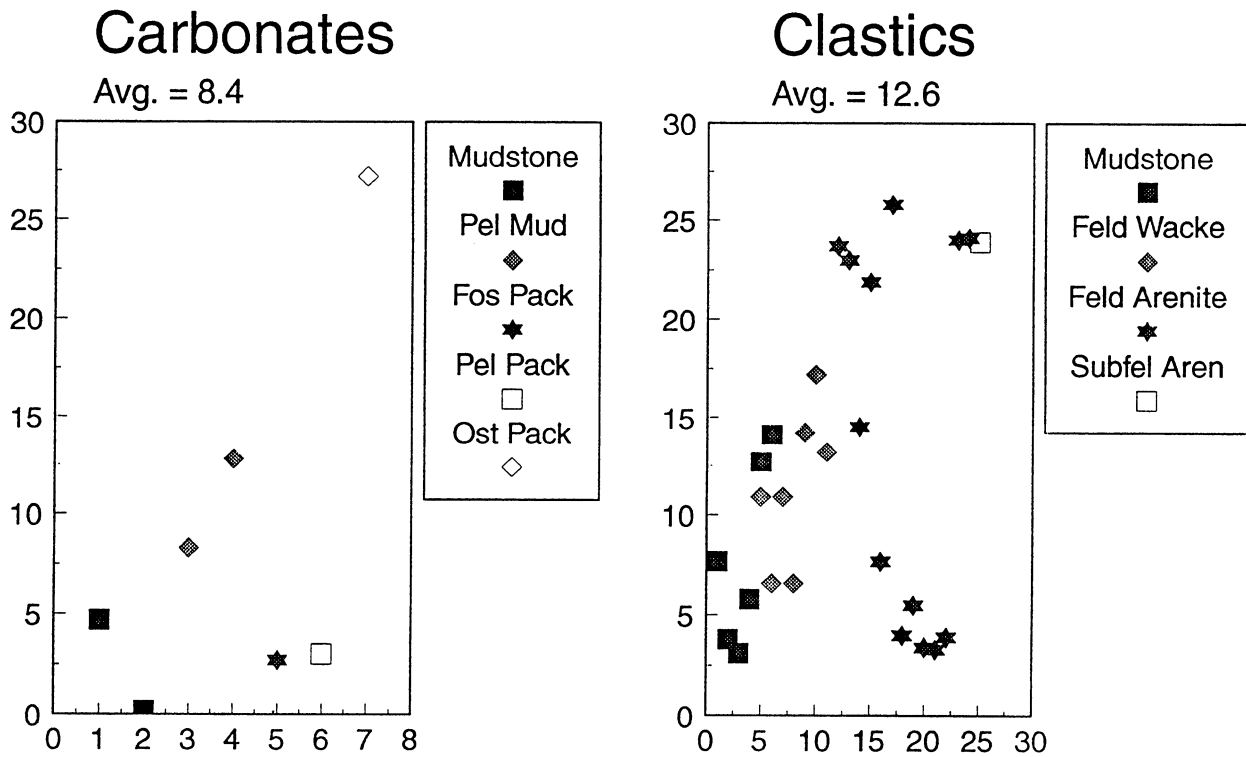


Figure 28. Core-plug porosity of carbonate and clastic outcrop samples. The vertical axis is percent porosity, the horizontal is the number of samples.

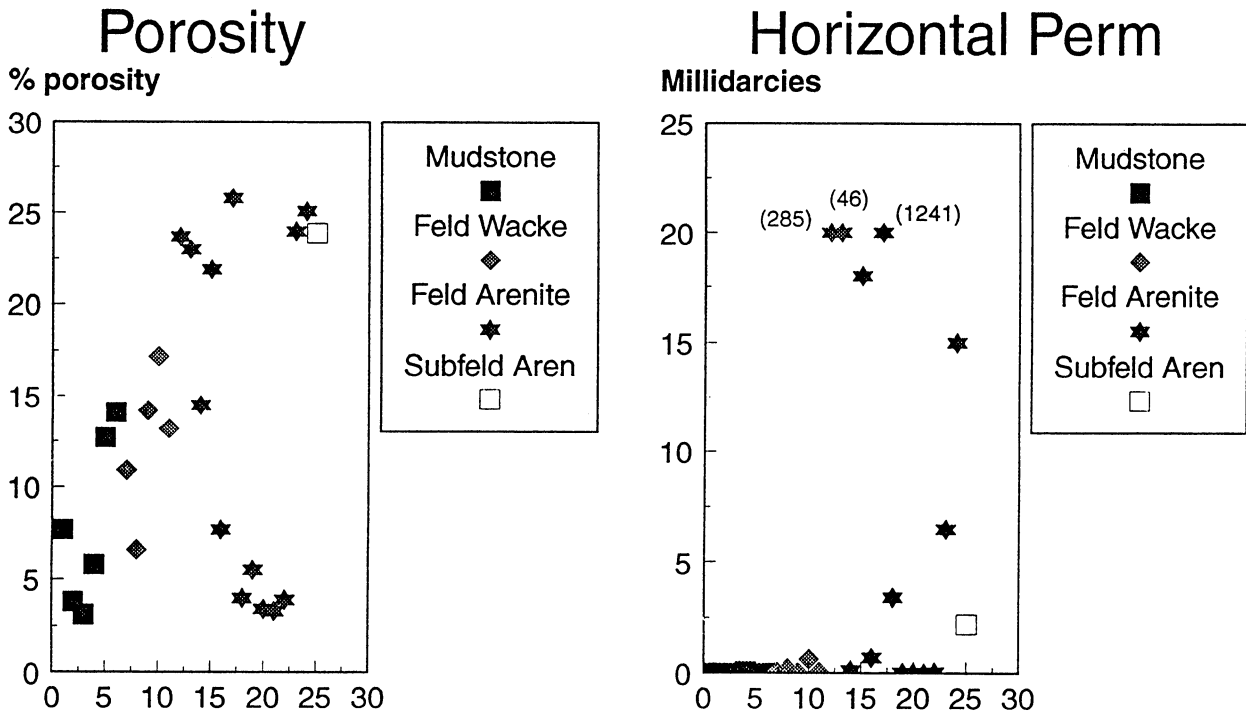


Figure 29. Porosity of clastic core-plug samples taken from the outcrop (the vertical axis is percent porosity, the horizontal is the number of samples) compared to the horizontal permeability (the vertical axis is millidarcies of permeability, the horizontal is the number of samples).

Hor Perm in md

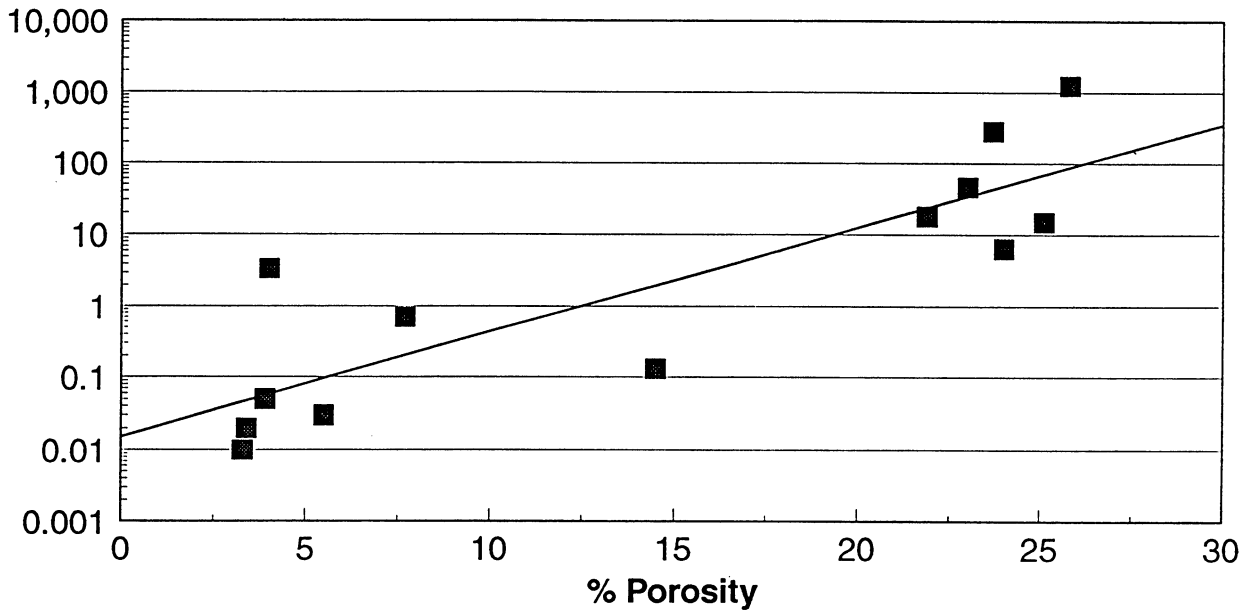


Figure 30. Porosity (percent) versus horizontal permeability (millidarcies) of core-plug samples classified as arenites.

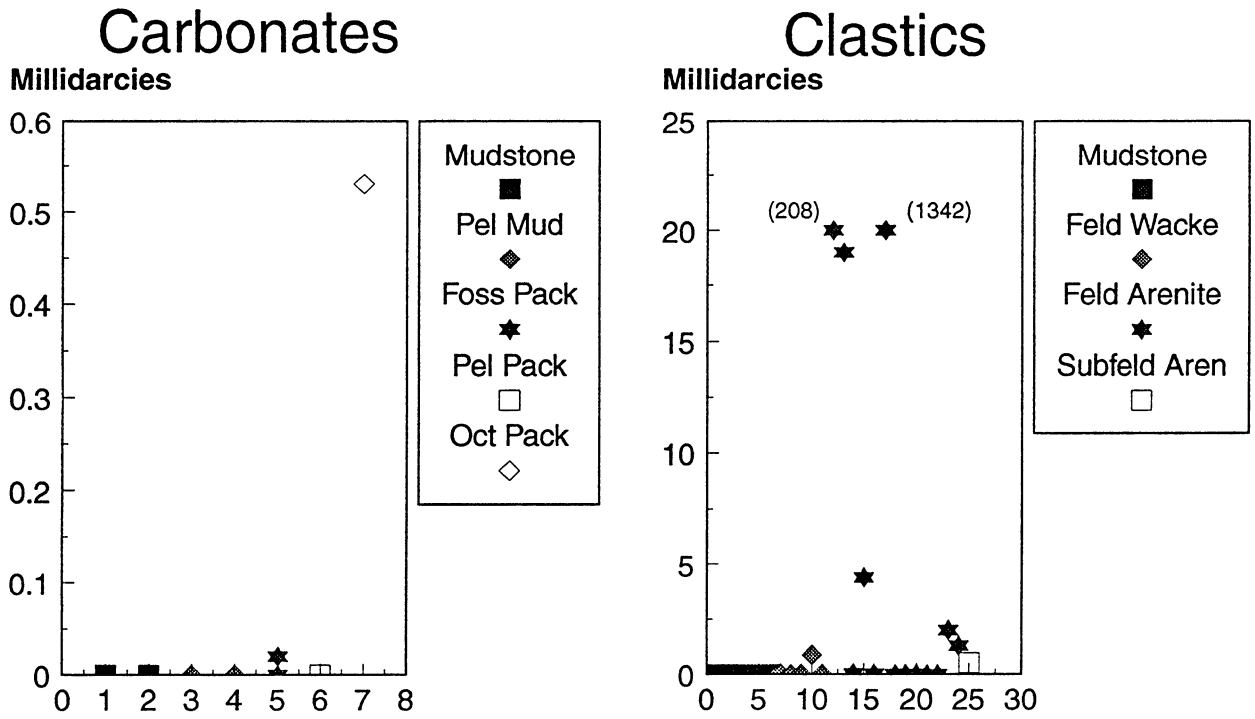


Figure 31. Vertical permeability of carbonate versus clastic core-plug samples taken from the outcrop. The vertical axes are millidarcies of permeability and percent porosity, the horizontal is the number of samples.

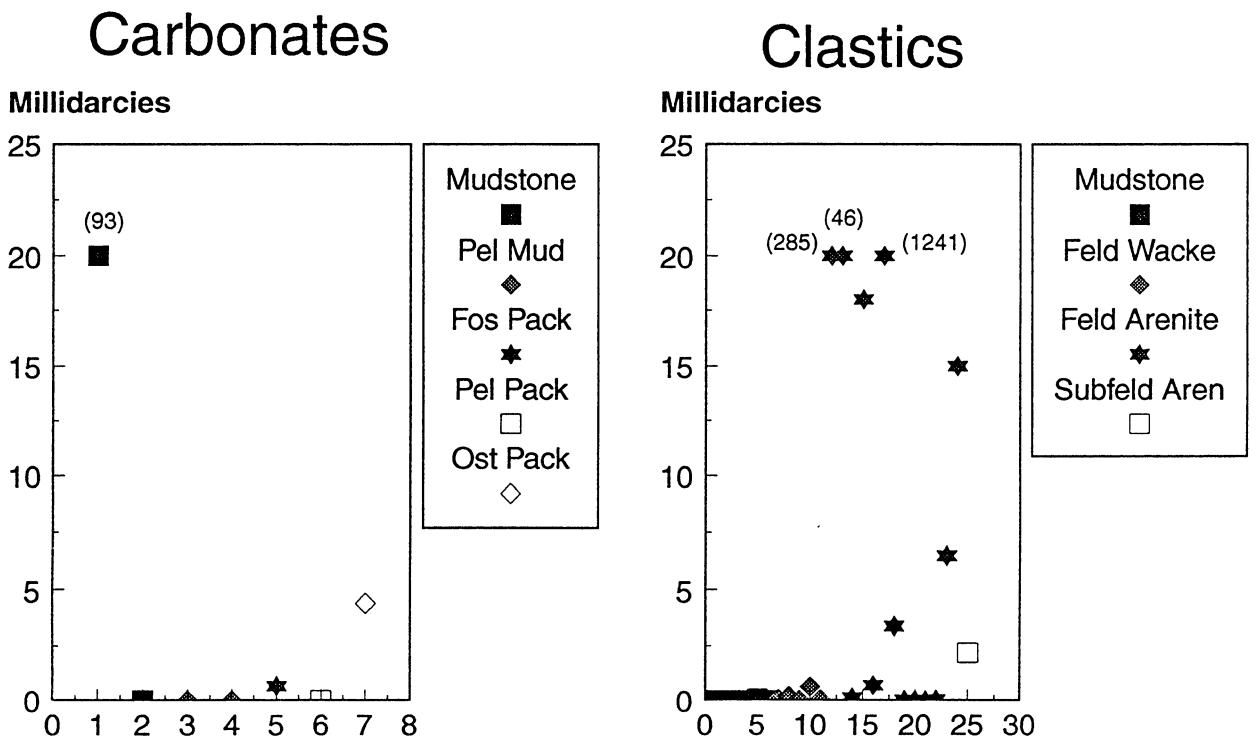


Figure 32. Horizontal permeability of carbonate compared to clastic core-plug samples taken from the outcrop. The vertical axes are millidarcies of permeability and percent porosity, the horizontal is the number of samples.

Table 2. Core from wells drilled in the Bluebell field that are being examined.

Well Number	Location	Min. Depth (ft)	Max. Depth (ft)
2-19A1E	SWSE 19, T1S R1E	9,160	9,720
2-22A1E	SWNE 22, T1S R1E	12,288	12,406
24-5	SENE 24, T1S R1W	12,180	12,238
3-17A2	NWSE 17, T1S R2W	13,580	13,692
1-12A2	SWSW 12, T1S R2W	10,480	10,630
1-7A1	NESW 7, T1S R1W	12,235	14,384
1-10A2	CSW 10, T1S R2W	11,105	11,158
1-18A1	CNE 18, T1S R1W	10,630	11,222
1-24A2	NESW 24, T1S R2W	12,135	12,193
9-4B1	SESW 4, T2S R1W	11,006	11,143
TOTAL 10 WELLS			TOTAL 1,635 FT OF CORE

Bow Valley Petroleum Ute 2-22A1E
22-T1S-R1E SWNE

Date logged: July 12, 1994

Logged by: MaryBeth Wegner

Ground: 0.00 ft KB: 0.00 ft

Remarks: The core is in poor condition, especially in the shaley units, therefore it is difficult to measure accurately. Core diameter is 2 1/2 inches.

LEGEND

LITHOLOGY

 SAND/SANDSTONE	 sandy shale	 LIMESTONE	 Silty Limestone
 SILT/SILTSTONE	 mud/mudstone		

CONTACTS

----- Uncertain

PHYSICAL STRUCTURES

 Ripple Lamination	 Flaser Bedding	 Microfault
 Horizontal fracture(s)	 Haphazard fractures	 Vertical fracture(s)
 Horizontal and vertical fractures		

LITHOLOGIC ACCESSORIES

 Calcareous	Py Pyrite	 Rip Up Clasts
--	-----------	---

ICHOFOSSILS

 Undifferentiated Bioturbation

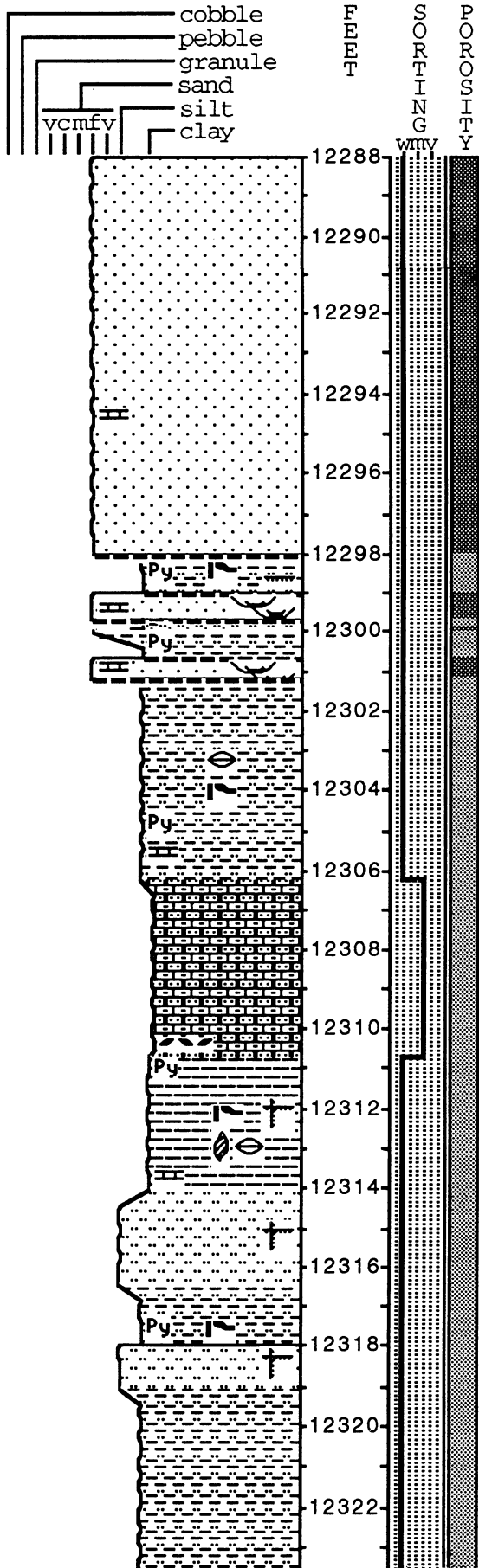
FOSSILS

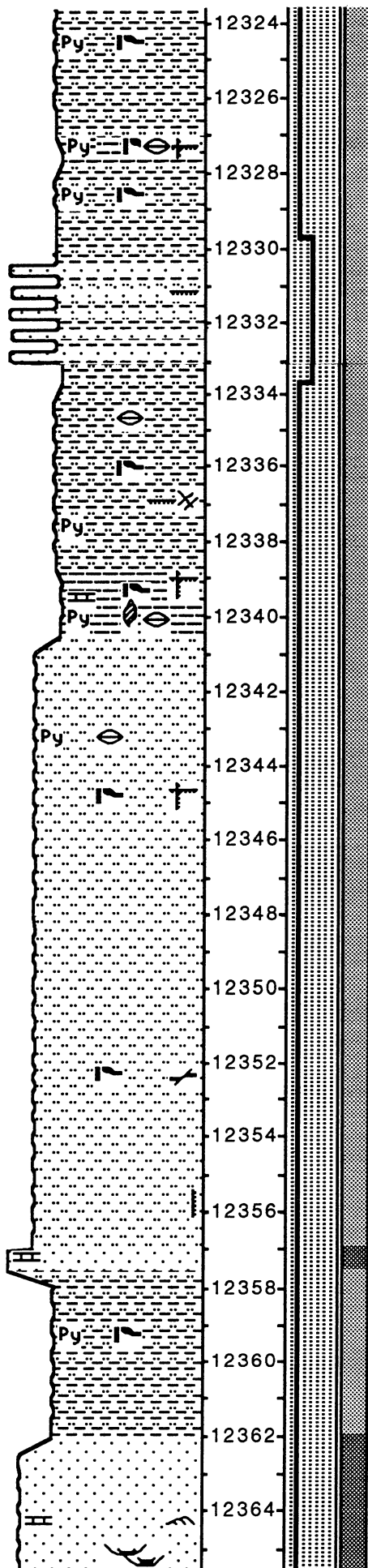
 Molluscs (undifferentiated)	 Gastropods
---	--

Figure 33. Description of the core taken in the Wasatch Formation from the 2-22A1E (section 22, T. 1 S., R. 1 E.) well.

GRAIN SIZE

- cobble
- pebble
- granule
- sand
- silt
- clay





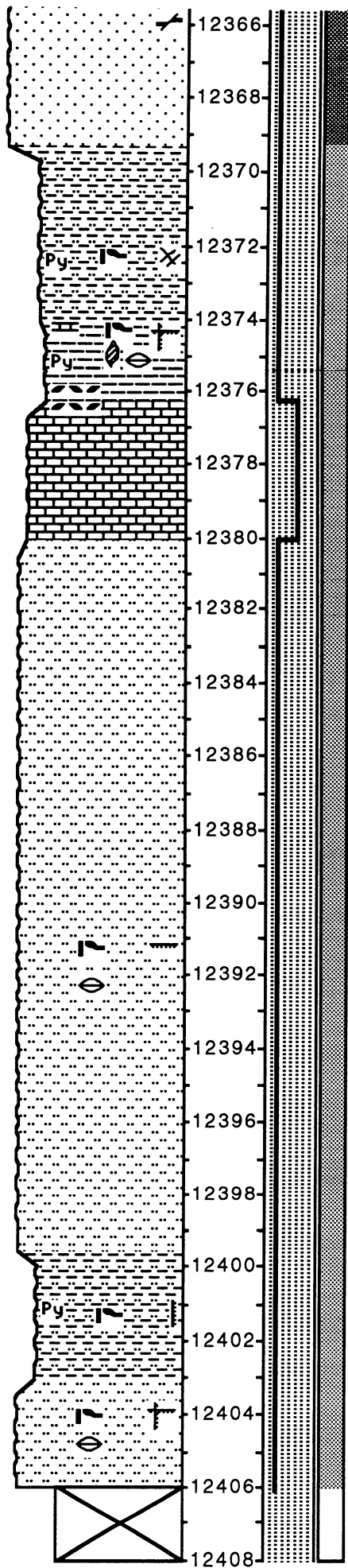
— Silty shale is like Unit 2, sandstone is similar to Unit 1. Each layer averages about 5 cm thick with undulatory contacts and some foundering.

— Fossils are mostly pyritized and up to 2.0 cm long (most are about 5.0 mm). They are concentrated in a zone about 4.5 cm thick at 12,334'.

— There is a major vertical fracture up to 3.0 mm wide and 30.5 cm long that is only about 5% calcite-filled.

— Top of Core 2; begins at 13,348'. This unit is very similar to unit 11, only it is slightly more fine-grained. There is a vertical fracture from 12,355' to 12,356' 10" up to 1.0 mm wide and 95% calcite-filled.

— Pyrite lenses up to 4.0 cm long and 3.0 mm wide at 12,360' 6".



More fine-grained than Unit 11. Occasional fossils. Appears to fine upward and the porosity is slightly better downcore where the grains are more coarse.

There is a vertical fracture up to 2.0 mm wide from about 12,402' to 12,406'. It is 95% calcite-filled and continues into Unit 30.

SURFACE FRACTURING PATTERNS

Bluebell Field Area

Surface fracturing patterns may provide clues to subsurface fracturing patterns in the Bluebell field, where oil and gas migration and production is often dependent upon fracturing. In addition, structures on fracture surfaces and relationships between fracture sets can provide important information leading to better understanding of timing and mode of fracture formation.

Surface outcrops in the Bluebell field are all in the Duchesne River Formation of Eocene-Oligocene age (Bryant, 1990; Hintze, 1988), which consists of sandstone, siltstone, claystone, and conglomerate deposited in fluvial, floodplain, and alluvial environments to the south of the Uinta uplift. Data were collected from 29 stations in or near the Bluebell field (figure 34). All data come from sandstone or pebble conglomerate beds and were collected on near-horizontal surfaces ($\pm 3^\circ$). Azimuth orientations were measured on vertical or near vertical fractures at each station. Approximately 75 to 100 orientations were collected at each locality. All stations show two major joint sets. These are shown in figure 34 with longer lines representing the sets with the most abundant measurements and the shorter lines representing the secondary set. In general, one fracture set tends to follow the regional structural trend (which bends) of the north margin of the Uinta Basin and the other set is nearly orthogonal to the first. This same pattern has been noted earlier by Narr (1977) in a broader study of fractures in the Uinta Basin.

The orientations of the older of the two fracture sets at each locality was determined by "T" intersections between fractures. The northwest oriented fractures predominate among the early formed fractures, but the data are certainly not uniform across the field. This may suggest that the two fracture sets formed at nearly the same time during the same fracturing event. Alternatively, the fractures may have formed during regional uplift which allowed simultaneous propagation of planes of weakness of microfractures which formed during entirely different fracturing events.

Fractures at the surface stations were not mineralized or filled, although some of them were stained with a black mineral or organic material. The fracture surfaces also did not preserve any features that could be used to determine direction or mode of fracture propagation.

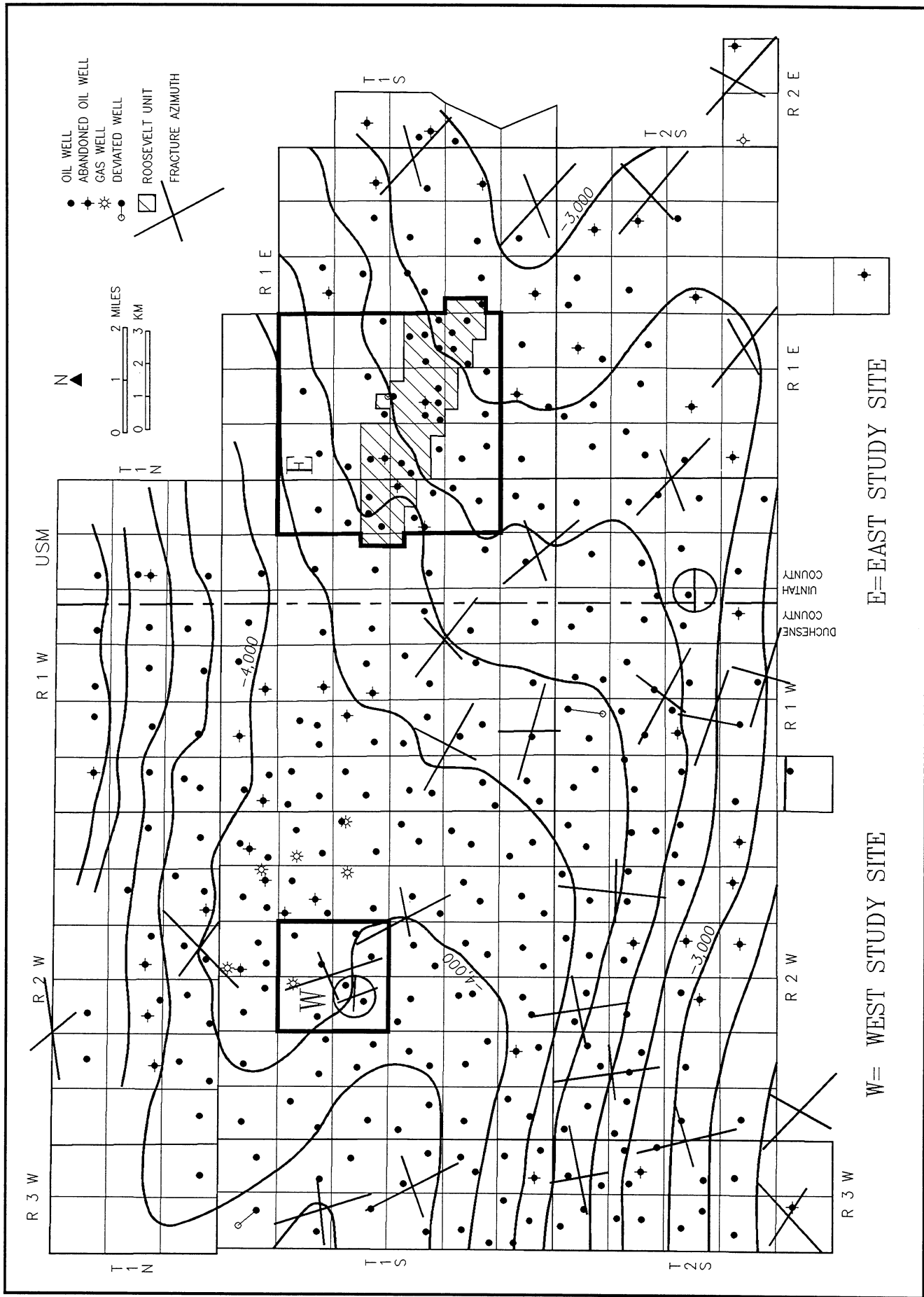


Figure 34. Structure contour map of the top of the middle marker, Green River Formation, Bluebell field, with azimuth orientations of surface fractures shown. Azimuth orientations enclosed in a circles are from subsurface borehole imaging logs run in the Green River and Wasatch productive intervals.

Indian Canyon Area

Good outcrops of the Green River Formation occur southwest of the town of Duchesne in Indian Canyon. Fracture orientations were measured and fracture surface features (plumose structure, hackle, arrest lines, and other features) were examined at eight localities spread along about 30 miles (48.3 km) of the Indian Canyon in the upper part of the Green River Formation. There are two fairly consistent sets (north-south and east-west) found at all the stations. At most of the stations in Indian Canyon, plumose structures were observed. In all cases the plumose structure was axially symmetric (see Pollard and Aydin, 1988, p. 1199) along the length of the joint, indicating that fracture propagation was horizontal and extensional rather than of shear origin. The principal horizontal stresses responsible for fracture origin were thus fracture parallel. We will now be able to compare present day in-situ stresses to fracture orientation to predict which fractures are open.

RESERVOIR DATA AND FLUID PROPERTIES

Reservoir simulation will be the tool for integrating all of the data generated during this project. Given a certain representation, reservoir simulation will help evaluate if production from the reservoir has been as expected. This in turn, will identify reservoir damage due to drilling or completion practices. If the geologic reservoir representation is reasonable, reservoir simulation could be used to identify zones with remaining oil production potential. Predictions from reservoir simulation are only as good as the data input to the simulator. Three essential elements of data required for reservoir simulator are:

1. Reservoir characteristics; depth, net pay, porosity, and so forth,
2. Oil and gas fluid properties; compositions, initial gas-oil ratios, bubble points, oil formation volume factors, solution gas-oil ratios, and so forth,
3. Porous media properties; permeabilities, relative permeabilities, and so forth.

Reservoir Data

The reservoir data for the Bluebell field are scattered. The task of constructing reservoir models is made even more difficult because the production is from multiple beds over large vertical intervals. The production data indicate extensively fractured reservoirs but fracture information on the field is practically nonexistent. The available data could be categorized broadly into: (1) reservoir characterization and geologic data (2) production data.

Reservoir Characterization and Geologic Data

Reservoir and geologic data was compiled from the following sources:

1. DST data on a number of wells in the Uinta Basin. This set contains one well from the Bluebell field. The data bank consists of data on permeability, extrapolated fluid pressure, net pay, average viscosity, temperature, and transmissibilities. DSTs of 16 wells from the Uinta Basin are reported.
2. Perforation information on the wells for which production information was also available.
3. Well completion logs on a number of wells from the field. These logs are essentially available on request to the respective operators.
4. Stratigraphic cross sections.
5. Correlations between Michelle Ute, Malnar Pike, Chasel Sprouse, 1-8 A1E, and Roosevelt Unit C-11 on the east side of the field and between State 3-10C, Lamicq 2-9C, Springfield 2-10C, Sundance 4-15A2, Lamb 2-16A2, Boren 3-15A2, and Boren 6-16A2 on the west side of the field, compiled by Utah Geological Survey (UGS). This information is based on gamma-ray, sonic, density, and resistivity logs. The data include pay-zone thicknesses and cross-plot porosities for a number of zones in the above wells.

Production Information

Monthly oil, gas, and water production data for the following wells are available on request from operators in the field or from the Utah Division of Oil, Gas and Mining.

East side of the Bluebell Field, the wells are (figures 1 and 11):

1. Michelle Ute,
2. Malnar Pike,
3. Chasel Sprouse,
4. 1-8 A1E,
5. Roosevelt Unit C-11 (RUC-11).

West side of the Bluebell Field, the wells are (figures 1 and 21):

1. State 3-10C (1-10A2 State),

2. Lamicq 2-9C (2-9A2 Lamicq),
3. Springfield 2-10C (1-10A2 Springfield).

These wells were selected in order to focus on the part of the Bluebell field where the Michelle Ute and Malnar Pike wells are and then expand the reservoir description and modeling to other parts of the field. The Michelle Ute and Malnar Pike are the proposed demonstration wells for the project. The west side was chosen because of the high-quality well data that is availability.

The cumulative gas-oil ratio (GOR) for most of the wells from the Bluebell field are close to their initial producing GOR values. The initial, cumulative (as of December 31, 1991) and peak GOR values for Michelle Ute were 859 standard cubic feet per stock tank barrel (SCF/STB), 943 SCF/STB and about 2,000 SCF/STB respectively. The Malnar Pike went on production with an initial GOR of 1,111 SCF/STB. The cumulative GOR for the well as of December 31, 1991, was 866 SCF/STB while the peak GOR was about 2,000 SCF/STB. The initial GOR for Chasel Sprouse was 740 SCF/STB. Chasel Sprouse had produced at a cumulative GOR of 903 SCF/STB (as of December 31, 1991) with a peak GOR of about 3,000 SCF/STB. The Roosevelt Unit C-11 (RU C-11) well had an initial GOR of 1,560 SCF/STB and a cumulative GOR of 2,258 SCF/STB (as of June 1993). The production from this well showed peak GOR values of about 4,000 SCF/STB. Thus the production history of RU C-11 differed significantly from the history of other wells in its vicinity. RU C-11 could be producing from zones significantly different from the producing zones of the other wells. The initial GOR for well 1-8A1E was 300 SCF/STB. After going through peak values of about 800 SCF/STB, the cumulative GOR for the well was only 500 SCF/STB. Thus, the production history of well 1-8A1E is also different from wells in its vicinity. This well could be producing from shallower zones or from partially depleted zones. In summary, the Michelle Ute, the Malnar Pike, and the Chasel Sprouse showed GOR behavior that is consistent with the reservoir oil/gas thermodynamic properties. The RU C-11 was gassier than expected, while 1-8A1E had lower than expected GORs.

The wells operated by Pennzoil Exploration and Development Company (Pennzoil) were first produced from the lower Green River, and then from the deeper Wasatch. During production from the lower Green River the trends in GOR were as follows: State 3-10C went on production with an initial GOR of 400 SCF/STB, the peak GOR was 68,400 SCF/STB and cumulative GOR was 875 SCF/STB (as of December 31, 1984). The initial, cumulative (May 31, 1974) and peak GOR values for Lamicq 2-9C were 324 SCF/STB, 365 SCF/STB and 3,630 SCF/STB respectively. Springfield 2-10C had an initial GOR of 300 SCF/STB, cumulative GOR of 356 SCF/STB and peak production GOR of 630 SCF/STB. The relevant GOR values for the wells in the Bluebell field are summarized in table 3.

Table 3. Compilation of gas-oil ratios (GOR) for a few selected wells.

Well	Initial GOR (SCF/STB)	Peak GOR (SCF/STB)	Cumulative GOR (SCF/STB)
Michelle Ute	859	2000	943
Malnar Pike	1111	2000	866
Chasel Sprouse	740	3000	903
RU C-11	1560	4000	2258
1-8A1E	300	800	500
State 3-10C	400	68,400	875
Lamicq 2-9C	324	3630	365
Springfield 2-10C	300	630	356

The overall GOR trends in all the wells suggest gas segregation and preferential oil production as is observed in classic naturally fractured reservoirs. A decline curve analysis was performed on Michelle Ute and Malnar Pike wells to evaluate remaining production potential.

Decline Curve Analysis

Decline curve analysis is a technique used to project the oil production from a particular well using available oil production data. The data is plotted as a log of average daily production rate versus time. A straight line is used to fit the data. The equation describing the straight line is used to calculate the average daily production rate for future production from the well, and thus the ultimate oil recovery. The monthly production data for the Michelle Ute and Malnar Pike wells were used for the analyses. Semi-log plots of average daily production rate versus time are shown in the figures 35 and 36. Straight line equations obtained from field data were used to project future production. Cumulative oil production projections for the two wells are shown in figures 37 and 38. Reasonable cumulative oil production estimates using decline curve analyses were difficult as the daily production rates for both the wells had already reached the economic limit of 20 STB/day (3.2 m³). Nevertheless, application of the technique establishes that Malnar Pike would produce 123 MSTB (19,600 m³), while Michelle Ute would produce 156 MSTB (24,800 m³) of oil over 20 years of production.

Reservoir Geologic Information

The Bluebell well in the DST data bank is 1-16 Gulf Ute located in section 16, T. 2 S., R. 2 W. The DST midpoint depth was 9,240 feet (2818.2 m), the net pay

was 50 feet (15.3 m), the reservoir temperature was 156° F (68.9° C). The extrapolated fluid pressure through the DST test was about 3,950 psi (27,235 KPa). The average oil viscosity was 0.6 centipoise and the flow was 144 STB/day (22.9 m³). The formation permeability as determined from the test was about 0.2 millidarcies (md). These data illustrate that the production is from low-permeability fractured formation.

The perforation information on the wells reveals that the wells have been completed in multiple zones. Each well has been perforated in 10 zones or more. The multiple zone completion makes reservoir history matching difficult because without further testing, it is impossible to determine the zones most responsible for production.

Michelle Ute had a total of 69 zones open over a vertical interval of about 4,500 feet (1370 m), while Malnar Pike had 50 zones open over a vertical interval of about 5,000 feet (1,530 m). A reserve analysis was performed to determine original oil-in-place (OOIP) using this data. The analysis revealed that even with conservative areal extent (40 acres [16.2 ha]), these zones contain significant amounts of oil. Michelle Ute had 3.8 MMSTB (604,200 m³) of oil, while Malnar Pike had 6.7 MMSTB

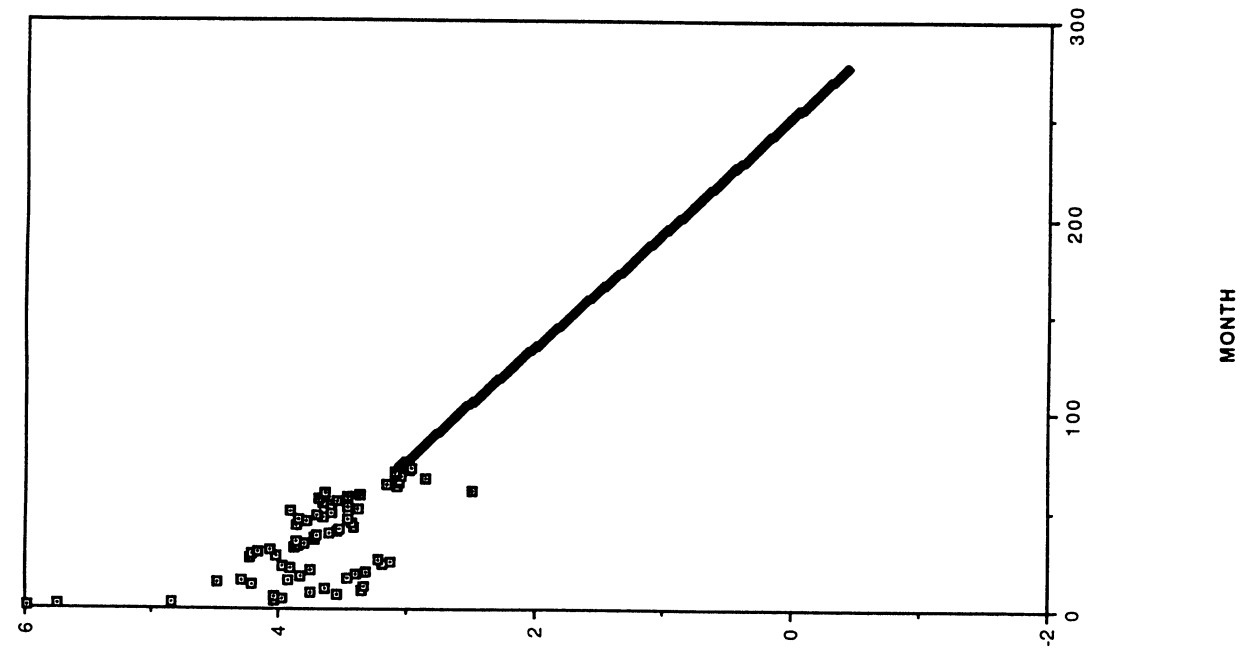


Figure 36. Decline curve analysis of the Malnar Pike well.

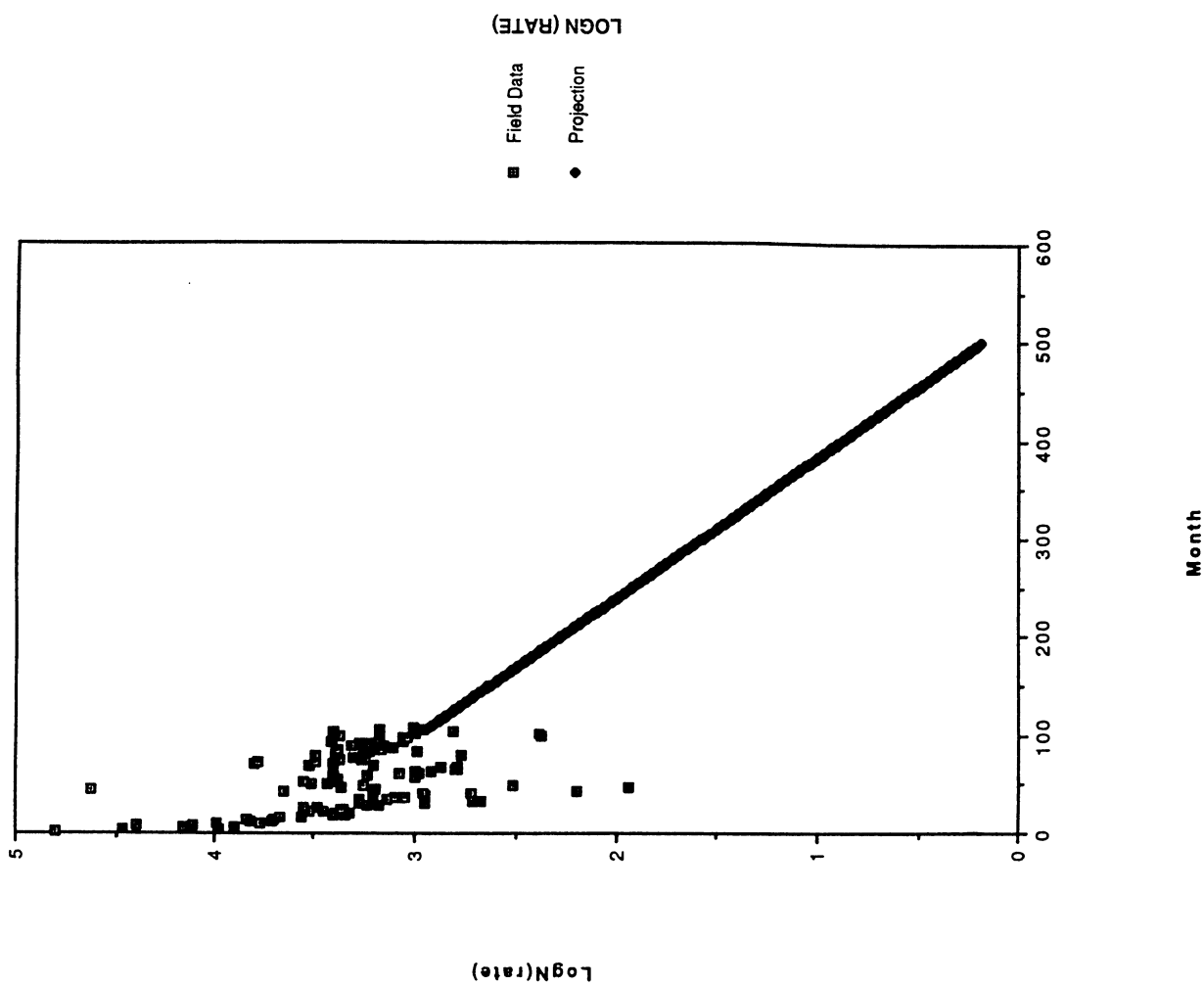


Figure 35. Decline curve analysis of the Michelle Ute well.

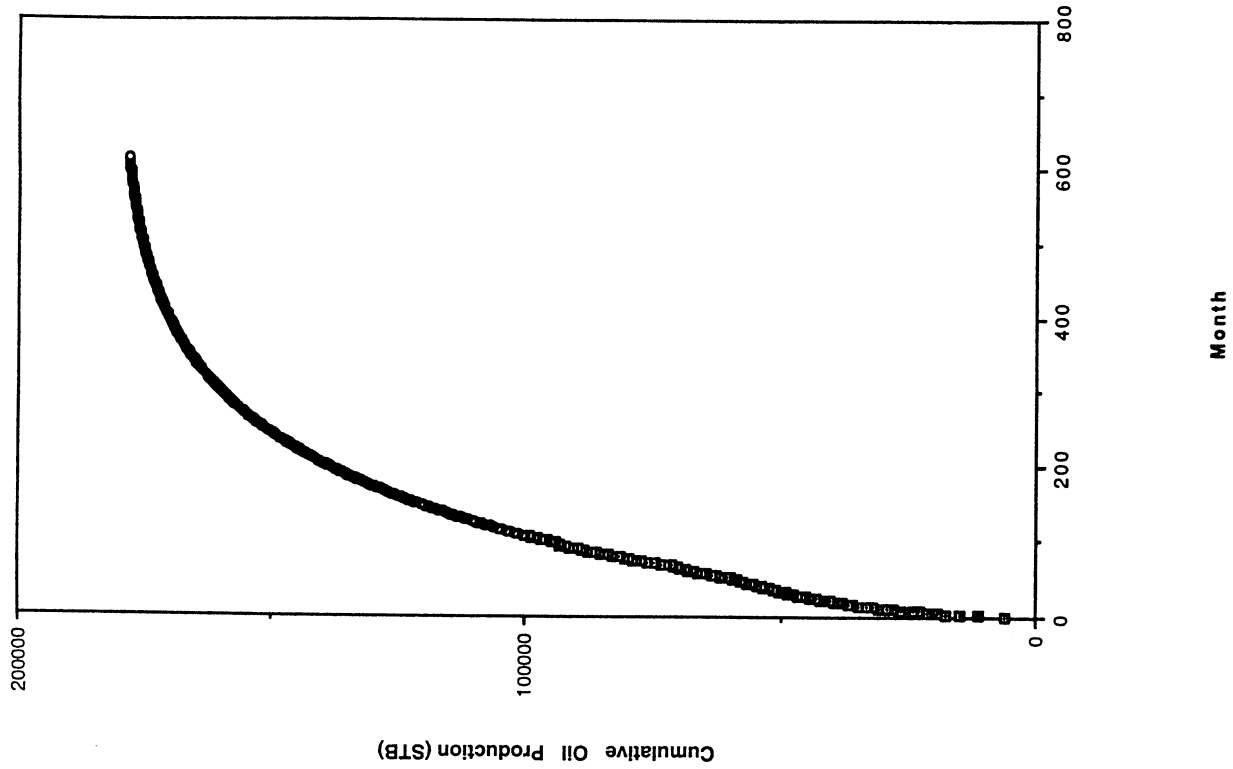


Figure 37. Cumulative oil production and projection for the Michelle Ute well.

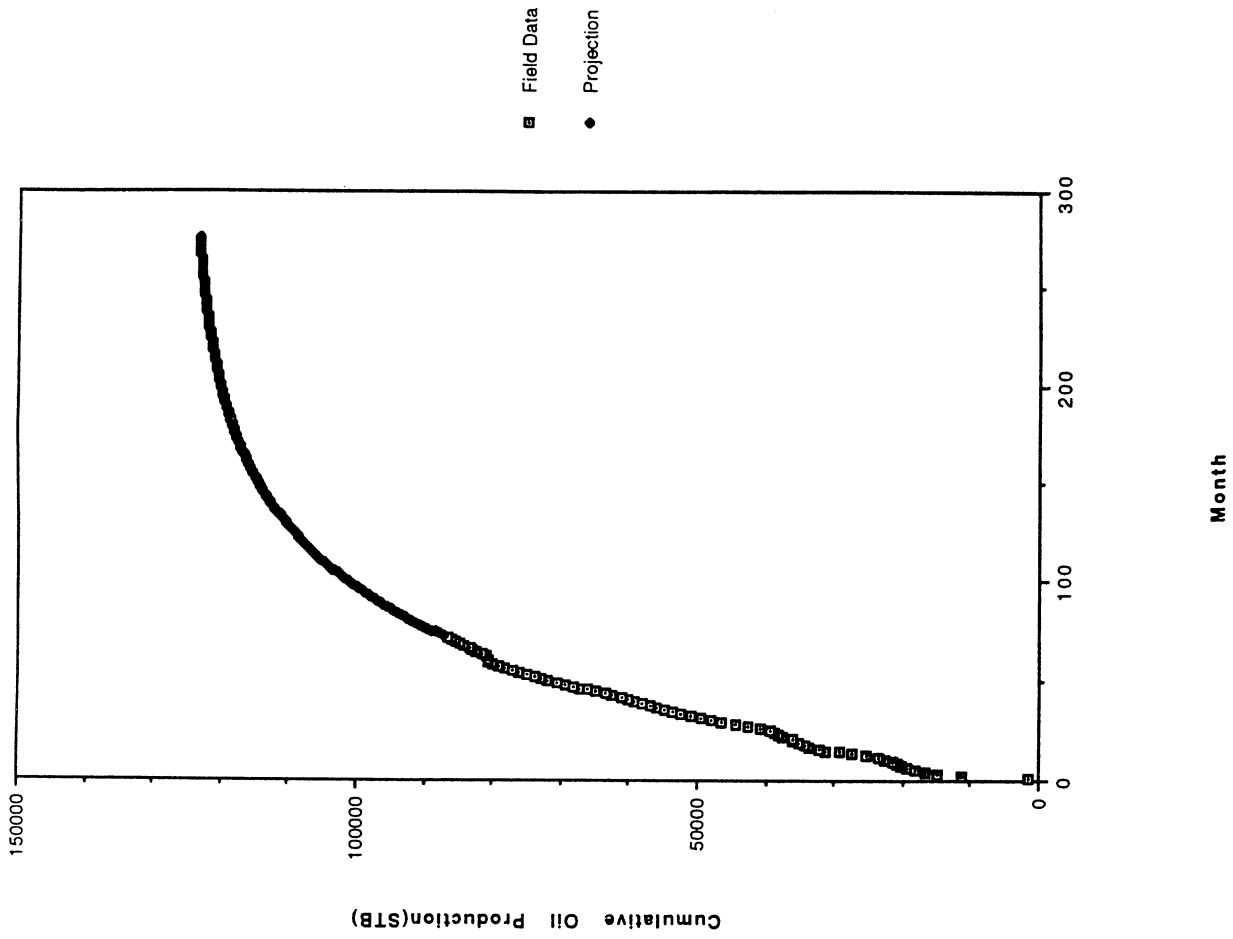


Figure 38. Cumulative oil production and projection for the Malnar Pike well.

(1,065,300 m³). Distributions of this oil in different zones is shown in figures 39 and 40. Cumulative production from Michelle Ute and Malnar Pike has been 99,000 STB (15,700 m³) and 88,000 STB (13,900 m³) respectively, which is less than 3 percent of OOIP for both the wells. These simple volumetric calculations indicate that there is substantial oil production potential for these two wells. Thickness and porosity were determined at 2-foot (0.6-m) resolution for five zones in the lower transition from the five wells listed under production on the east side. Bed correlations were established between these five wells. This geologic reservoir characterization was used in constructing a five-well reservoir model. Similar information was provided for the seven wells on the west side of the Bluebell field. Bed correlations were available for nine zones in that area. The west side reservoir, model discussed later, was constructed using this information. Data on porosities and permeabilities of outcrop and well-core samples are also being gathered and will be integrated into reservoir models later in the project.

Reservoir Fluid Properties

The data available on the fluid properties can be divided into the following categories:

1. Water analysis reports from wells in the Bluebell field,
2. Crude oil characterization report compiled by the U.S. Bureau of Mines Laboratory in Laramie, Wyoming,
3. Data on the pour points, API gravity, and viscosity of the oils from the Green River Formation,
4. Gas chromatography analysis, viscosity, and pour points of oils from the John 2-7B2 and Leslie Taylor 24-5 wells, operated by Quinex Energy Corporation (Quinex),
5. Differential liberation data on four wells operated by Pennzoil.

The water analyses data were for the Deep Creek, Red Cap, Jodie 3-36A3, Malnar Pike, Emerson, and Allred wells. Most of the produced waters appeared to have an alkaline pH of between 7.8 and 8.5. With the exception of two samples, the dissolved solid concentrations were between 5,000 to 8,000 mg/l. The samples from Deep Creek and Allred wells had dissolved solids concentrations of about 15,000 mg/l. The implications of these water analyses on reservoir clay stability or possible mineral precipitation in the reservoir will be assessed later in the project.

The U.S. Bureau of Mines oil analysis was for a well located in NW1/4NW1/4, section 11, T. 1 S., R. 2 W. The sample was collected from the interval 10,359 to 10,517 feet (3,159.5-3,207.7 m). The oil API gravity was 31.5, pour point was 90^o F (32.2^o C). Detailed distillation cuts from 122^o F to 572^o F (50^o-300^o C) were given

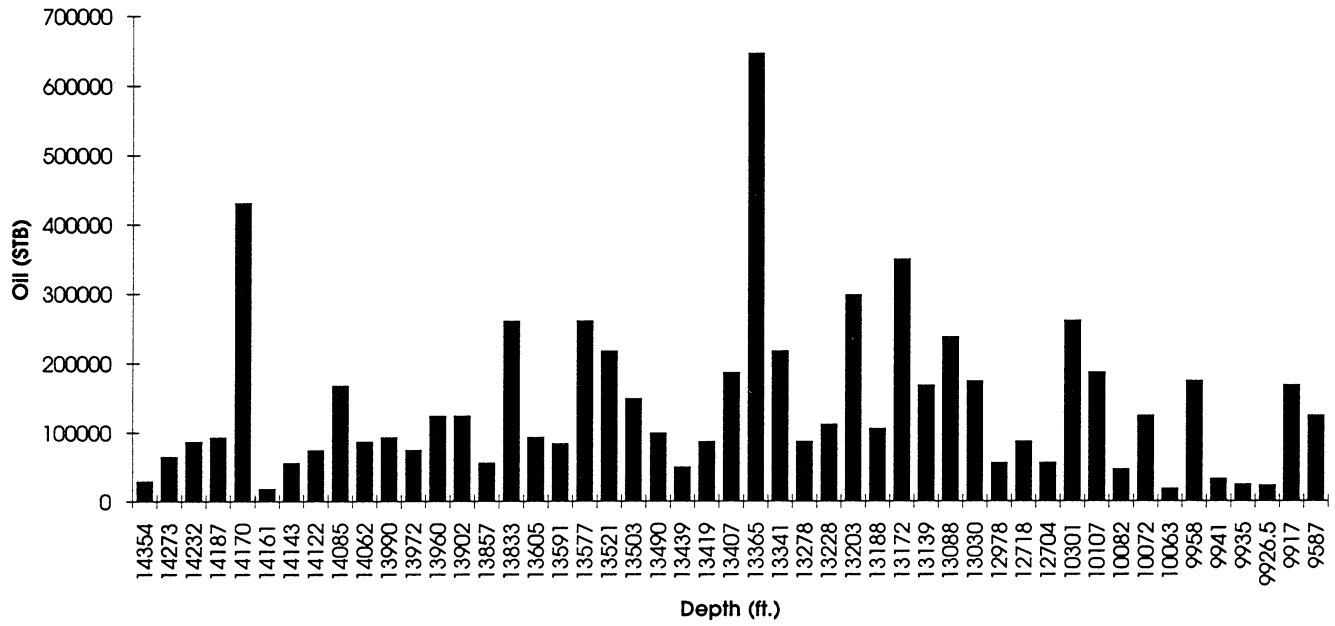


Figure 40. Original oil-in-place calculations for all perforated zones in the Malnar Pike well.

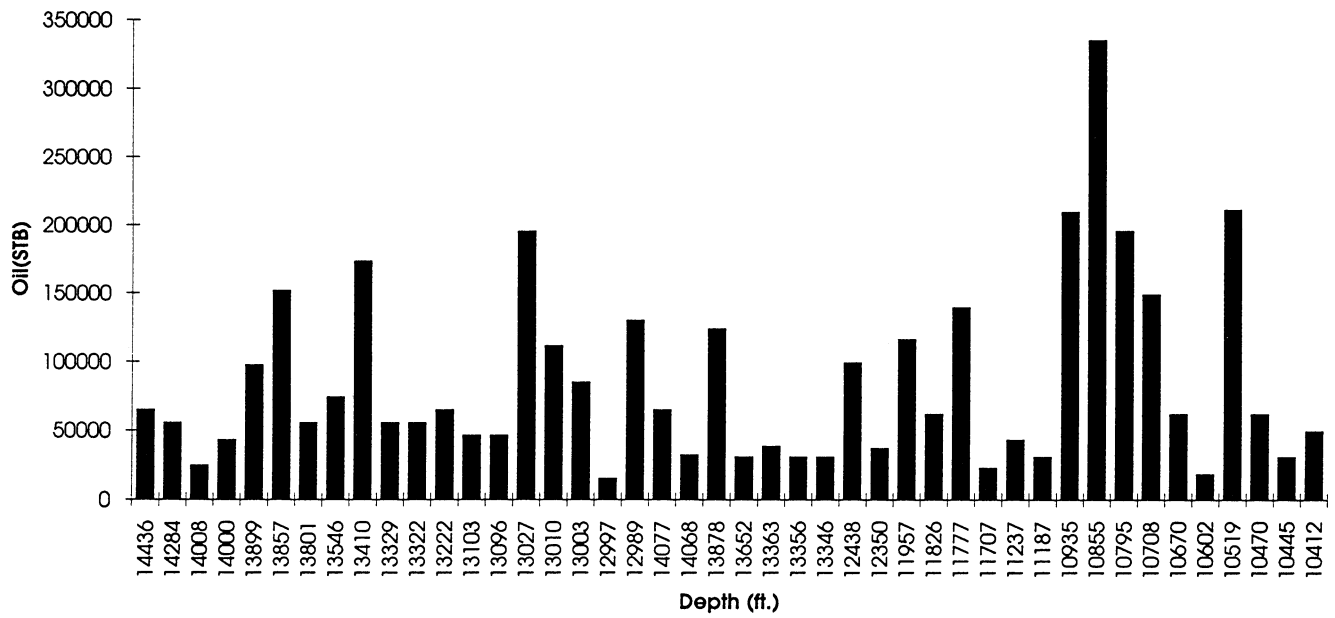


Figure 39. Original oil-in-place calculations for all perforated zones in the Michelle Ute well.

at 45° F (7.2° C) intervals. The brownish-black oil contained 43.3 percent residue or 572° F (300° C) plus material.

Quinex provided oil analyses on the yellow wax crude oil from the John 2-7B2 (section 7, T. 2 S., R. 2 W.) and black wax crude oil from the Leslie Taylor 24-5 (section 24, T. 1 S., R. 1 W.) well. These analyses indicated that the paraffin content of the oil samples was 7.4 percent and 12.2 percent by weight respectively. The paraffins were defined as C₂₀+ n-paraffins. Correspondingly, the Leslie Taylor oil had a cloud point of 157° F (69.4° C) compared to a cloud point of 132° F (55.6° C) for John 2-7B2. The oil from Leslie Taylor had a pour point of 120° F (48.9° C) and the oil from John 2-7B2 had a pour point of 95° F (35.0° C). The high concentration of paraffins in the samples makes paraffin precipitation in the reservoir (with temperature and pressure changes) a possibility.

The short and the long column compositional analysis of the two oils provided by Quinex were completed in the Fluid Characterization Laboratories at the University of Utah. The long-column analysis provided the carbon number distribution from C₅-C₄₄ and a C₄₄+ fraction. The yellow wax crude had a C₄₄+ fraction of 0.28 and the amount of this high-boiling fraction in black wax crude was found to be 0.48. This data was consistent with the API gravities of these crude oils, which were reported to be 39° API and 33° API respectively. The lighter yellow wax was found to have the lower residual high-boiling fraction. The short-column analysis revealed that all of the yellow wax crude oil eluted before the residence time for carbon number C₉₀. Thus the 28 percent of the C₄₄+ fraction had a carbon number distribution between C₄₄ and C₉₀. Combined results of the long column analysis of the yellow and black wax have been presented in figure 41.

The data on Green River Formation oils did not include any samples from the Bluebell field. Gas analyses also did not include samples from the Bluebell field. The most comprehensive data on the oil and gas properties was provided by Pennzoil. Data on four reservoir fluids were provided, three of which were from the Altamont field and one from the Bluebell field. The data from the Bluebell field was for well 1-7B1E. The sample was collected at 8,000 feet (2,400 m). The original GOR was 404 SCF/STB and the saturation pressure at this GOR at 182° F (83.3° C) temperature was 2,026 psi (13,969 KPa). The oil formation volume factor at the bubble point was 1.247. The stock tank gravity of the liquid was 35° API. The gas gravity was 0.8. The initial producing GOR for most wells of interest (Roosevelt Unit area) were about two to three times the initial GOR for the well reported on by Pennzoil. The Altamont wells in the Pennzoil data set had producing GOR values of 673 SCF/STB to 1,805 SCF/STB. The data set provided a confirmation of the thermodynamic properties generated for reservoir simulations. Generation of thermodynamic data for reservoir simulation is discussed next.

Thermodynamic Properties

Properties like bubble point pressures, oil formation volume factors for different GORs, reservoir temperature, oil API gravity, and gas specific gravity were calculated using Glaso's (1980) empirical thermodynamic correlations. Laboratory data on North Sea crude oils were used for developing these equations. Variations in the thermodynamic properties with respect to oil and gas gravities are presented in table 4. Bubble point pressure and oil formation volume factor increase almost linearly with GOR. Changes in oil API gravity and changes in specific gas gravity produce considerable change in the bubble point pressure. Change in the oil API gravity does not affect oil formation volume factor significantly, but change in gas specific gravity does produce significant change in the formation volume factor.

Table 4. Table of thermodynamic properties.

Oil API Gravity	Gas Specific Gravity	GOR (SCF/STB)	Bubble Point Pressure (psi)	Oil Formation Volume Factor (RB/STB)
35	0.60	100	617	1.06
35	0.60	1000	4853	1.45
35	0.80	100	446	1.06
35	0.80	1000	3945	1.53
30	0.80	100	552	1.06
30	0.80	100	370	1.06

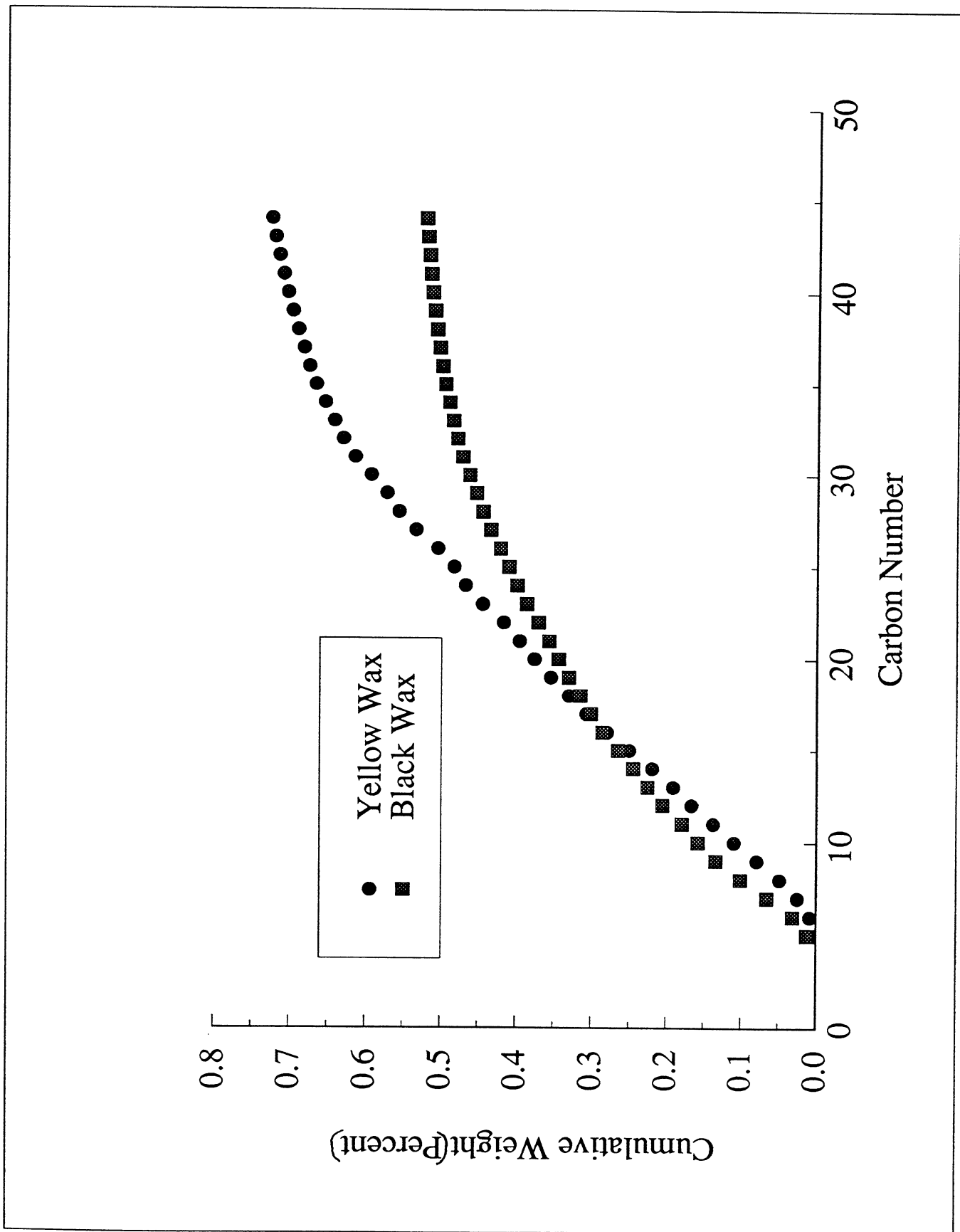


Figure 41. Long column gas chromatography analyses of the yellow wax crude from the John 2-7B2 well (section 7, T. 2 S., R. 2 W.) and the black wax crude from Leslie Taylor 24-5 well (section 24, T. 1 S., R. 1 W.).

RESERVOIR SIMULATIONS

Reservoir simulators solve partial differential equations resulting from material balances on oil, gas and water components, coupled with Darcy's law. In this work, a three-dimensional, three-phase, black-oil simulator (oil represented as a single component), was used. The partial differential equations are solved using finite-difference representation. The simulator allows simulation of geologically homogeneous reservoirs as well as fractured reservoirs. Fractured reservoirs are represented using the well-known dual-porosity, dual-permeability approach, first proposed by Warren and Root (1963) and later developed by Gilman and Kazemi (1983). This particular approach assumes that a fractured reservoir consists of essentially two different interacting continua; a matrix system and a fracture system. Most of the storage capacity of the reservoir is in the matrix while almost all of flow takes place through the fractures.

Reservoir simulation was used to study progressively more complex reservoir models. The idea was to start with simple single-well models with limited number of producing zones, which would later be expanded to multi-well models covering as much of the field as possible. Geologic information provided by manually interpreted logs was used in these preliminary simulation studies. The general idea is to proceed toward geostatistical reservoir representation using digitized logs.

The cumulative GOR for most of the wells in the Bluebell field are close to the initial producing GOR values. Naturally fractured reservoirs display this GOR trend. Hence, single-well fractured reservoir models were studied first. We also wanted to investigate if the observed trend in GOR could have been a result of production from multiple zones. The single-well reservoir models were later expanded to a four-square mile (10.4 km²) portion of the field on the east side and a four-square mile (10.4 km²) area on the west side. Thus, reservoir simulation model discussion has been categorized into:

1. Single-well fractured reservoir models for Michelle Ute and Malnar Pike wells: These wells are operated by Quinex and are likely to be the project demonstration wells. The producing zones for Michelle Ute well were represented by five lumped zones and for Malnar Pike well by 3 lumped zones.
2. Comprehensive single-well models: These were also reservoir models for Michelle Ute and Malnar Pike wells. All of the producing zones (69 in Michelle Ute and 50 in Malnar Pike) were represented separately in these models. At the present time a homogeneous reservoir model has been employed; fractured reservoir representation will be attempted later in the project as more fracture information becomes available.

3. East study-site model: The single-well models for Michelle Ute and Malnar Pike were later extended to a four-square mile (10.4 km²) area in the Roosevelt unit area. The idea was to see how the wells performed when they were considered as a unit producing from the same reservoir.
4. West study-site model: A great deal of high-quality data is available for some wells on the west side of the Bluebell field. The idea was to construct reservoir models for this portion of the field, for comparison with the east side models and with the ultimate objective of developing an integrated, unified model.

Preliminary Single-Well Models

The reservoir parameters employed for the preliminary single-well models are summarized below. The simulations were performed using a dual porosity, dual permeability simulator.

Properties	Michelle-Ute	Malnar-Pike
Reservoir extent	10,400-14,400 feet (ft) (3,170-4,390 m)	10,000-14,400 ft (3,050-4,390 m)
Grid	5 * 5 * 8	5 * 5 * 5
Grid size (x and y)	264 ft. (80.5 m)	264 ft. (80.5 m)
Number of fractures (x and y)	2 each	1 each
Porosity	0.05 - 0.11	0.112 (constant)
Permeability (matrix)	0.011 md	0.0236 md
Permeability (fracture)	0.11 md	1.0 md
Pressure	4,000 psi (27,580 KPa)	4,000 psi (27,580 KPa)
Oil gravity	42 API	42 API
Gas gravity	0.068	0.068
Initial GOR	900 SCF/STB	900 SCF/STB
Initial bubble point pressure	3,200 psi (22,064 KPa)	3,200 psi (22,064 KPa)
Initial oil saturation	0.7 (constant)	0.7 (constant)
Bottom hole pressure	3,000 psi (20,685 KPa)	3,000 psi (20,685 KPa)

It should be noted that only two fractures were used in the Michelle Ute model and only one fracture was employed for Malnar Pike simulations. The areal extent of the reservoir in both the models was 40 acres (16.2 ha). The porosities of the oil-bearing layers were calculated from geophysical well logs. This was done by lumping the 69 open intervals in Michelle Ute into four oil producing zones in the model and by representing the 50 zones in Malnar Pike by three oil producing layers. The permeabilities for the matrix and for the fractures were adjusted to match the production history. The cumulative oil and gas production from the model are plotted

with the field data in figures 42 and 43 for Michelle Ute well and figures 44 and 45 for Malnar Pike well. The oil production match is better than the gas production prediction. This could have been due to the fact that pressure variations between different zones were not accounted for in the model.

The simulation predictions compared with field production indicate that the model predictions were reasonable. However, since the analysis was limited to only a few lumped zones, this model would have to be adopted with caution when considering future production. Extremely low matrix and fracture permeabilities indicate possible wellbore damage. Low fracture permeabilities also may mean that most of the fractures are partially or completely filled. Low fracture frequency was adequate in matching production. This suggests that even though the reservoir may be extensively fractured, only a few fractures are contributing to flow.

Comprehensive Single-Well Models

A total of 69 zones are open in the Michelle Ute well, while Malnar Pike has been perforated in 50 zones. Porosities and thicknesses of each of the individual zones were determined from geophysical logs. This information formed the basis for the most comprehensive single-well models constructed in this study. Results of the Michelle Ute model have been discussed in this report. The comprehensive single-well model for Malnar Pike well is still being developed.

The reservoir parameters for the Michelle Ute model have been summarized below.

Reservoir extent	10,400 - 14,400 ft. (3,170-4,390 m)
Grid	8 * 8 * 69
Grid size (x and y)	165 ft. (50.3 m)
Porosity	0.0 - 0.16
Pressure gradient	0.5 psi/ft (11 KPa/m)
Oil gravity	35 API
Gas gravity	0.75
Initial GOR	900 SCF/STB
Initial bubble point pressure	3,200 psi (22,064 KPa)
Initial oil saturation	0.7 (constant)
Bottom hole pressure	2,000 - 3,000 psi (13,800-20,700 KPa)

It should be noted that variations in initial reservoir pressure in the different zones were accounted for by using a constant pressure gradient of 0.5 psi/ft (11 KPa/m). The bottom-hole pressure (a production constraint) was 3,000 psi (20,700 KPa) in the first year and 2,000 psi (13,800 KPa) in subsequent years of production. The field production operations were essentially duplicated by opening perforations at appropriate times. Once again, the permeabilities were adjusted to match field oil and gas production. Permeabilities of the zones first open were adjusted first. In a given time interval (when additional perforations came on-line), permeabilities of only those additional zones were varied in order to match production. Permeabilities varied from

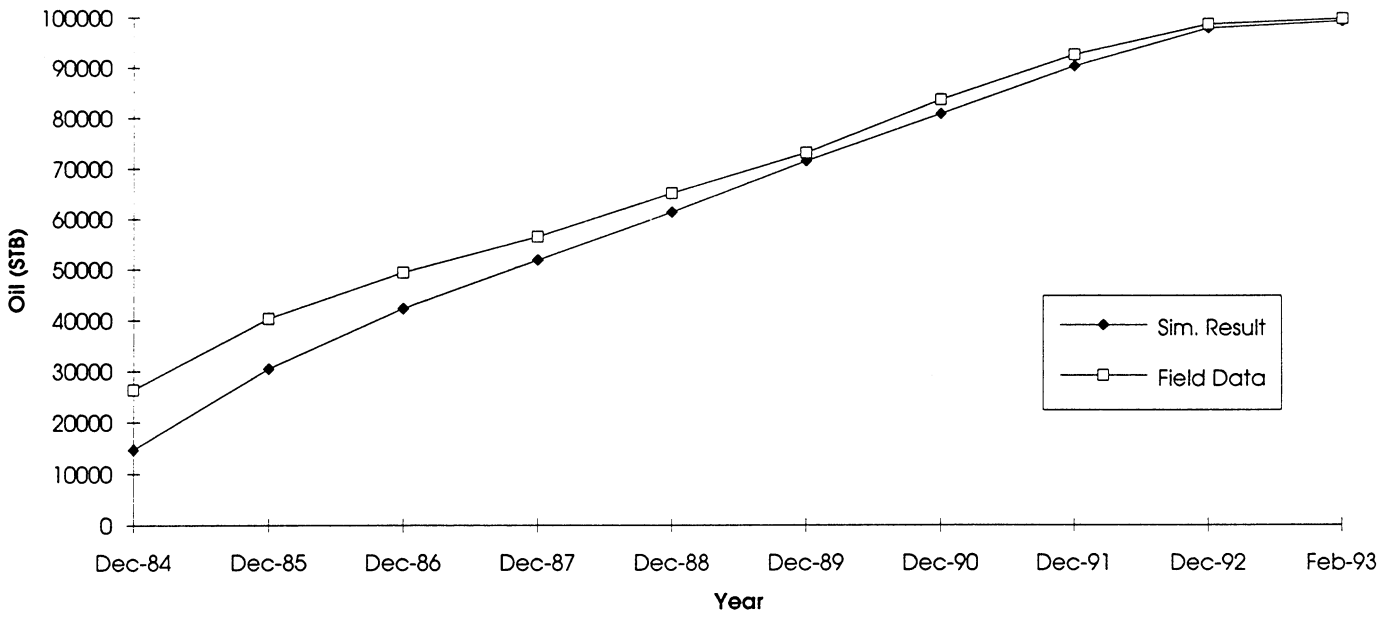


Figure 42. Actual versus preliminary single-well model simulated cumulative oil production for the Michelle Ute well.

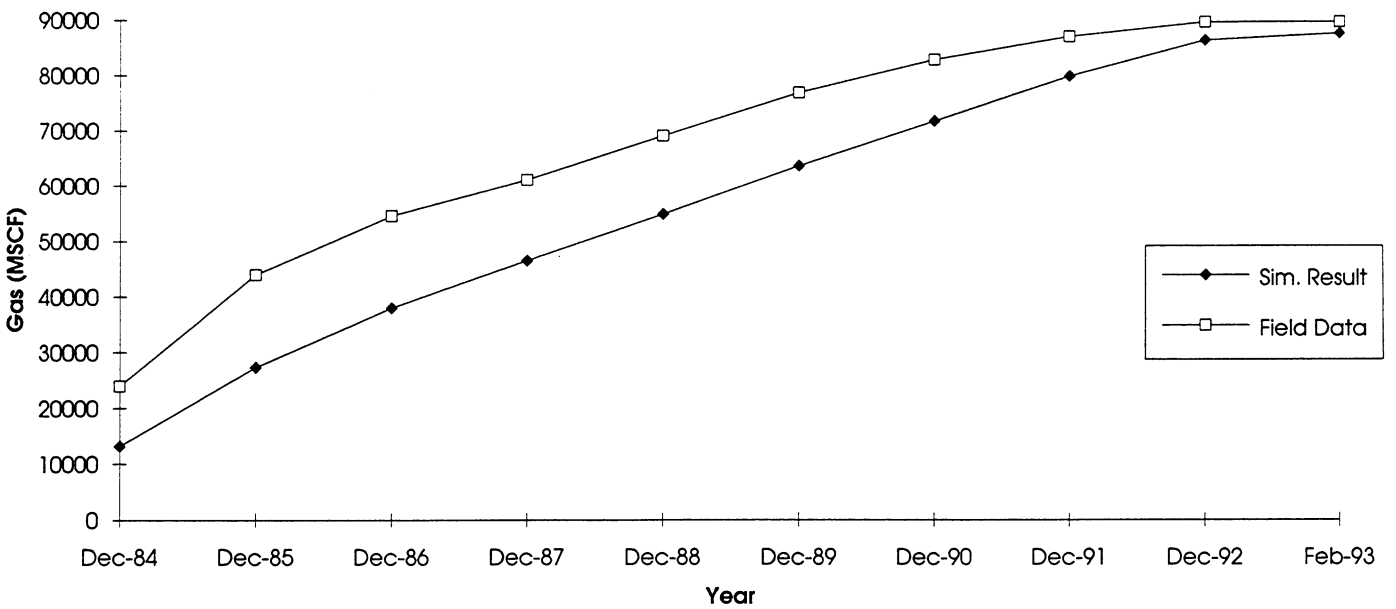


Figure 43. Actual versus preliminary single-well model simulated cumulative gas production for the Michelle Ute well.

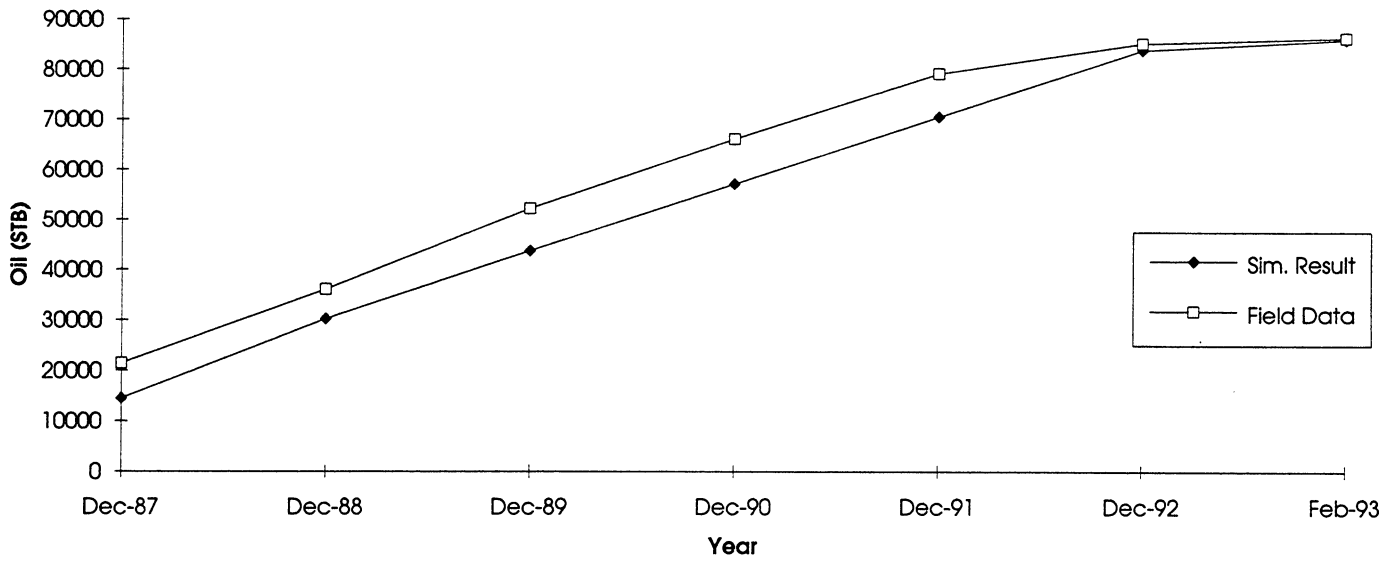


Figure 44. Actual versus preliminary single-well model simulated cumulative oil production for the Malnar Pike well.

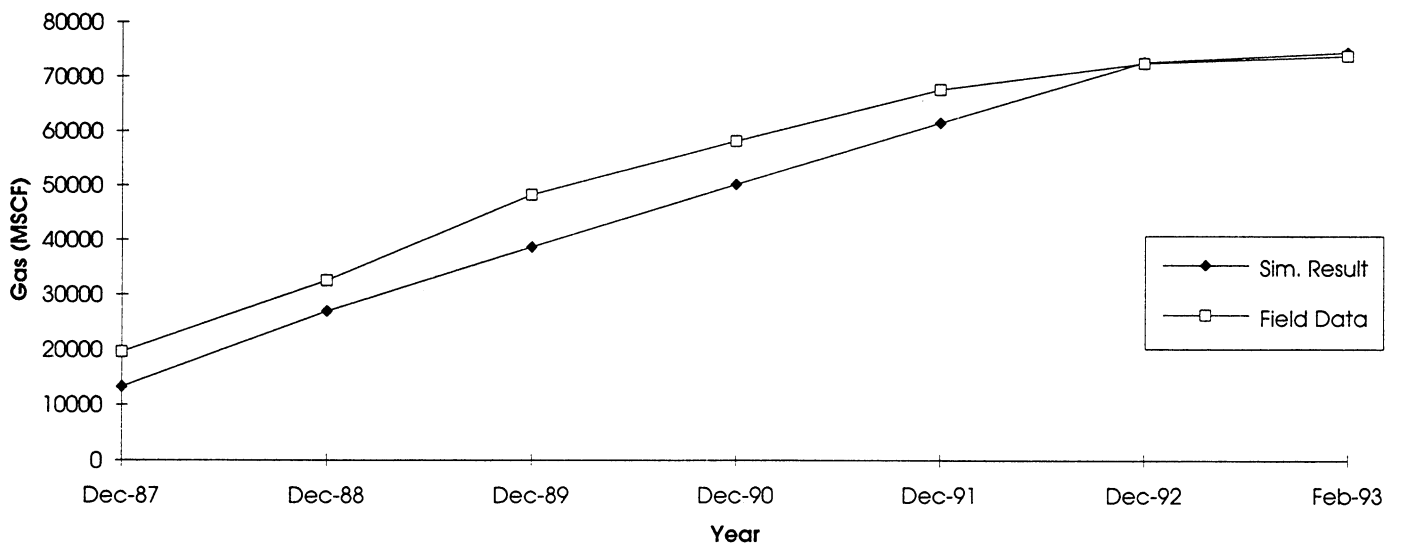


Figure 45. Actual versus preliminary single-well model simulated cumulative gas production for the Malnar Pike well.

0.03 md to 1.25 md. The permeability values are well within the range of values measured for outcrop samples. Once core permeabilities become available, they will be used directly in the simulator to assess the production potential of the well. The oil and gas production predictions from the model are compared with field data in figures 46 and 47. It is viewed that the model provides an excellent match with the field history. An internal model analysis could be undertaken to assess pressurized zones with oil production potential. These zones could then be targeted for either recompletion or deviated drilling.

East Study-Site Model

Five zones in the lower Wasatch transition were correlated between five wells in the Roosevelt unit area. The four-square mile (10.4 km²) area around the Michelle Ute and Malnar Pike wells (sections 17, 18, 19 and 20, T. 1 S., R. 1 E.), was modeled. This was a homogeneous reservoir model and it was decided that fracture description would be included once it became available. Only the five zones were considered for which correlations were developed. Only five wells perforated in these zones were considered in the model. These were Michelle Ute, 1-8A1E, Chasel Sprouse, Malnar Pike, and Roosevelt Unit C-11, the wells for which production information was compiled and discussed in an earlier section. Since only the five zones were considered, all of the model production was attributed to these zones. Reservoir parameters used in the model are summarized below.

Reservoir extent	13,000 - 14,000 ft. (3,970-4,270 m)
Grid	20 * 20 * 9
Grid size (x and y)	528 ft. (161.0 m)
Porosity	0.0 - 0.18
Pressure	7,050 psi(constant) (48,600 KPa)
Oil gravity	35 API
Gas gravity	0.75
Initial GOR	900 SCF/STB
Initial bubble point pressure	4,146 psi (28,587 KPa)
Initial oil saturation	0.7 (constant)
Bottom hole pressure	3,000 psi (20,690 m)

Figures 48 and 49 show a comparison of the cumulative oil and gas production for the four-square mile (10.4 km²) model with total production from the five wells. It should be noted that the individual block permeabilities were adjusted to match the total area production. The permeabilities varied from 0.018 md to 0.5 md. Production from remaining zones would have to be accounted for in order to provide a more realistic reservoir picture. This was however, our first attempt at developing reservoir-wide models for the Bluebell field. Since the production from the field was matched by adjusting permeabilities, the cumulative oil production from the model matches the field production data reasonably well. The gas production, however, is not predicted to the same accuracy by the model. Not considering other producing

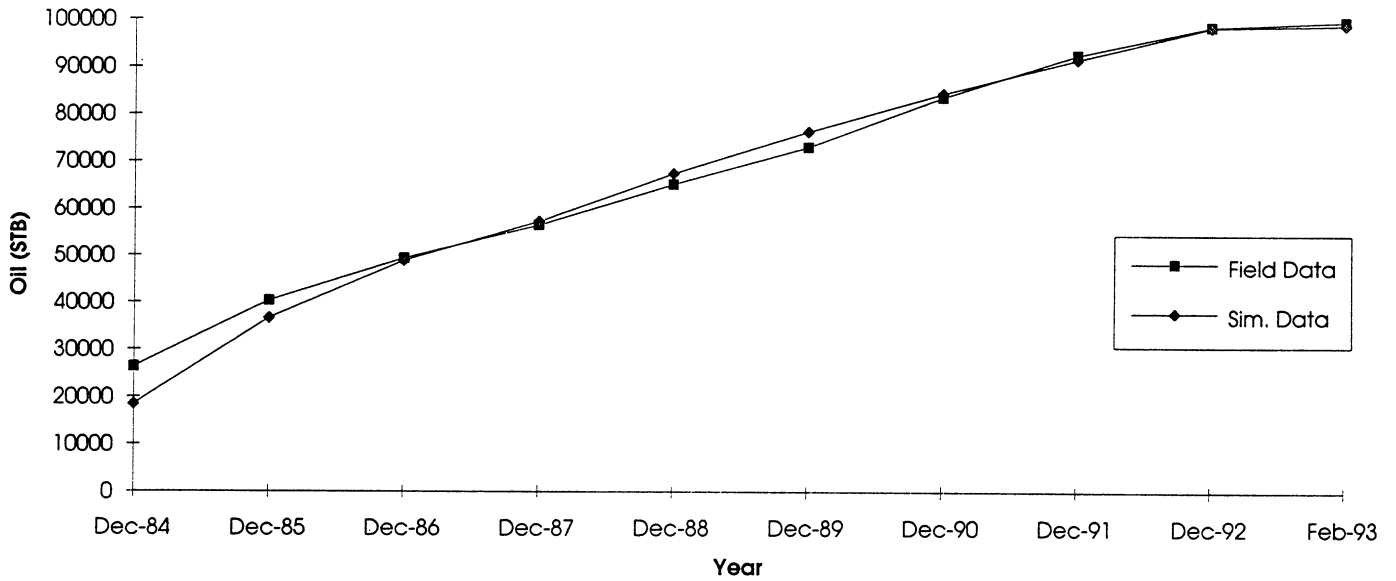


Figure 46. Actual versus comprehensive single-well model simulated cumulative oil production for the Michelle Ute well.

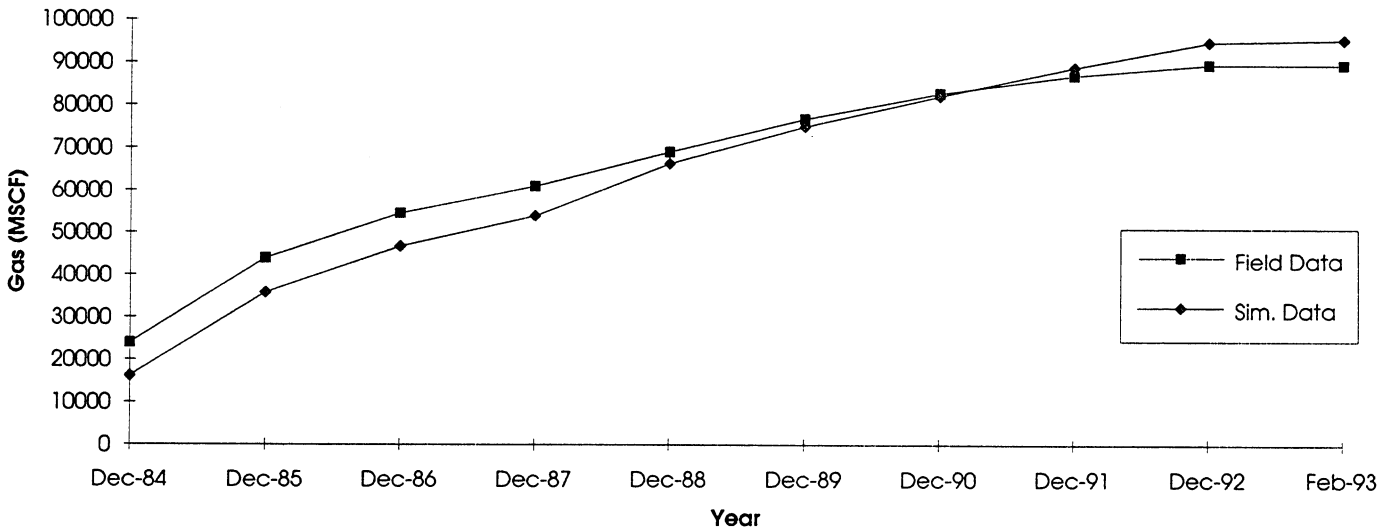


Figure 47. Actual versus comprehensive single-well model simulated cumulative gas production for the Michelle Ute well.

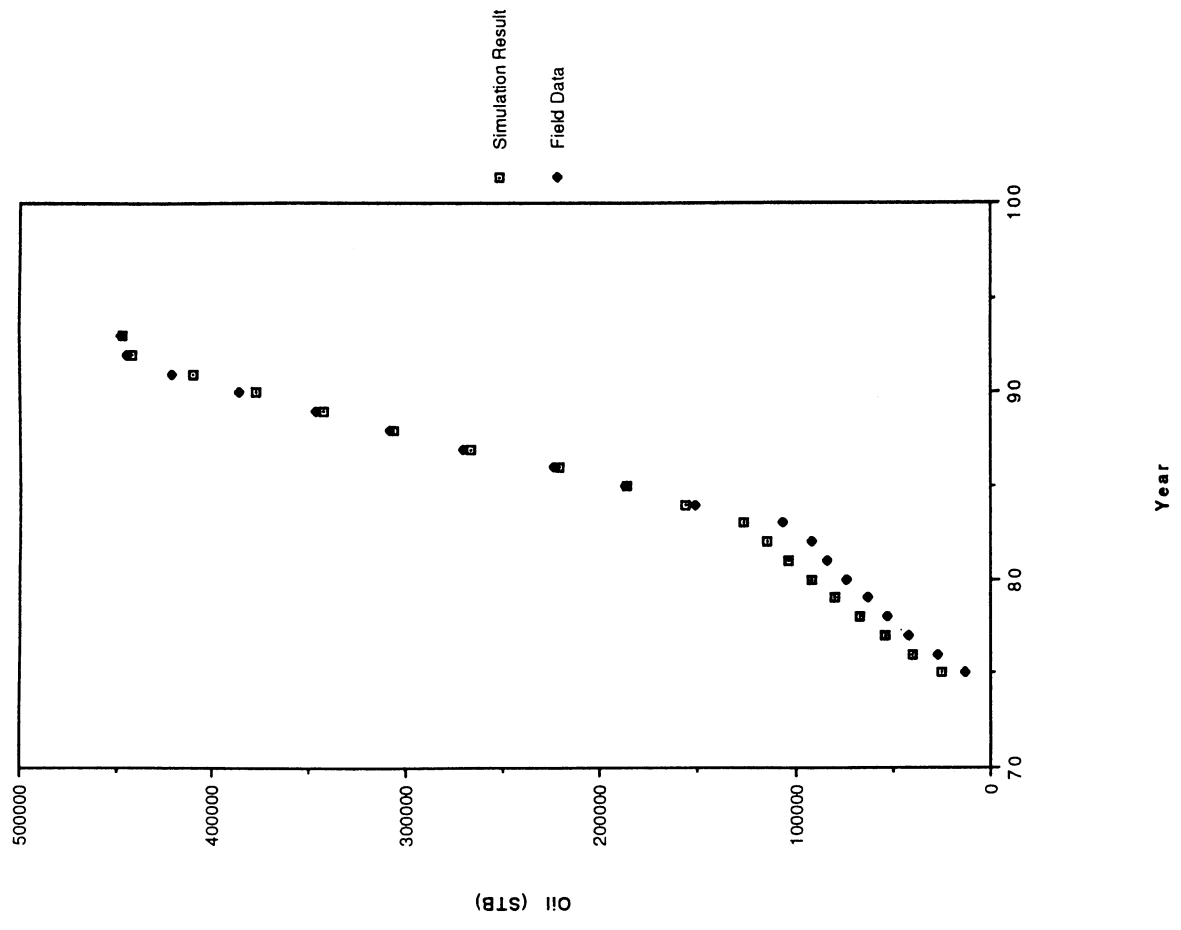


Figure 48. Actual versus simulated cumulative oil production from five zones in five wells in the four-square mile east study site (sections 7, 8, 17 and 18, T. 1 S., R. 1 E.).

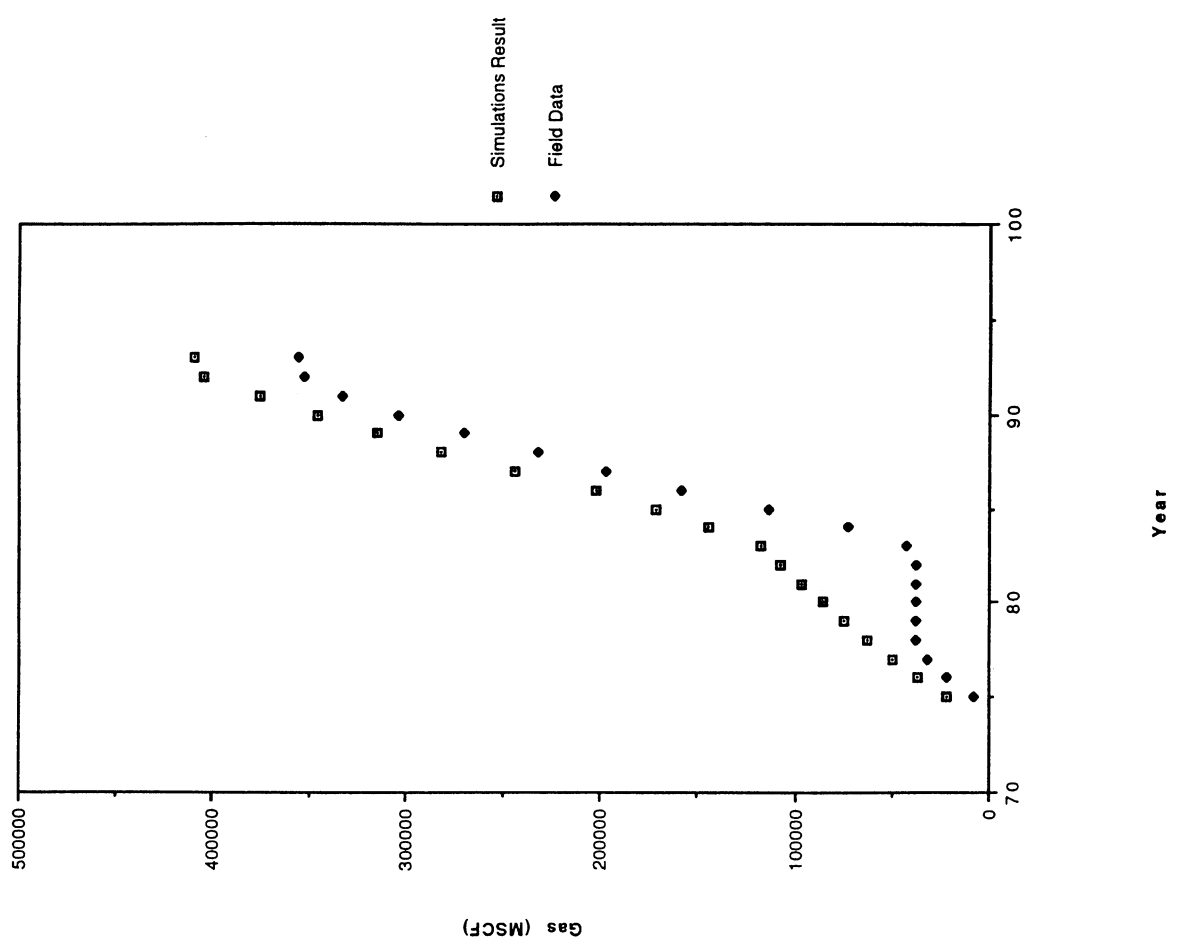


Figure 49. Actual versus simulated cumulative gas production from five zones in five wells in the four-square mile east study site (sections 7, 8, 17 and 18, T. 1 S., R. 1 E.).

zones may be the important reason for this observation. Individual well histories from the model were also compared with their respective field values. Figures 50 to 51 show cumulative oil and gas productions for Michelle Ute and figures 52 and 53 show oil and gas production for Malnar Pike. As can be seen from the figures, the oil production is well matched. The gas production results for the individual wells do not match the field values as well, just like the cumulative gas production. A possible reason (apart from other producing zones) for these deviations may be the fact that fractures were not considered in this model and at least, limited fracturing would have to be considered for a realistic field-wide model. Model internal analysis reveals that due to low permeabilities, number of regions in the four-square mile (10.4 km²) area remain pressurized. This shows that there is a definite potential for selected infill drilling in the field.

West Study-Site Model

The lower Green River Formation/upper Wasatch transition (upper perforations) in the four-square mile (10.4 km²) west study-site area (sections 9, 10, 15 and 16, T. 1 S., R. 2 W.), was modeled. Once again, a homogeneous representation was used. Lamicq 2-9C, Springfield 2-10C, State 3-10C, Sundance 4-15A2, Lamb 2-16A2, Boren 3-15 A2, and Boren 6-16A2 were the wells in this area. Out of these wells, only Lamicq 2-9C, Springfield 2-10C, and State 3-10C were perforated in the upper part of the formation. The primary features of the model were as follows;

Reservoir extent	10,250 - 10,628 ft. (3,126-3,242 m)
Grid	20 * 20 * 21
Grid size (x and y)	528 ft. (161.0 m)
Porosity	0.0 - 0.26
Pressure	4,800 psi(constant) (33,000 KPa)
Oil gravity	35 API
Gas gravity	0.75
Initial GOR	400 SCF/STB
Initial bubble point pressure	2,100 psi (14,500 KPa)
Initial oil saturation	0.7 - 0.9
Bottom hole pressure	2,500 psi (17,200 KPa)

A field production history match was obtained for permeability values varying from well to well and from layer to layer. The values were between 0.18 md and 0.62 md with a base permeability of 0.5 md.

The cumulative oil and gas production results for this model are shown in figures 54 to 55. Figures 54 and 55 show the cumulative oil and gas production for the entire field, while figures 56 and 57 show the history match for the well State 3-10C. The comparison attempted here is more realistic than for the east-side of the field since the zones considered in this model were the only producing zones during that time period. It can be observed from figure 54 that the oil production lags the field production over almost the entire time period even though the ultimate production

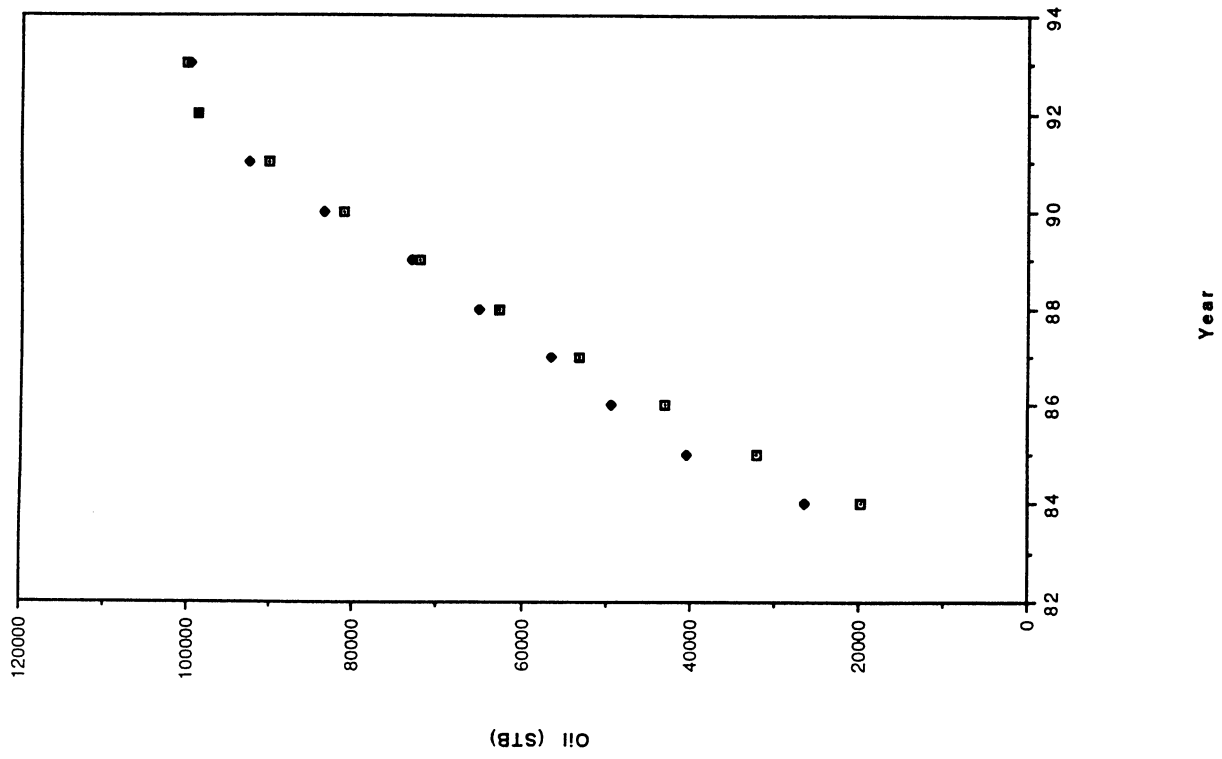


Figure 50. Actual versus simulated cumulative oil production (based on the four-square mile model) for the Michelle Ute well.

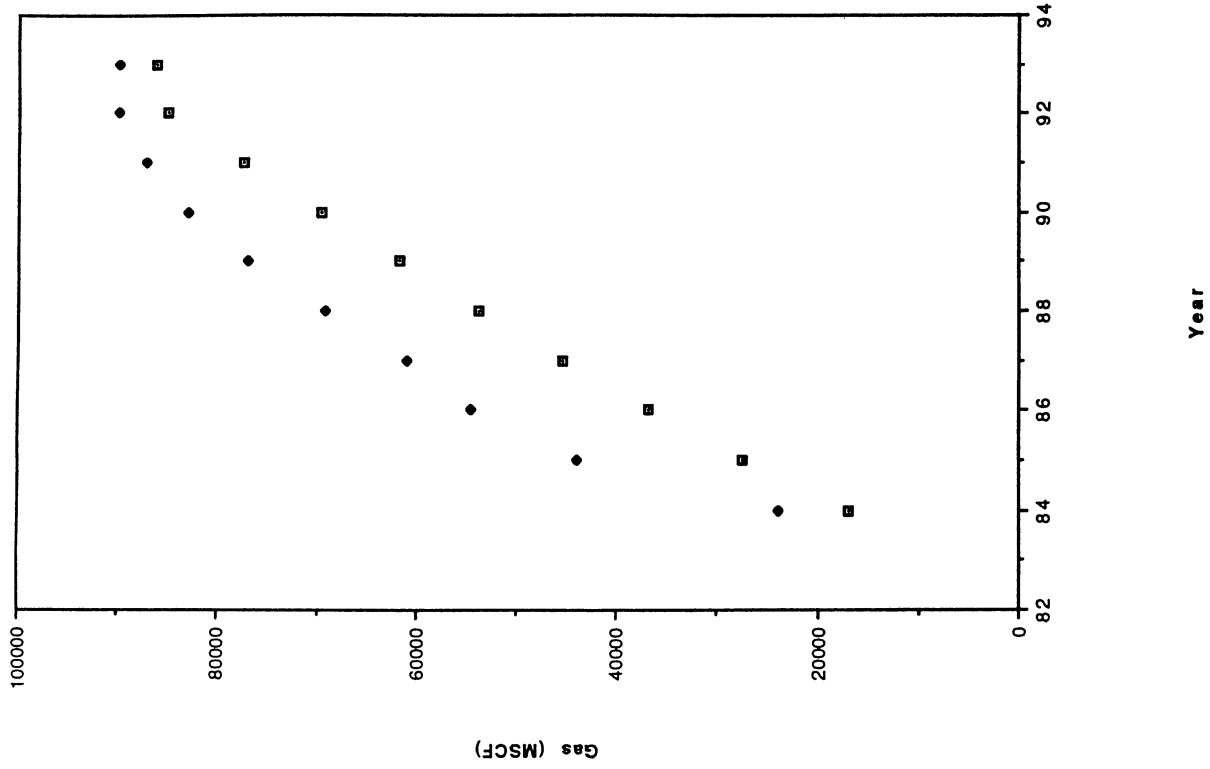


Figure 51. Actual versus simulated cumulative gas production (based on the four-square mile model) for the Michelle Ute well.

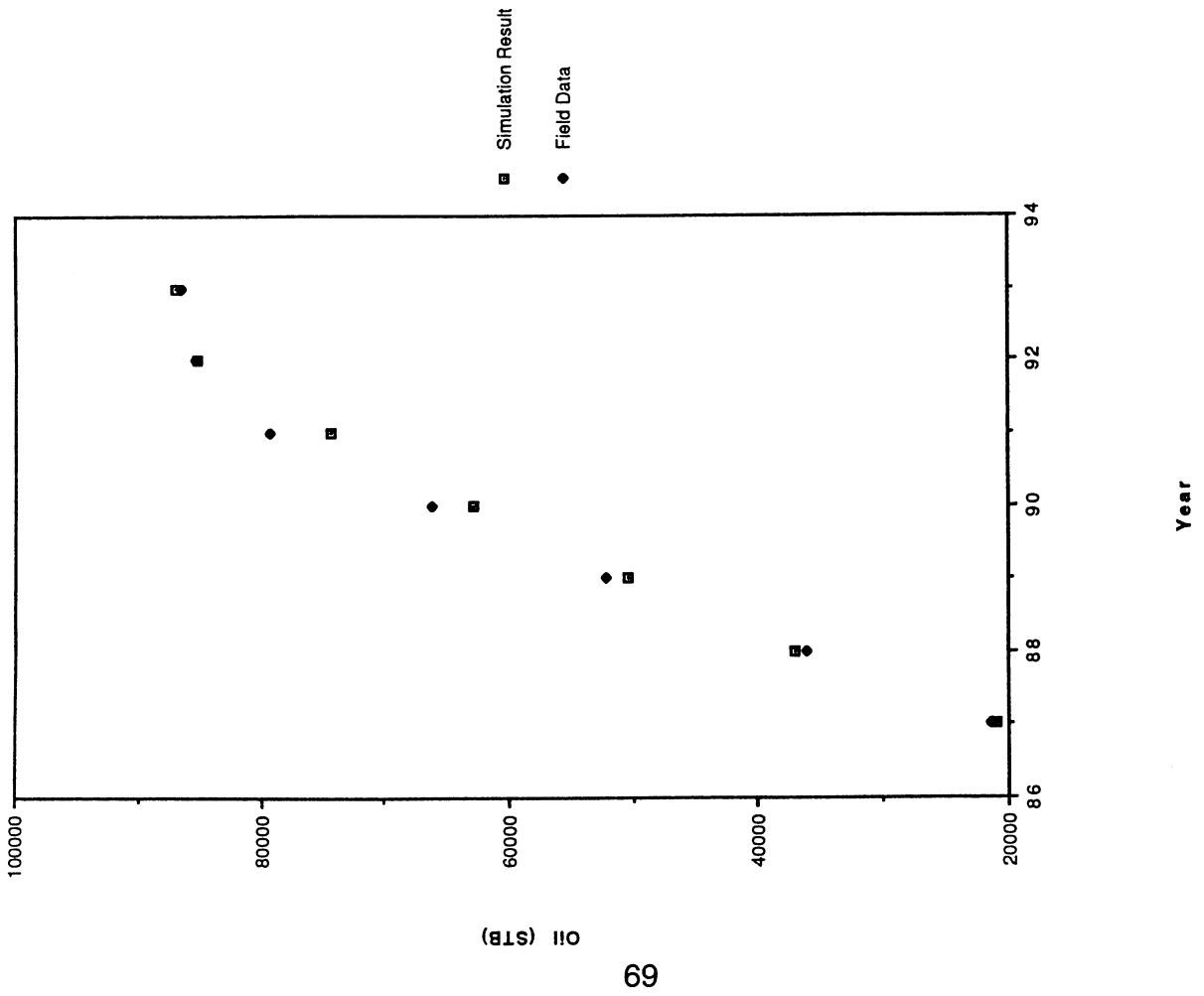


Figure 52. Actual versus simulated cumulative oil production (based on the four-square mile model) for the Mainar Pike well.

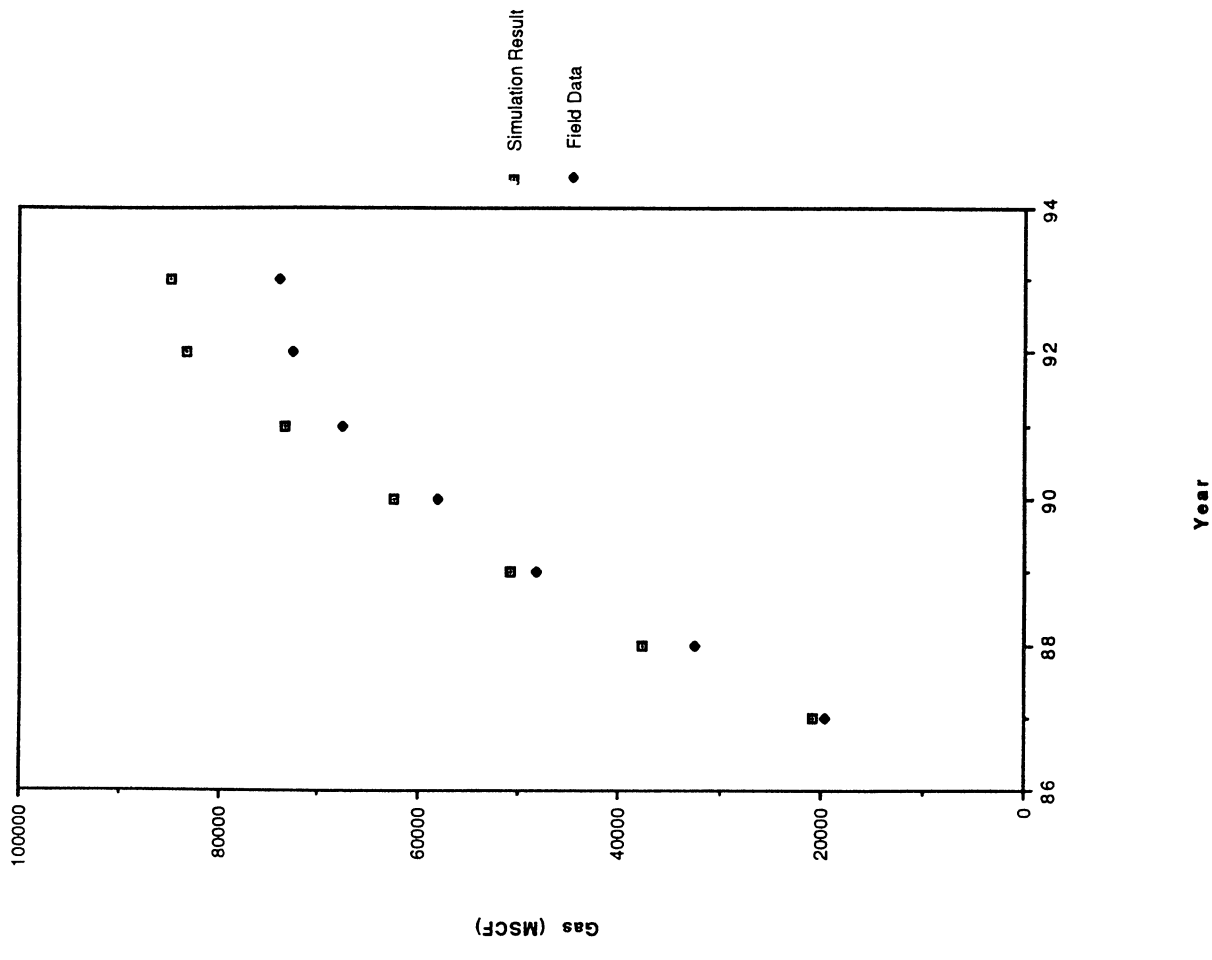


Figure 53. Actual versus simulated cumulative gas production (based on the four-square mile model) for the Mainar Pike well.

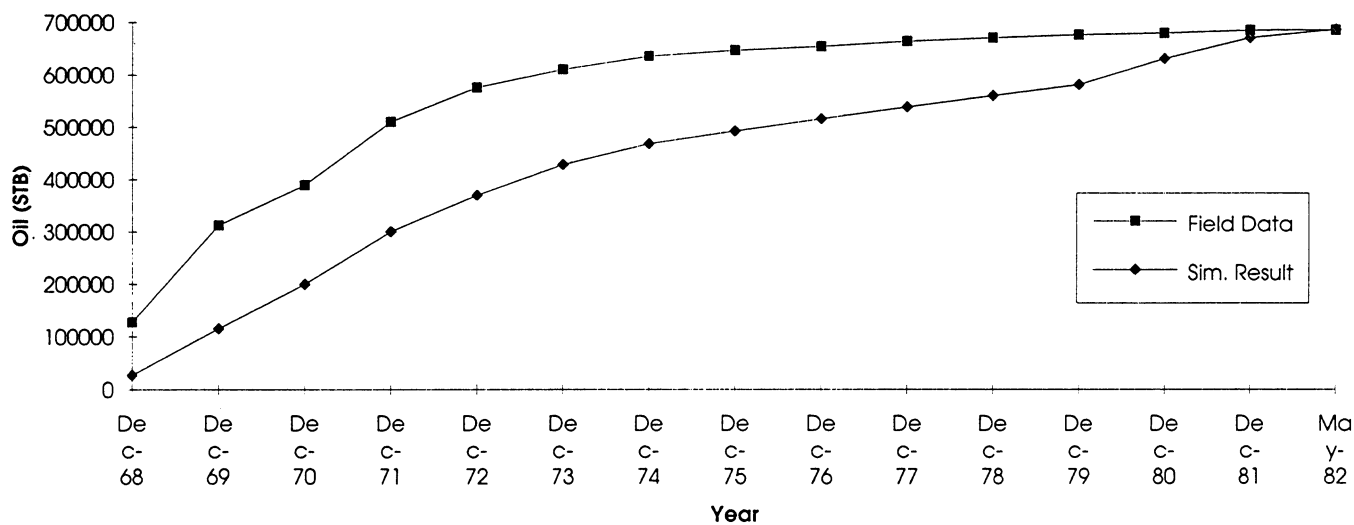


Figure 54. Actual versus simulated cumulative oil production of the lower Green River Formation/upper Wasatch transition from three wells in the four-square mile (10.4 km²) west study-site (sections 9, 10, 15, and 16, T. 1 S., R. 2 W.).

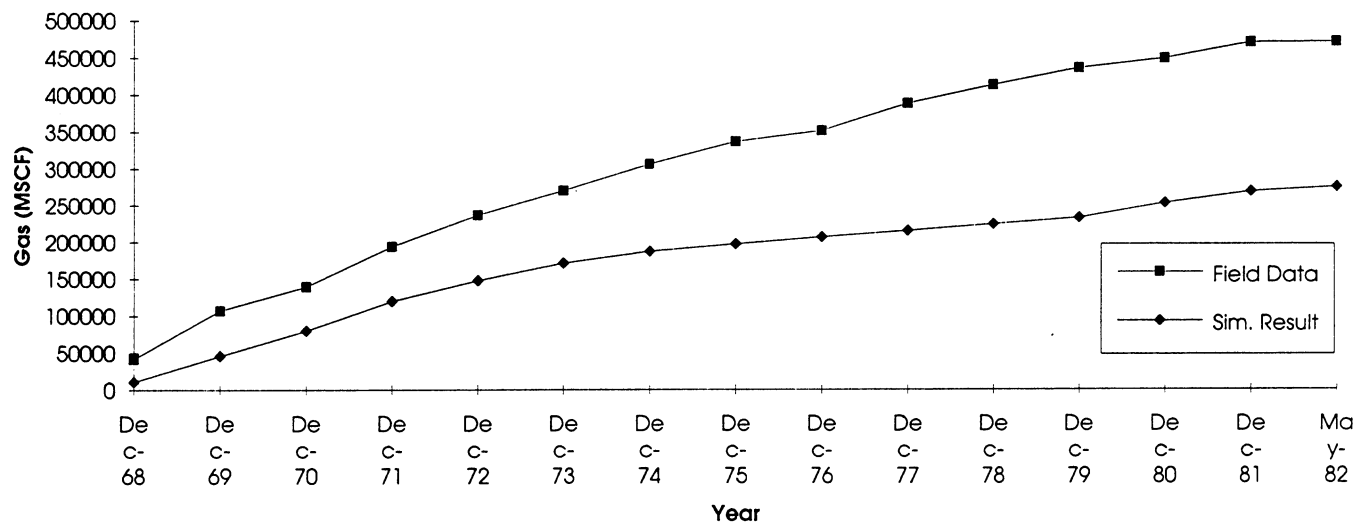


Figure 55. Actual versus simulated cumulative gas production of the lower Green River Formation/upper Wasatch transition from three wells in the four-square mile (10.4 km²) west study-site (sections 9, 10, 15, and 16, T. 1 S., R. 2 W.).

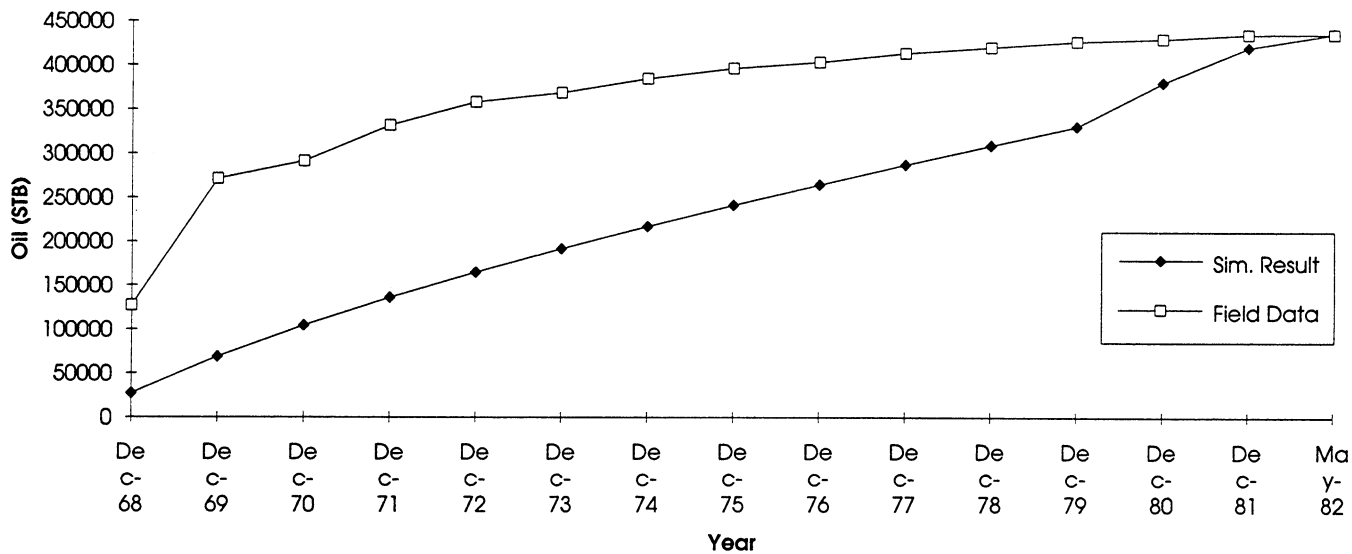


Figure 56. Actual versus simulated cumulative oil production (based on the four-square mile model) for the State 3-10C well (section 10, T. 1 S., R. 2 W.).

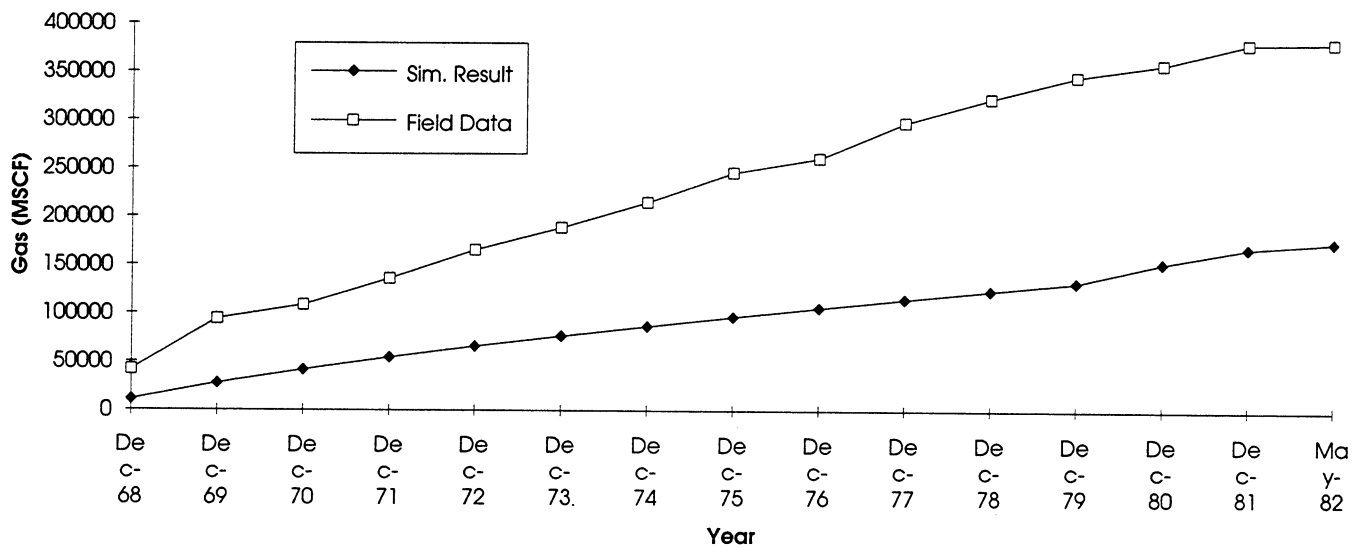


Figure 57. Actual versus simulated cumulative gas production (based on the four-square mile model) for the State 3-10C well (section 10, T. 1 S., R. 2 W.).

is close to the field value. The gas production from the model lags the field production over the entire interval. Once again, considering fractures may be essential in matching the field history more closely. Internal analysis once again reveals that a considerable amount of oil at producible pressures is left in the reservoir pointing to the possibility of increasing reserves by infill drilling.

REFERENCES

- Bruhn, R.L., Picard, M.D., and Beck, S.L., 1983, Mesozoic and early Tertiary structure and sedimentology of the central Wasatch Mountains, Uinta Mountains and Uinta Basin: Utah Geological and Mineral Survey Special Studies 59, p. 63-105.
- Bryant, B., 1990, Geologic and structure maps of the Salt Lake City 1° X 2° Quadrangle, Utah and Wyoming: U. S. Geological Survey Map I-1997.
- Carozzi, A.V., 1993, Sedimentary Petrography: Englewood Cliffs, N.J., Prentice Hall, 263 p.
- Castle, J.W., 1991, Sedimentation in Eocene Lake Uinta (lower Green River Formation), northeastern Uinta Basin, Utah, *in* Katz, B.J., editor, Lacustrine basin exploration-case studies and modern analogs: American Association of Petroleum Geologists Memoir 50, p. 243-263.
- Chidsey, T.C., Jr., 1993, Uinta Basin [UN] plays-overview, *in* Atlas of major Rocky Mountain gas reservoirs: New Mexico Bureau of Mines and Mineral Resources, p. 83.
- Dott, R.H., Jr., 1964, Wacke, graywacke and matrix - what approach to immature sandstone classification?: *Journal of Sedimentary Petrology*, v. 34, p. 625-632.
- Dunham, R.J., 1962, Classification of carbonate rocks according to depositional texture, *in* Ham, W.E., editor, Classification of Carbonate Rocks: American Association of Petroleum Geologists Memoir 1, p. 108-121.
- Fouch, T.D., 1975, Lithofacies and related hydrocarbon accumulations in Tertiary strata of the western and central Uinta Basin, Utah, *in* Bolyard, D.W., editor, Symposium on deep drilling frontiers in the central Rocky Mountains: Rocky Mountain Association of Geologists Special Publication, p. 163-173.
- , 1976, Revision of the lower part of the Tertiary system in the central and western Uinta Basin, Utah: U.S. Geological Survey Bulletin 1405-C, 7 p.
- , 1981, Distribution of rock types, lithologic groups, and interpreted depositional environments for some lower Tertiary and Upper Cretaceous rocks from outcrops at Willow Creek - Indian Canyon through the subsurface of Duchesne and Altamont oil fields, southwest to north-central parts of the Uinta Basin, Utah: U.S. Geological Survey Oil and Gas Investigations Map, Chart OC-81, 2 sheets.

- Fouch, T.D., Nuccio, V.F., and Chidsey, T.C., Jr., editors, 1992, Hydrocarbon and mineral resources of the Uinta Basin, Utah and Colorado: Utah Geological Association Guidebook 20, 366 p.
- Fouch, T.D., and Pitman, J.K., 1991, Tectonic and climate changes expressed as sedimentary cycles and stratigraphic sequences in the Paleogene Lake Uinta system, central Rocky Mountains, Utah and Colorado (abstract): American Association of Petroleum Geologists Bulletin, v. 75, no. 3, p. 575.
- , 1992, Tectonic and climate changes expressed as sedimentary and geochemical cycles - Paleogene Lake systems, Utah and Colorado - implications for petroleum source and reservoir rocks, *in* Carter, L.J., editor, U.S. Geological Survey research on energy resources, 1992 McKelvey forum program and abstracts (abstract): U.S. Geological Survey Circular 1074, p. 29-30.
- Fouch, T.D., Pitman, J.K., Wesley, J.B., Szantay, Adam, and Ethidge, F.G., 1990, Sedimentology, diagenesis, and reservoir character of Paleogene fluvial and lacustrine rocks, Uinta Basin, Utah - evidence from the Altamont and Red Wash fields, *in* Carter, L.M., editor, Sixth V. E. McKelvey forum on mineral and energy resources, U.S. Geological Survey research on energy resources - 1990 - program and abstracts: U.S. Geological Survey Circular 1060, p. 31-32.
- Franczyk, K.J., Fouch, T.D., Johnson, R.C., Molenaar, C.M., and Cobban, W.A., 1992, Cretaceous and Tertiary paleogeographic reconstructions for the Uinta-Piceance Basin study area, Colorado and Utah: U. S. Geological Survey Bulletin 1787-Q, 37 p.
- Gilman, J.R., and Kazemi, H., 1983, Improvements in simulation of naturally fractured reservoirs: Journal of Petroleum Technology, v. 35, p. 695-707.
- Glaso, O., 1980, Generalized pressure-volume-temperature correlations: Journal of Petroleum Technology, v. 32, no. 5, p. 785-795.
- Hintze, L.F., 1988, Geologic history of Utah: Provo, Brigham Young University Geology Studies, Special Publication 7, 202 p.
- Morgan, C.D., 1994, Oil and gas production maps of the Bluebell field, Duchesne and Uintah Counties, Utah: Utah Geological Survey Oil and Gas Fields Studies 15, 5 p., 8 pl., 1" = 0.8 mile.
- Narr, W.M., 1977, The origin of fractures in Tertiary strata of the Altamont field, Uinta Basin, Utah: Toronto, University of Toronto, M.S. Thesis, 132 p.

- Pitman, J.K., Anders, D.E., Fouch, T.D., and Nichols, D.J., 1986, Hydrocarbon potential of nonmarine Upper Cretaceous and Lower Tertiary rocks, eastern Uinta Basin, Utah, *in* Spencer, C.W., and Mast, R.F., editors, *Geology of tight gas reservoirs: American Association of Petroleum Geologists Studies in Geology* 24, p. 235-252.
- Pitman, J.K., Fouch, T.D., and Goldaber, M.B., 1982, Depositional setting and diagenetic evolution of some Tertiary unconventional reservoir rocks, Uinta Basin, Utah: *American Association of Petroleum Geologists Bulletin*, v. 66, no. 10, p. 1581-1596.
- Pollard, D.D., and Aydin, A., 1988, Progress in understanding jointing over the past century: *Geological Society of America Bulletin*, v. 100, p. 1181-1204.
- Ryder, R.T., Fouch, T.D., and Elison, J.H., 1976, Early Tertiary sedimentation in the western Uinta Basin, Utah: *Geological Society of America Bulletin*, v. 87, p. 496-512.
- Smith, J.D., 1986, Depositional environments of the Tertiary Colton and basal Green River Formations in Emma Park, Utah: Provo, Brigham Young University *Geology Studies*, v. 33, p. 135-174.
- Smouse, DeForrest, 1993, Altamont-Bluebell, *in* Hill, B.G., and Bereskin, S.R., editors, *Oil and gas fields of Utah: Utah Geological Association Publication* 22, unpaginated.
- Stokes, W.L., 1986, *Geology of Utah: Utah Geological Survey Miscellaneous Publication* S, 317 p.
- Warren, J.E., and Root, P.J., 1963, The behavior of naturally fractured reservoirs: *Journal of Petroleum Technology*, v. 15, p. 245-253.

APPENDIX A

**Petrographic Description of Lower Green River Formation
Samples Taken in Willow Creek Canyon**

5-DN5--300 point count.

Constituent	Number = Percent	Constituent	Number = Percent
Quartz	85 = 28.3	Polyxline Quartz	0 = 0.0
Feldspar	56 = 18.6	Fe-oxide	0 = 0.0
Lithics	12 = 4.0	Chert	15 = 5.0
Cement	32 = 10.6	Porosity	14 = 4.6
Matrix	53 = 17.6	Mica	4 = 1.3
Organics	29 = 9.6	Fossils	0 = 0.0

Moderately sorted, angular, lower fine-grained to lower very fine-grained feldspathic wacke with very little interparticle porosity. The cement in this thin section looks like a fairly equal mixture of calcite and quartz. The feldspars are highly altered. The lithic count may be low due to the difficulty of exactly identifying some of the smaller fragments. The organic count may all be Fe-oxides but there was not enough biotite to account for all the iron.

7-DN7--Fossiliferous packstone with fragments of ostracodes, gastropods, and bivalves with original aragonite. There are also some phosphatic fossils in this section which may be fish debris. Most of the fossil fragments have two sizes of calcite cement. There has been solution enlargement and spar filling in the areas around the fragments. Some of the intraparticle porosity has been filled with organic material. There is some minimal open fracture porosity.

37-DN37--Ostracodal packstone with micrite and calcite reduced to filled intra- and interparticle porosity. Some of the calcite cement has been followed by silica cement and a lot of the matrix has undergone aggrading neomorphism from micrite to microspar. The ostracodes have all been lined up perpendicular to the up direction of the thin section and many of them have been crushed, indicating compaction. Bits of organic material have also been lined up roughly perpendicular to the up direction of the thin section.

43--Mudstone with about 5 percent fossil hash and solution enlarged spar filled mesomoldic porosity. Organic material has been collected along concentrations of moldic porosity. (Percentage is visual estimate only).

47-DN47--Mudstone with ostracod fragments(?) and organic-rich matrix. There

is no open porosity. There are some small variations in the blue tinge of the thin section due to some layers that seem to be made up of small peloids glued together with fossil fragments by micrite.

102-EH47--Mudstone with lighter and darker colored micritic laminae (varves?). The darker color may be due to a concentration of very fine-grained organic material. There are a few bits of quartz and mica. Some of the mud clasts (peloids) look like they may have some intraparticle porosity but the amounts are not significant. Vertical fractures and microfaults have been sealed with micrite.

113-EH58 block--Mudstone with about 1 percent solution enlarged, cement reduced micromoldic and microvuggy intraparticle porosity. (Percentage is visual estimate only).

140-EH85--300 point count.

Constituent	Number = Percent	Constituent	Number = Percent
Quartz	94 = 31.3	Polyxline Quartz	2 = 0.6
Feldspar	60 = 20.0	Fe-oxide	29 = 9.6
Lithics	1 = 0.3	Chert	14 = 4.6
Cement	20 = 6.6	Porosity	72 = 24.0
Matrix	6 = 2.0	Mica	2 = 0.6
Organics	0 = 0.0	Fossils	0 = 0.0

Well sorted, subrounded, upper to lower fine-grained feldspathic arenite with interparticle porosity. A lot of the quartz grains have overgrowths. The cement in this section looks like fragments or grains which are approximately the same size as the mineral grains. There is not very much mica in this sample so that which is listed as Fe-oxide could be organic material.

140-EH85A--300 point count.

Constituent	Number = Percent	Constituent	Number = Percent
Quartz	110 = 36.6	Polyxlline Quartz	21 = 7.0
Feldspar	78 = 26.0	Fe-oxide	3 = 1.0
Lithics	0 = 0.0	Chert	5 = 1.6
Cement	1 = 0.3	Porosity	52 = 17.3
Matrix	20 = 6.6	Mica	1 = 0.3
Organics	9 = 3.0	Fossils	0 = 0.0

Very well sorted, subangular to subrounded, lower fine-grained feldspathic arenite with interparticle porosity. Some of the quartz grains have overgrowths. Both organic material and Fe-oxides can be found in this thin section. The organics are a reddish brown and the Fe-oxides are black and are associated with disintegrating biotite fragments.

265-RP18--300 point count.

Constituent	Number = Percent	Constituent	Number = Percent
Quartz	35 = 11.6	Polyxlline Quartz	1 = 0.3
Feldspar	54 = 18.0	Fe-oxide	1 = 0.3
Lithics	0 = 0.0	Chert	8 = 2.6
Cement	86 = 28.6	Porosity	16 = 5.3
Matrix	78 = 26.0	Mica	2 = 0.6
Organics	5 = 1.6	Fossils	14 = 4.6

Well sorted, angular, lower very fine-grained feldspathic wacke with a lot of biotics, some of which are calcite replaced. The biotics are oriented parallel to fractures. Most of the porosity is fracture porosity but there is also some interparticle porosity. The feldspars are so highly altered that it is difficult to determine whether they should be considered a feldspar grain or calcite cement. Because of this, the point count may be skewed toward cement.

282-RP35--300 point count.

Constituent	Number = Percent	Constituent	Number = Percent
Quartz	79 = 26.3	Polyxline Quartz	1 = 0.3
Feldspar	59 = 19.6	Fe-oxide	4 = 1.3
Lithics	1 = 0.3	Chert	7 = 2.3
Cement	99 = 33.0	Porosity	17 = 5.6
Matrix	25 = 7.6	Mica	9 = 3.0
Organics	0 = 0.0	Fossils	1 = 0.3

Well sorted, subangular, upper fine-grained to upper very fine-grained feldspathic arenite with interparticle and mesovuggy porosity. The matrix of this section looks like it has undergone aggrading neomorphism from micrite to microspar. Most of the feldspar grains in this sample are only slightly altered. The porosity count may be low because it occurs as tiny spots randomly scattered throughout the cement. The porosity stain can also be seen on top of mineral fragments which were counted as grain.

424-AA25--300 point count.

Constituent	Number = Percent	Constituent	Number = Percent
Quartz	94 = 31.3	Polyxlline Quartz	4 = 1.3
Feldspar	108 = 36.0	Fe-oxide	10 = 3.3
Lithics	3 = 1.0	Chert	6 = 2.0
Cement	14 = 4.6	Porosity	46 = 15.3
Matrix	4 = 1.3	Mica	10 = 3.6
Organics	0 = 0.0	Fossils	0 = 0.0

Well sorted, angular, upper to lower fine-grained feldspathic arenite with interparticle porosity. Some of the quartz grains have abraided overgrowths and the feldspars are highly altered. The micas are oriented perpendicular to the up direction and, where there is a concentration of biotite fragments, it seems that a lot of them have been altered to Fe-oxides.

451-AA52--Peloidal quartz mudstone with very few fossil fragments and no obvious open porosity. There are a few random fragments of Fe-oxide or organic material and there seems to be some solution enlarged cement filled microvuggy porosity. Some of the micritic matrix has been neomorphosed to microspar.

479-CC4--Peloidal mudstone that has been interlaminated with silty peloidal mudstone. There is no open porosity and some of the matrix has undergone aggrading neomorphism from micrite to microspar.

608-RC2--300 point count.

Constituent	Number = Percent	Constituent	Number = Percent
Quartz	70 = 23.3	Polyxlline Quartz	2 = 0.6
Feldspar	86 = 28.6	Fe-oxide	9 = 2.9
Lithics	7 = 2.6	Chert	5 = 1.6
Cement	98 = 32.6	Porosity	9 = 3.0
Matrix	11 = 3.6	Mica	3 = 1.0
Organics	0 = 0.0	Fossils	0 = 0.0

Well sorted, subangular, lower medium-grained to lower fine-grained feldspathic arenite with interparticle and vuggy porosity and poikilotopic calcite cement. The feldspars in this section vary from being clean to highly altered. Most of the lithics looked like quartz grains with altered feldspar lathes in them.

632-RC17--Mudstone with about 15 percent organic filled wispy fracture porosity. Much of the matrix of this thin section has undergone aggrading neomorphism from micrite to microspar. (Percentage is a visual estimate only).

638-RC32--Mudstone that looks like a small scale turbidity sequence that coarsens upward within each layer but fines upward through the whole sequence. Part of this sequence has been fractured and brecciated and has been injected with a silty mudstone. There is about 1 percent open fracture porosity. There is also a stylolite through this section that looks like it has organic material and/or Fe-oxides concentrated along it. (Percentage is a visual estimate only).

GB2--Interlaminations of well sorted, subangular, very fine-grained quartz wacke with some fossil fragments, micrite clasts (very few), about 50 percent calcite cement (after micrite) and silty mudstone. Mica fragments are evenly distributed throughout the whole section. There is not any obvious open porosity but the entire thin section has a blue tinge from the porosity staining, especially in the sandy areas.

J3--300 point count.

Constituent	Number = Percent	Constituent	Number = Percent
Quartz	68 = 22.6	Polyxlline Quartz	1 = 0.3
Feldspar	59 = 19.6	Fe-oxide	2 = 0.6
Lithics	12 = 4.0	Chert	3 = 1.0
Cement	48 = 16.0	Porosity	42 = 14.0
Matrix	54 = 18.0	Mica	10 = 3.3
Organics	0 = 0.0	Fossils	1 = 0.3

Well sorted, subrounded, lower fine-grained to lower very fine-grained feldspathic wacke with interparticle porosity. This rock is very dirty and the edges of many of the altered grains are blurred into the cement or matrix. Consequently, the cement and matrix counts may be a little high.

2nd J7--300 point count.

Constituent	Number = Percent	Constituent	Number = Percent
Quartz	101 = 33.6	Polyxlline Quartz	8 = 2.6
Feldspar	62 = 20.6	Fe-oxide	0 = 0.0
Lithics	12 = 4.0	Chert	9 = 3.0
Cement	58 = 19.3	Porosity	45 = 15.0
Matrix	2 = 0.6	Mica	3 = 1.0
Organics	0 = 0.0	Fossils	0 = 0.0

Well sorted, subrounded, lower medium-grained to lower fine-grained feldspathic arenite with interparticle and mesovuggy porosity and poikilotopic calcite cement. There are some quartz overgrowths and the feldspar grains are clean to moderately altered. The porosity count may be low because numerous large vugs were not crossed during counting.

4th J7--Well sorted, subangular, lower medium-grained to upper fine-grained feldspathic arenite with some fragments of mica as well as grains of feldspar and chert. About 50 percent poikilotopic calcite cement-filled interparticle porosity. Only about 1 percent of the viewing area is open interparticle porosity. (Percentages are visual estimates only).

4th J7 with clasts--300 point count.

Constituent	Number = Percent	Constituent	Number = Percent
Quartz	58 = 19.3	Polyxlline Quartz	8 = 2.6
Feldspar	60 = 20.0	Fe-oxide	2 = 0.6
Lithics	43 = 14.3	Chert	16 = 5.3
Cement	110 = 36.6	Porosity	0 = 0.0
Matrix	2 = 0.6	Mica	1 = 0.3
Organics	0 = 0.0	Fossils	0 = 0.0

Well sorted, angular to subangular, upper medium-grained to upper fine-grained feldspathic arenite with interparticle and moldic porosity. There are also some micritic/fossiliferous clasts and some random bivalve(?) fragments.

RC?--Peloidal and micritized ostracodal packstone with 5 percent quartz grains and some solution enlarged cement reduced inter- and intraparticle porosity. This grades upward into a peloidal wackestone with 15 percent quartz grains and the same porosity. A few of the quartz grains in this section are polycrystalline. Many of the peloids look like intraclasts or superficially coated grains. (Percentages are visual estimates only).

11-10-12-1a--300 point count.

Constituent	Number = Percent	Constituent	Number = Percent
Quartz	103 = 34.3	Polyxline Quartz	0 = 0.0
Feldspar	58 = 19.3	Fe-oxide	1 = 0.3
Lithics	12 = 4.0	Chert	8 = 2.6
Cement	95 = 31.6	Porosity	15 = 5.0
Matrix	6 = 2.0	Mica	1 = 0.3
Organics	1 = 0.3	Fossils	0 = 0.0

Very well sorted, subangular, lower medium-grained to upper fine-grained feldspathic arenite with interparticle and moldic porosity and poikilotopic calcite cement. Some of the quartz grains have overgrowths and the feldspars vary from clean to highly altered.

11-10-12-2--300 point count.

Constituent	Number = Percent	Constituent	Number = Percent
Quartz	89 = 29.6	Polyxline Quartz	0 = 0.0
Feldspar	52 = 17.3	Fe-oxide	1 = 0.3
Lithics	23 = 7.6	Chert	2 = 0.6
Cement	115 = 38.3	Porosity	16 = 5.3
Matrix	0 = 0.0	Mica	2 = 0.6
Organics	0 = 0.0	Fossils	0 = 0.0

Very well sorted, subangular, lower medium-grained to upper fine-grained feldspathic arenite with interparticle and moldic porosity and poikilotopic calcite cement. Most of the lithics look like quartz with altered feldspar laths embedded in them. The porosity count may be slightly low because the porosity stain often coated grains that didn't have obvious holes between them. These were counted as grains.

11-10-12-3a--300 point count.

Constituent	Number = Percent	Constituent	Number = Percent
Quartz	67 = 22.3	Polyxlline Quartz	3 = 1.0
Feldspar	79 = 26.3	Fe-oxide	2 = 0.6
Lithics	10 = 3.3	Chert	4 = 1.3
Cement	103 = 34.3	Porosity	30 = 10.0
Matrix	1 = 0.3	Mica	1 = 0.3
Organics	0 = 0.0	Fossils	0 = 0.0

Well sorted, angular, upper medium-grained to upper fine-grained feldspathic arenite with interparticle, mesovuggy and fracture porosity and poikilotopic calcite cement. There are some quartz overgrowths and the feldspar grains vary from being clean to highly altered. The lithics seem to be both metamorphic (schist) and igneous (quartz with feldspar laths).

11-10-13-1b--300 point count.

Constituent	Number = Percent	Constituent	Number = Percent
Quartz	80 = 26.6	Polyxlline Quartz	2 = 0.6
Feldspar	80 = 26.6	Fe-oxide	5 = 1.6
Lithics	1 = 0.3	Chert	2 = 0.6
Cement	2 = 0.6	Porosity	75 = 25.0
Matrix	23 = 7.6	Mica	30 = 10.0
Organics	0 = 0.0	Fossils	0 = 0.0

Very well sorted, subangular, lower fine-grained to lower very fine-grained feldspathic arenite with interparticle and moldic porosity. The mica fragments are oriented roughly parallel to the low angle laminations that are evident in hand sample.

11-10-13-1c--300 point count.

Constituent	Number = Percent	Constituent	Number = Percent
Quartz	90 = 30.0	Polyxlline Quartz	0 = 0.0
Feldspar	46 = 15.3	Fe-oxide	3 = 1.0
Lithics	38 = 12.6	Chert	5 = 1.6
Cement	6 = 2.0	Porosity	68 = 21.9
Matrix	32 = 10.6	Mica	14 = 4.6
Organics	0 = 0.0	Fossils	0 = 0.0

Moderately sorted, angular to subrounded, lower medium-grained to lower very fine- grained feldspathic arenite with interparticle, moldic and vuggy porosity. The lithics are peloids with very small fragments of quartz, feldspar, mica, Fe-oxide and some fossil hash. The larger fragments of mica in this section are oriented roughly perpendicular to the up direction of the section.

11-10-13-1f--300 point count.

Constituent	Number = Percent	Constituent	Number = Percent
Quartz	72 = 24.0	Polyxlline Quartz	0 = 0.0
Feldspar	73 = 24.3	Fe-oxide	8 = 2.6
Lithics	0 = 0.0	Chert	3 = 1.0
Cement	6 = 2.0	Porosity	98 = 32.6
Matrix	22 = 7.3	Mica	18 = 6.0
Organics	0 = 0.0	Fossils	0 = 0.0

Very well sorted, subrounded, upper fine-grained to upper very fine-grained feldspathic arenite with interparticle porosity. There is very little obvious cement and the feldspars are slightly to highly altered. The mica fragments in this thin section are oriented roughly parallel to the low angle laminations that are evident in hand sample. The porosity count may be high because of overcompensation for the occurrence of porosity stain on top of mineral grains.

21-DN21--Fossiliferous wackestone to packstone with ostracod and gastropod fragments. There is compaction breakage of the ostracodes and the matrix is organic rich. There are solution enlarged spar filled intraparticle porosity and there is about 3 percent solution enlarged fracture porosity. (Percentage is a visual estimate only.)

36-DN36--Wackestone with organic rich matrix, 20 percent potato chip looking fossils and 10 percent wispy fracture porosity. (Percentages are visual estimates only).

438-AA39--Mudstone with about 5 percent fossil fragments and some solution enlarged cement filled mesomoldic and microvuggy porosity. There is one small open fracture and some random bits of organic material or Fe-oxide.

MB1-A--Algal and micritic concretions around something, possibly twigs(?), which has since been dissolved. Some of the micrite has also been dissolved. The resulting porosity has been filled in by a pore reducing microspar then by a pore filling poikilotopic calcite cement. There was a secondary dissolution of some of the micrite and cement leaving mesovuggy pore spaces, some of which have been filled in with organic material.

APPENDIX B

Lower Green River - Willow Creek

Date logged: March 25, 1994

Logged by: Tom Morris, Ann Garner, and undergrads, Spring - '92, '93

Datum elevation: 0.00 m

Remarks: Section was measured along road outcrops of Hwy 33 (191) on the south flank of the Roan Cliffs. Section begins in NW1/4 if SE1/4 of Sec. 23, T11S, R8W, Matts Summit 7 1/2 Minute Quadrangle and ends in W1/2 of SE1/4 of Sec. 11, T7S, R8W, Jones Hole 7 1/2

LEGEND

LITHOLOGY

 Sand/Sandstone  Silty Sand  Silt/Siltstone  Sandy Silt  Shaley Silt  Shale	 Sandy Shale  Silty Shale  Mud/Mudstone  Organic Shale with int  Oil Shale  Matrix Supported	 Silty Limey Mudstone  Ash  Limestone  Dolomite  Dolomitic Lst  Limey Mudstone	 Dolomitic Mudstone  Chert  Silty Limestone  slope cover  Sandy Limestone  Graded Pebble Conglom
--	---	---	---

CONTACTS

 Sharp	 Scoured	 Uncertain	 Undulating
---	---	---	--

PHYSICAL STRUCTURES

 Ripple Lamination	 Trough Cross-strat.	 Planar Lamination
 High Angle Tabular Bedding	 Low Angle Tabular Bedding	 Flaser Bedding
 Wavy Parallel Bedding	 Lenticular Bedding	 Convolute Bedding
 Scour	 Reverse Graded Bedding	 Mud Cracks
 Synaeresis Cracks	 Load Casts	 Stylolites
 Low angle trough cross sets	 Rip-up lag	 Flute Casts

LITHOLOGIC ACCESSORIES

 Sand Lamina	 Silt Lamina	 Shale Lamina
 Pebbles/Granules	 Coal Lamina	 Organic Shale Lamina
 Calcareous	 Dolomitic	 Cherty
 Fe Ferruginous	 Rip Up Clasts	 Micaceous
 Fecal Pellets	 Anhydritic	
 Silty	 Concretion/Nodule	

ICHTHOFOSSILS

^^ Hootlets
 UU Inclined Burrows

v Vertical Burrows

┌ Undifferentiated Bioturbation

FOSSILS

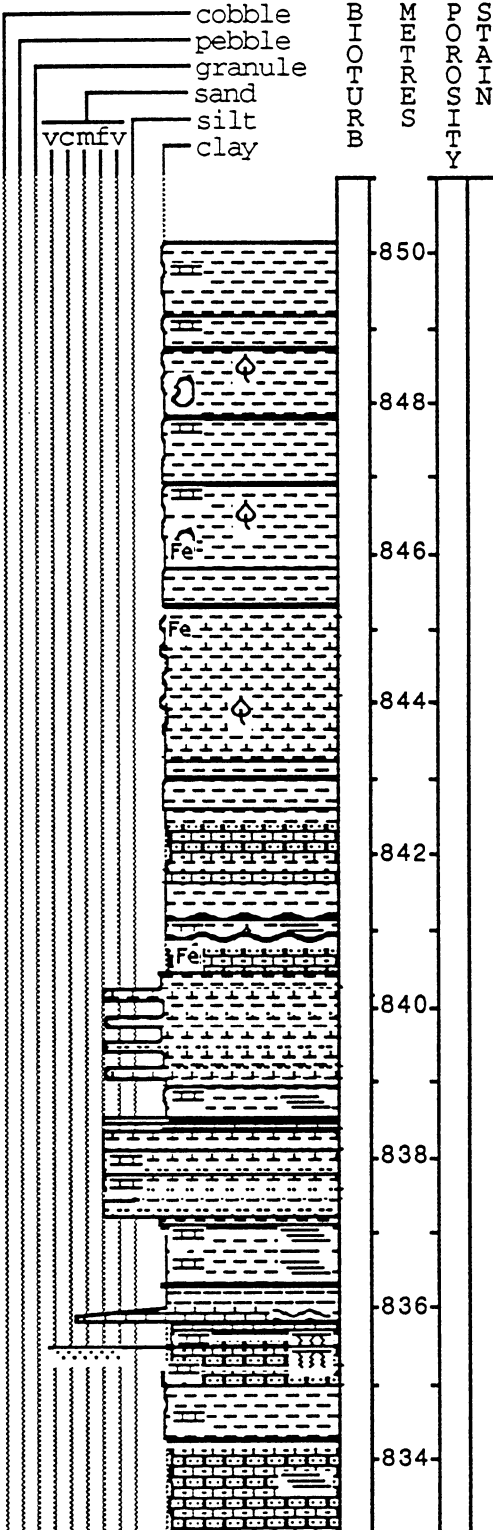
Algal Stromatolite
 Gastropods
 Vertebrates

Fish Remains
 Ostracods

Molluscs (undifferentiated)
 Plant Remains

GRAIN SIZE

cobble
 pebble
 granule
 sand
 silt
 clay



Three lenticular limestone interbeds (2 cm. thick)

Banded - 8 to 12 cm. thick in "cycles"

Color banded

Unit contains bands of fine-grained sand that are 2 mm. thick; pyrite blebs

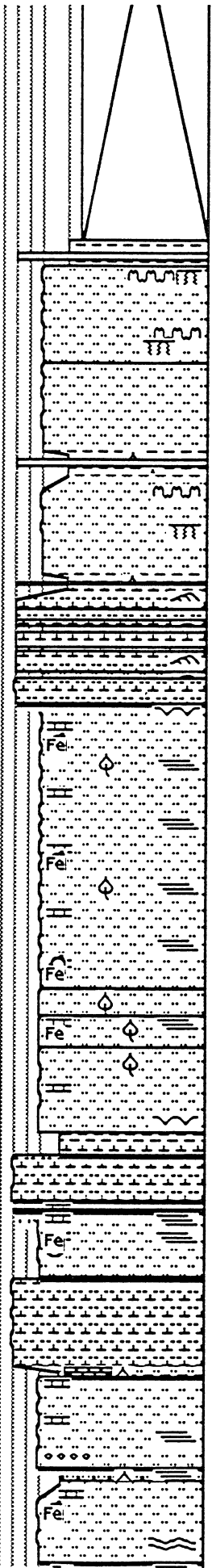
Sandy, pyritic dolomite; fills syneresis cracks of lower bed

Sandy, pyritic dolomite that pinches out and swells

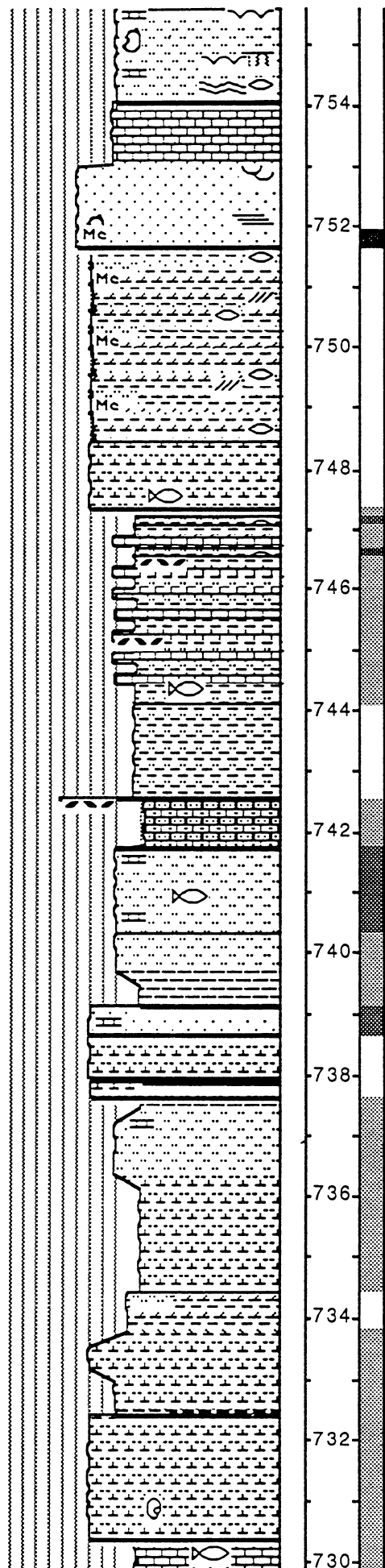
Syneresis cracks at top of unit are filled by overlying unit but do not penetrate the claystone interbeds

Color bands 8-12 cm. thick and are somewhat "cyclic"; pyrite nodules in a 5 cm. band midway up the unit; top is vertical

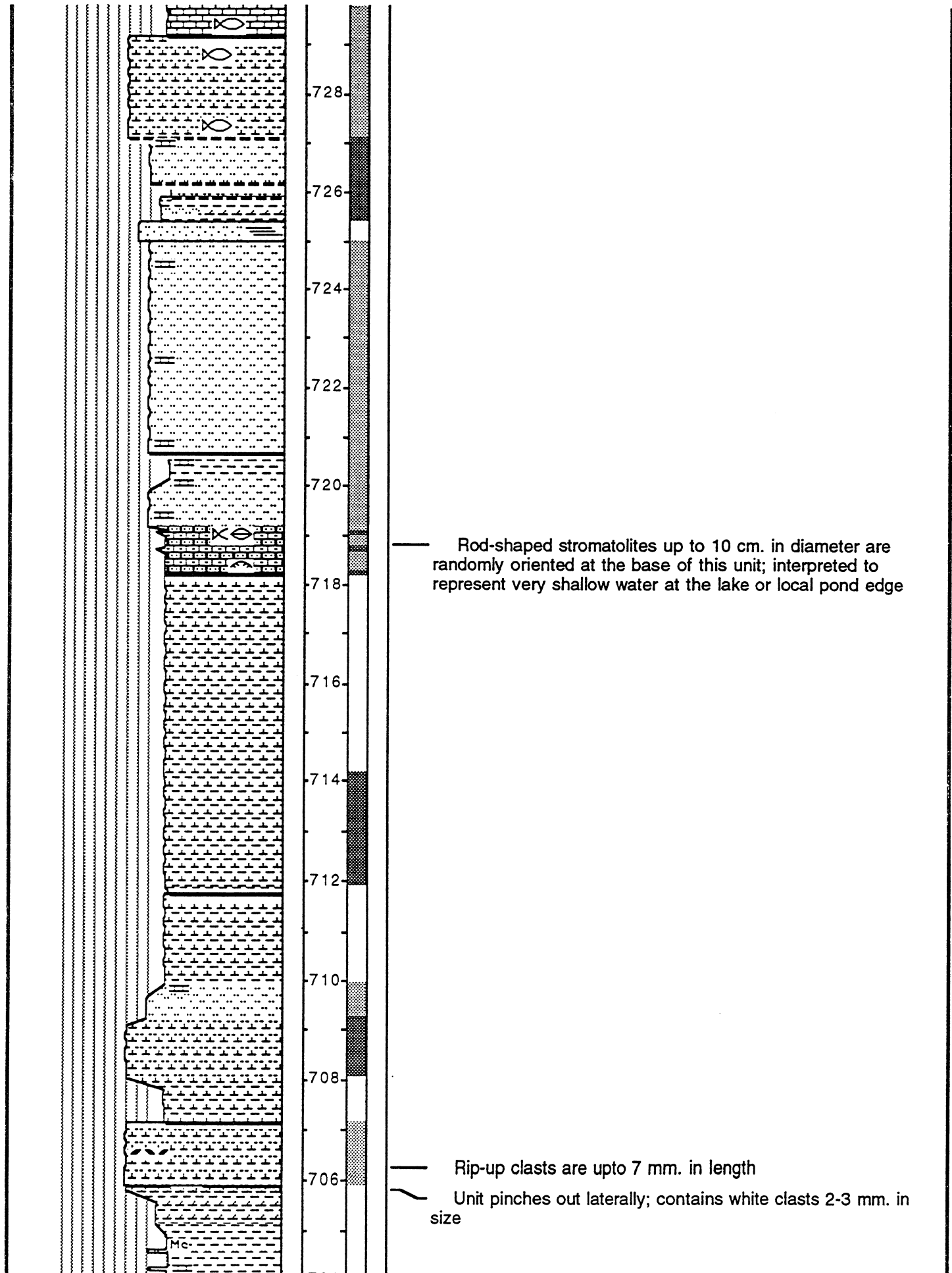
780
778
776
774
772
770
768
766
764
762
760
758
756

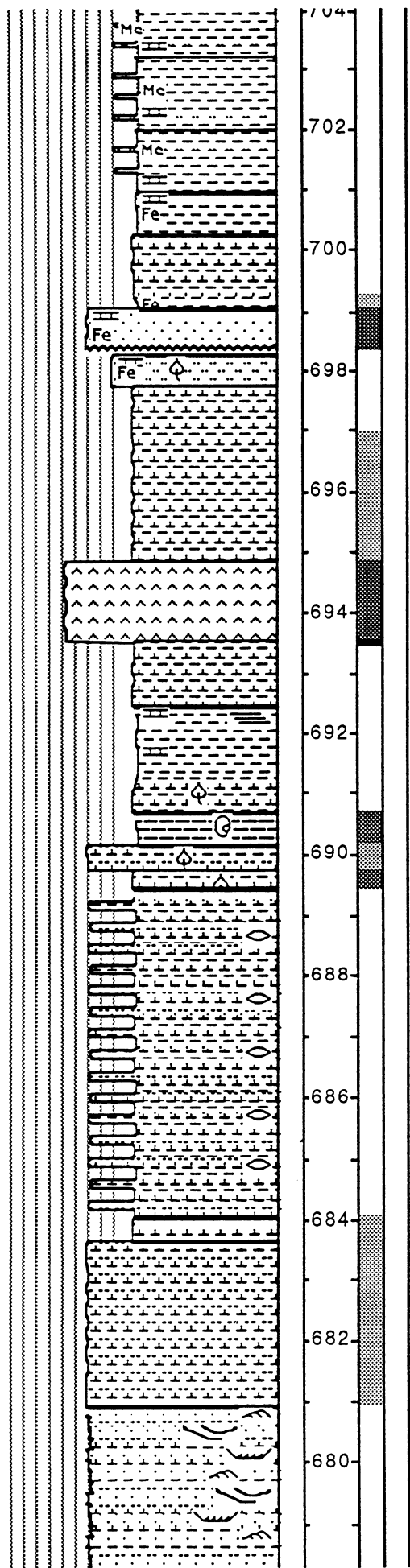


- Black-brown shale
- Black-brown shale
- Thin Sections 638-RC32 A and 638-RC32B; Syneresis dikes and stylolites within this varved-like unit
- Black-brown shale
- Black-brown shale
- Syneresis dikes and stylolites are found within this varved-like unit
- Black-brown shale
- Paper shale with woody fragments
- Hematite-filled fractures
- Some hematite filled fractures
- Thin Section 623-RC17; Oil shale; varve-like laminations; faintly odoriferous; Mahagony Marker(?)
- Carbon staining from organic matter
- Basal 2 cm. is a poorly sorted matrix supported pebble conglomerate
- Upper portion contains "organic hash"

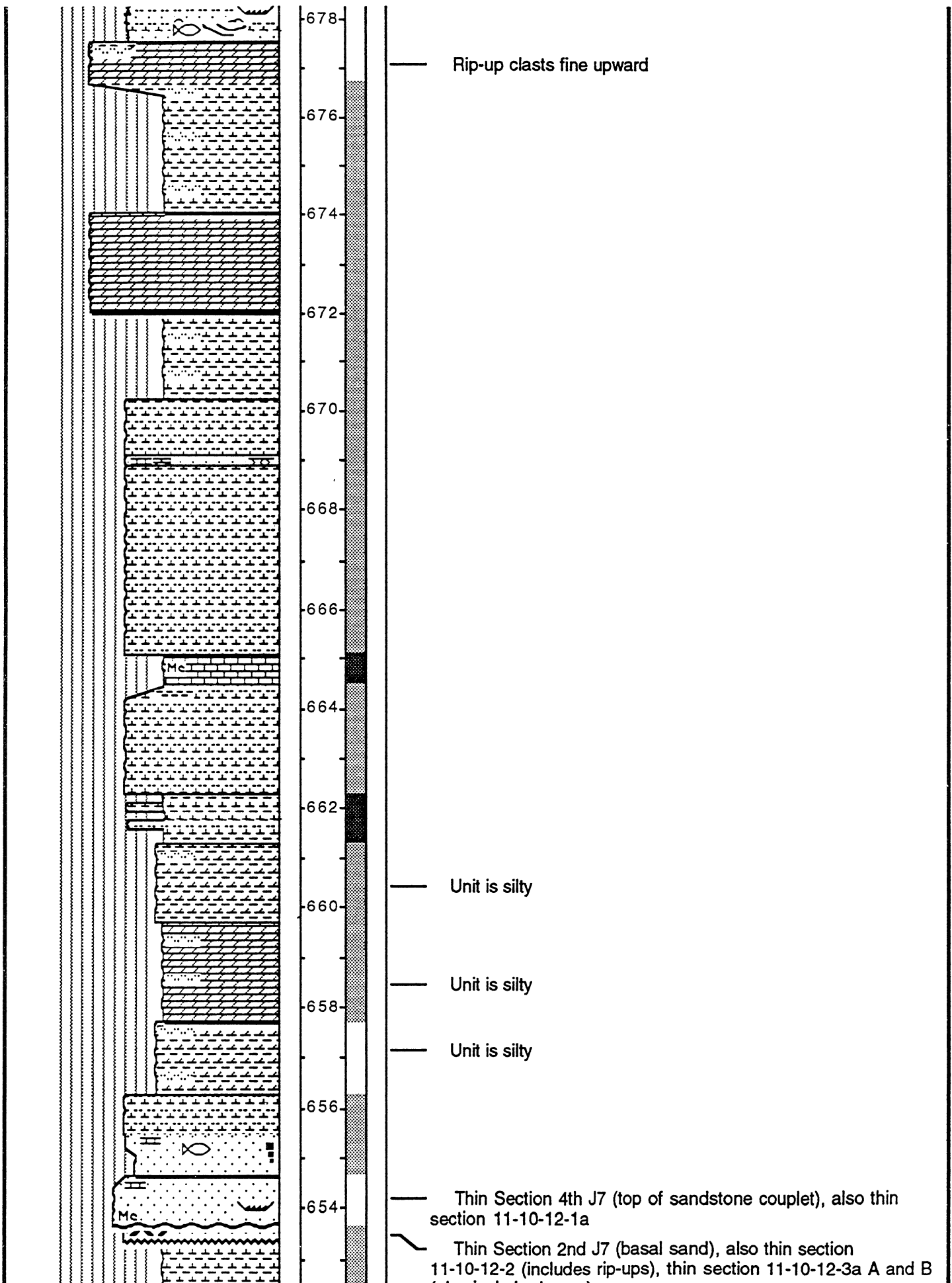


- Unit has 1-3 cm. iron concretions; syneresis dikes (possibly mud cracks) are found within this unit and are filled with the same lithology
- Limestone clasts (upto 3 cm. in diameter) and shell hash packstone occasionally tar saturated; note that tar within unit pinches and swells and is not ubiquitous
- There is a large channel-form sandstone (with mudstone drape) complex laterally offset from the sections measured; the complex shows lateral and vertical accretion of thin bedded sandstone and mudstone; sandstones are very fine-grained; moderate porosity
- Thin Section 608-RC2; Tar sand with some zones being odoriferous; contains iron and mica-rich concretions
- Interbeds of silty mudstone and fossiliferous (fish scales) carbonate rip-up limestone packstone; upper portion of unit has interbeds of sandy limestone
- 5 cm. thick bed with rip-up clasts upto 7 mm. in diameter
- Laterally equivalent unit was sampled - Thin Section GB2 (this unit has pebble conglomerate rip-ups)

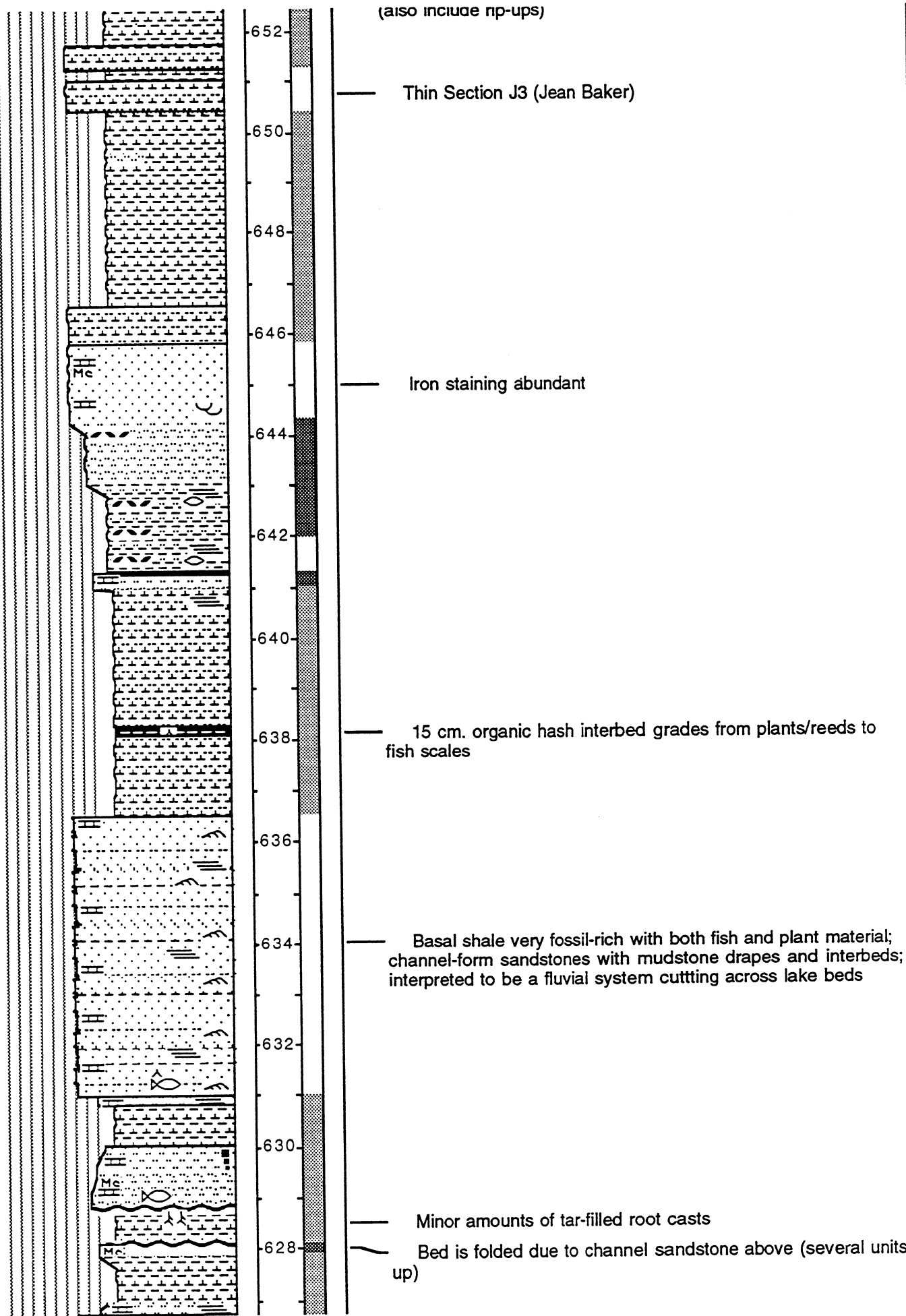




- Grayish brown blotches that do not fizz
- Flat yellow-orange clasts 3 mm. in size; iron flecks and dendritic staining
- Thins and pinches out laterally
- Gritty ash with poorly sorted and irregular shaped carbonate(?) clasts that compose up to 20% of the rock, average size of clast is 3 mm.
- Thin Section H-10
- Alternating layers of limy mudstone (60% and recessive) and silty limy mudstone; the silty limy mudstones (40%) form more resistive lensoidal bodies from 6 cm. to 50 cm. in thickness, several are very flat bottomed with crested tops that give the appearance of preserved large foresets as in a bar; biotite flakes in the silty limy mudstone; Tentative interpretation is a storm/wave generated near shore bar (upper shoreface)



(also include np-ups)



Thin Section J3 (Jean Baker)

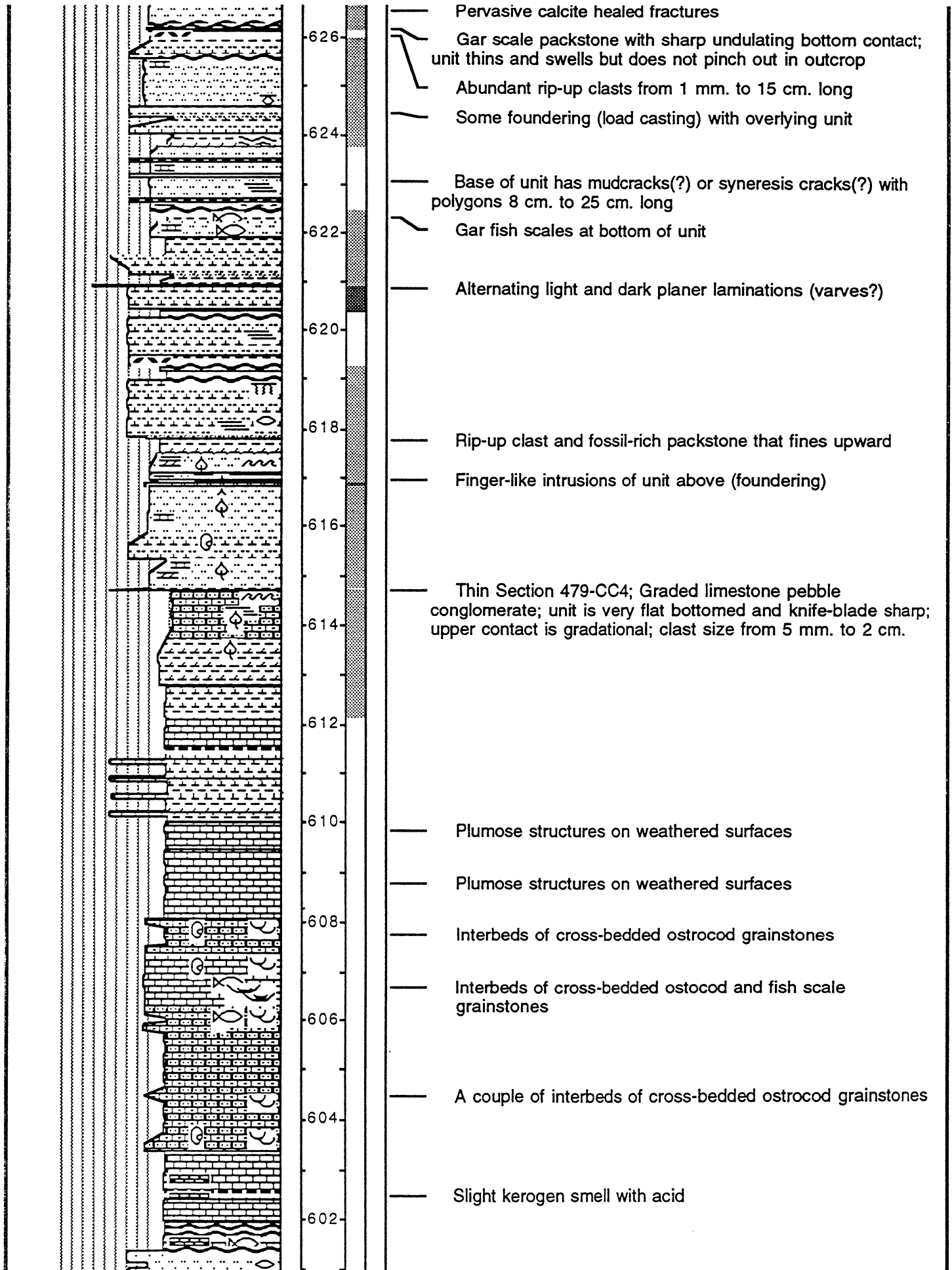
Iron staining abundant

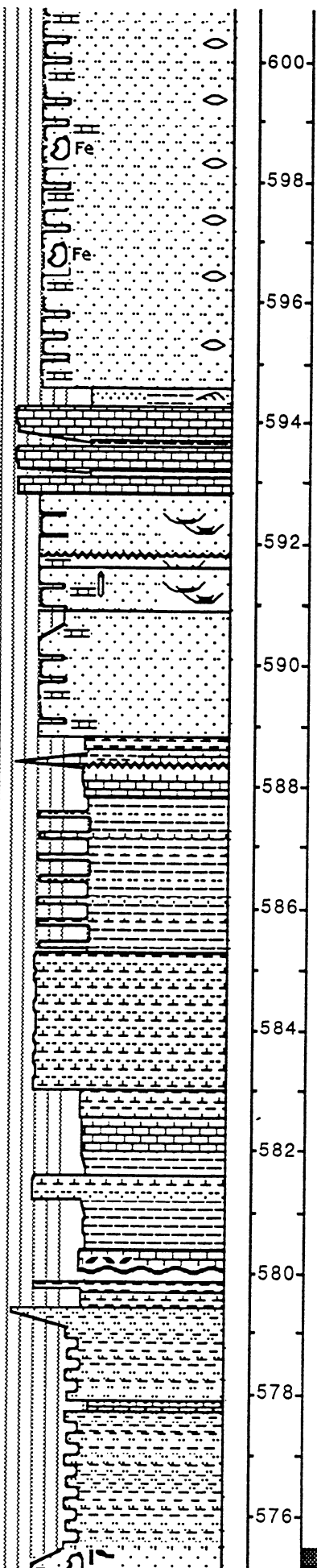
15 cm. organic hash interbed grades from plants/reeds to fish scales

Basal shale very fossil-rich with both fish and plant material; channel-form sandstones with mudstone drapes and interbeds; interpreted to be a fluvial system cutting across lake beds

Minor amounts of tar-filled root casts

Bed is folded due to channel sandstone above (several units up)





- Sigmoidal and lensoidal sandstone channel-forms scour the underlying mudstone but not the sandstone

- White limestone bed has a laminae of gar fish scales; light gray limestone has cross beds of bone and organics, uppermost layer is orange colored similar to the ash bed farther down in the section

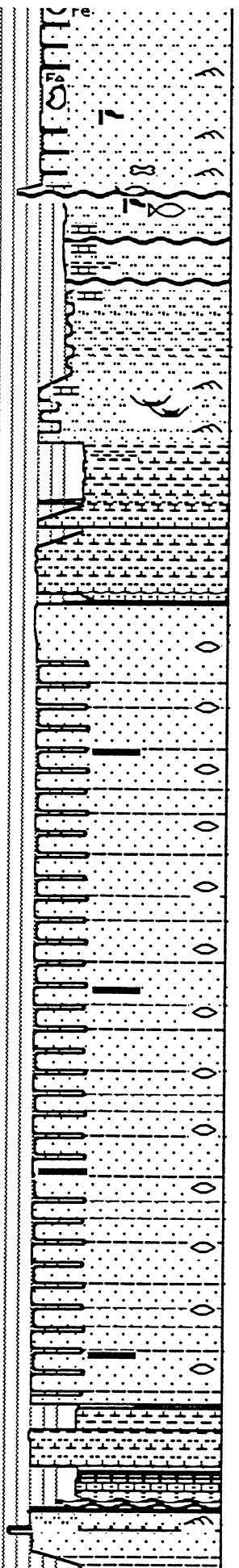
- Multilateral accretion sets; bone fragment and gar scales in channel; skolithos on top of channel sandstone

- Thin Section 451-AA52

- Finely crystalline limestone

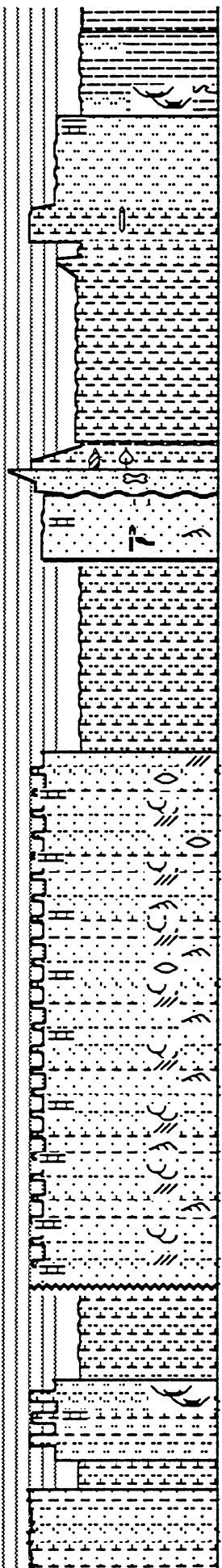
- Clay rip-ups dip 20 degrees to the south

- Weathered surface has "leopard" spots and good plumose fracture surfaces



574
572
570
568
566
564
562
560
558
556
554
552
550

- Vertical burrows up to 7mm in diameter
- Channel-form sandstones and interbedded siltstones; alligator tooth at the base
- Calcite replaced fish vertebrae
- Greenish gray and gray-red alternating beds
- Red bed
- Fresh color changes from red to gray
- Thickens toward a channel to the south; interpreted to be a splay sandstone
- Thin Section 424-AA25; Lensoidal and sigmoidal channel-form sandstones with mudstone/siltstone drapes. Coal lenses are less than 4 mm. thick
- Weathered surface has excellent plumose structures



— Turtle bone, mammal limb bone, and another tumbled bone at upper contact

— Alternating red and green beds

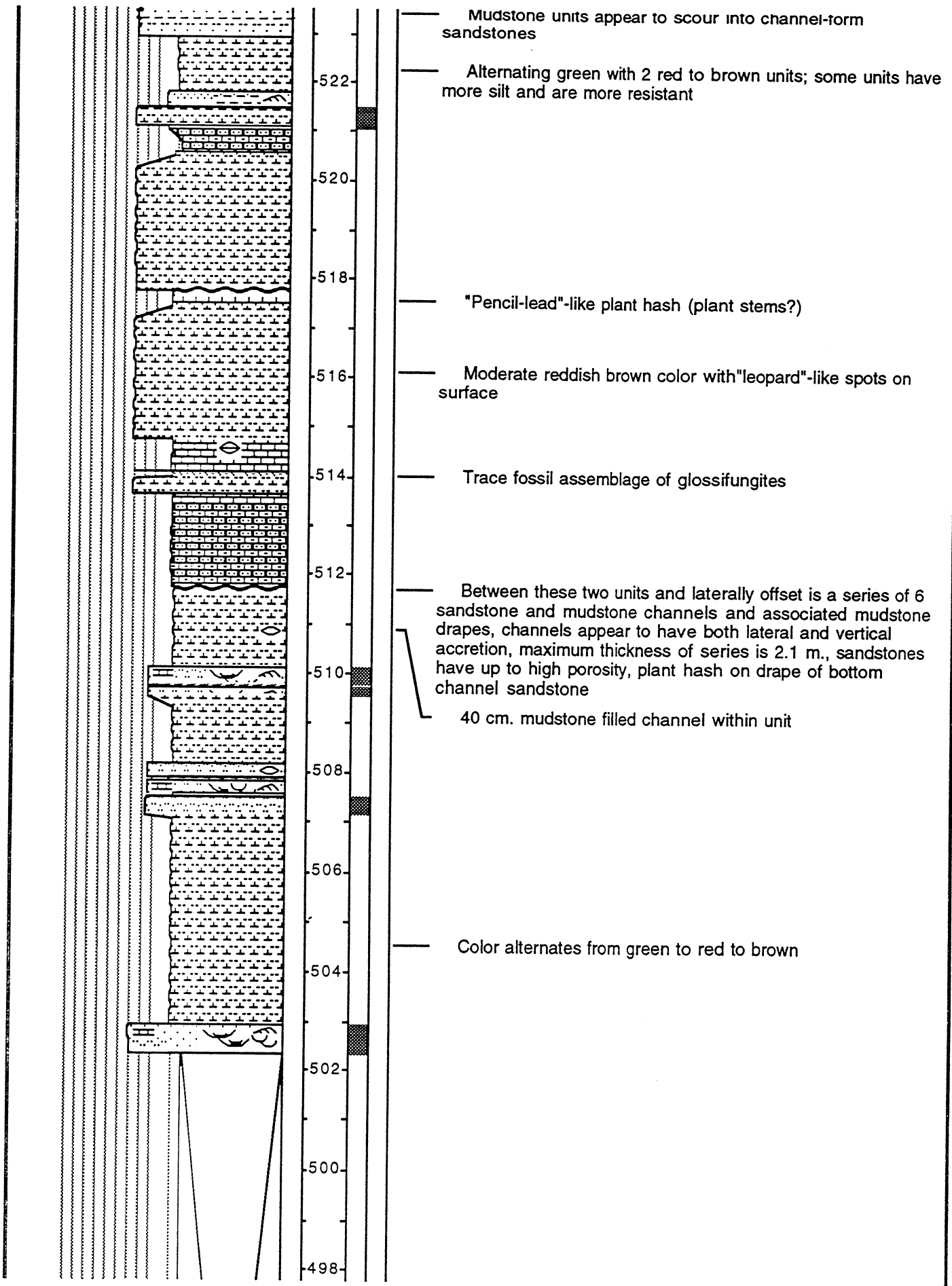
— Thin Sections 11-10-13-1b (middle of channel-form sandstone above a 7 inch lag deposit), 11-10-13-1c (channel-form lag deposit), 11-10-13-1f (top of channel-form sandstone 1.5 inches above sample 11-10-13-1b, a fossil log was directly above this sample); Two large aggrading channel complexes compose this unit; mudstones are variegated in color

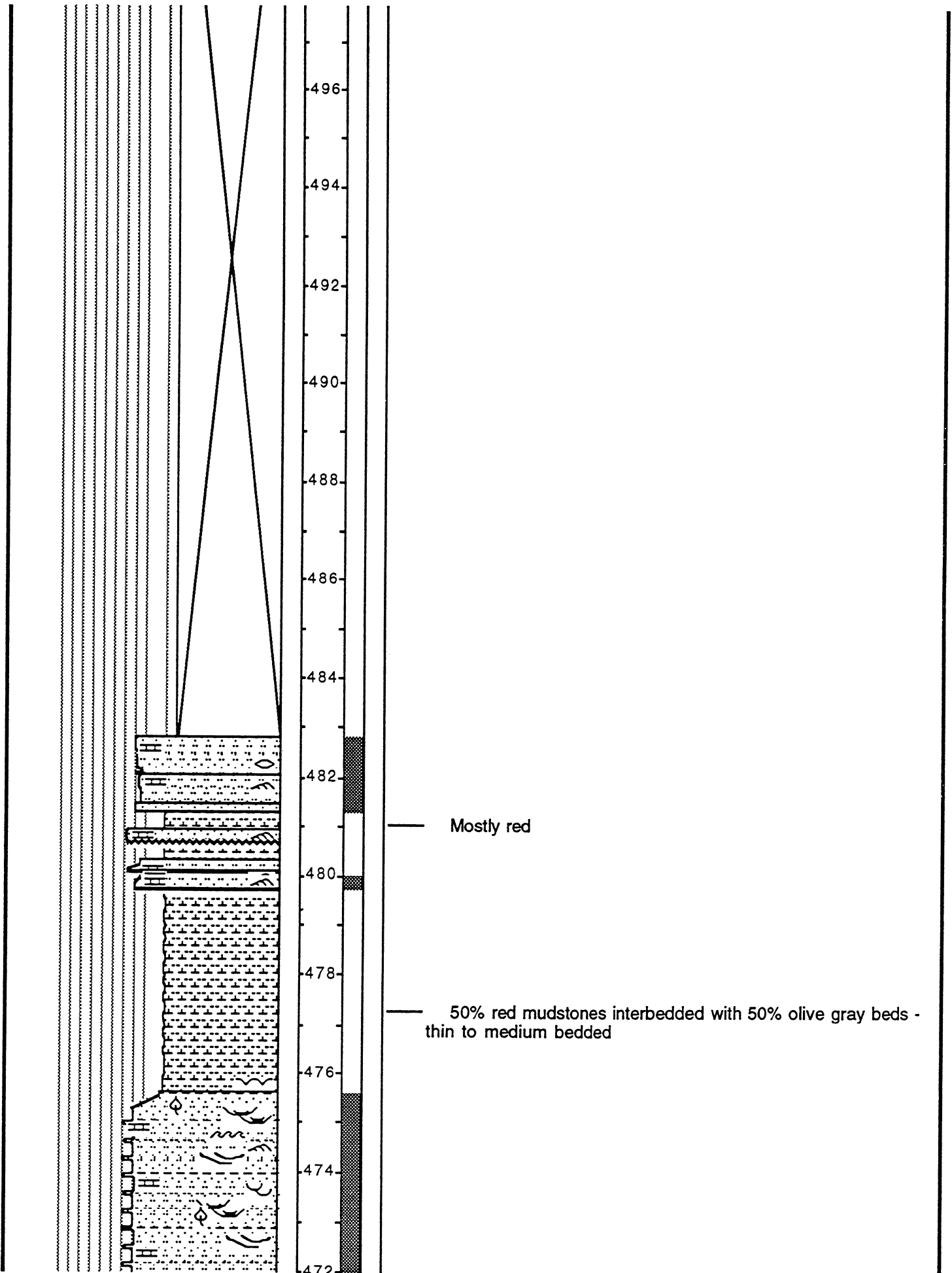
— Interbeds of reds, maroons, purples, and greens; upper contact scoured by overlying sandstones

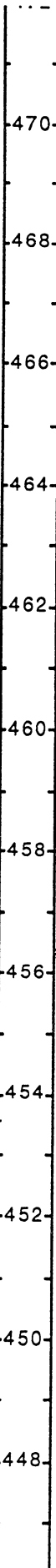
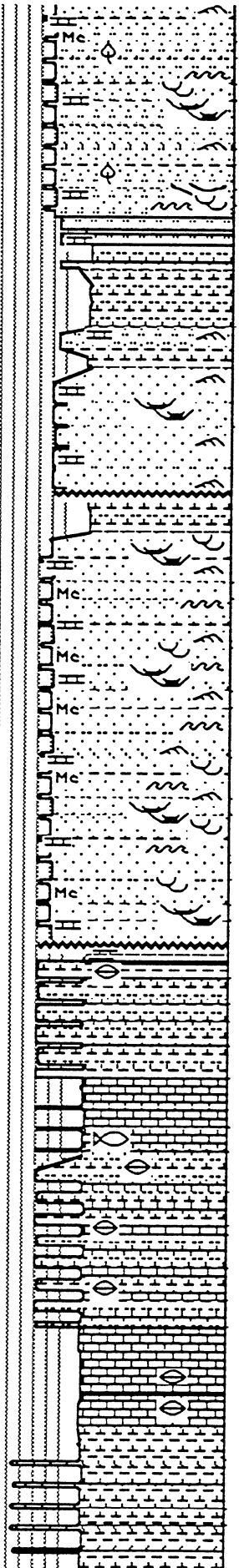
— Undulatory contacts between alternating green and red thin beds

— Blotchy green in uppermost red mudstone channel-form unit

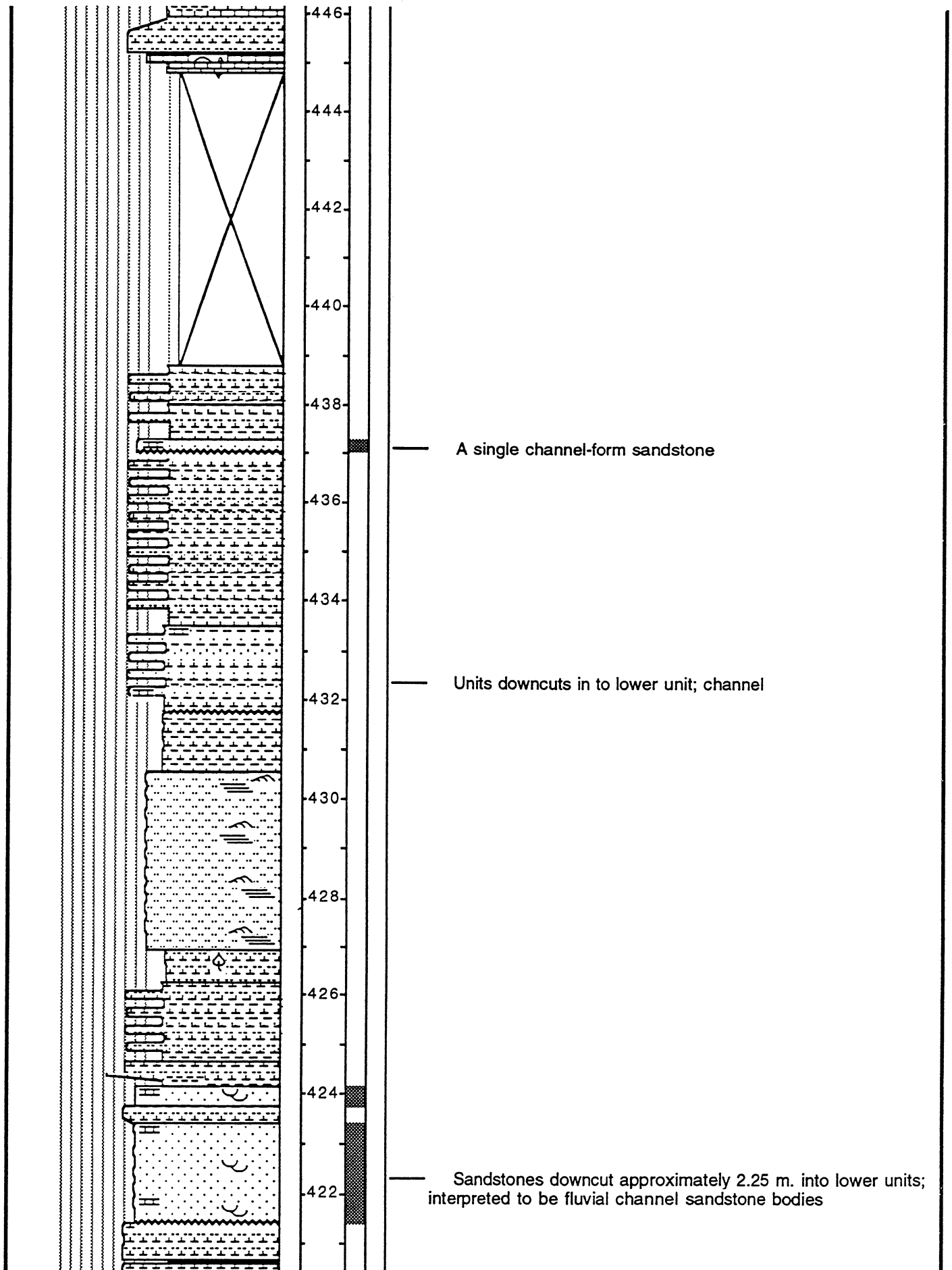
— Alternating red and green beds

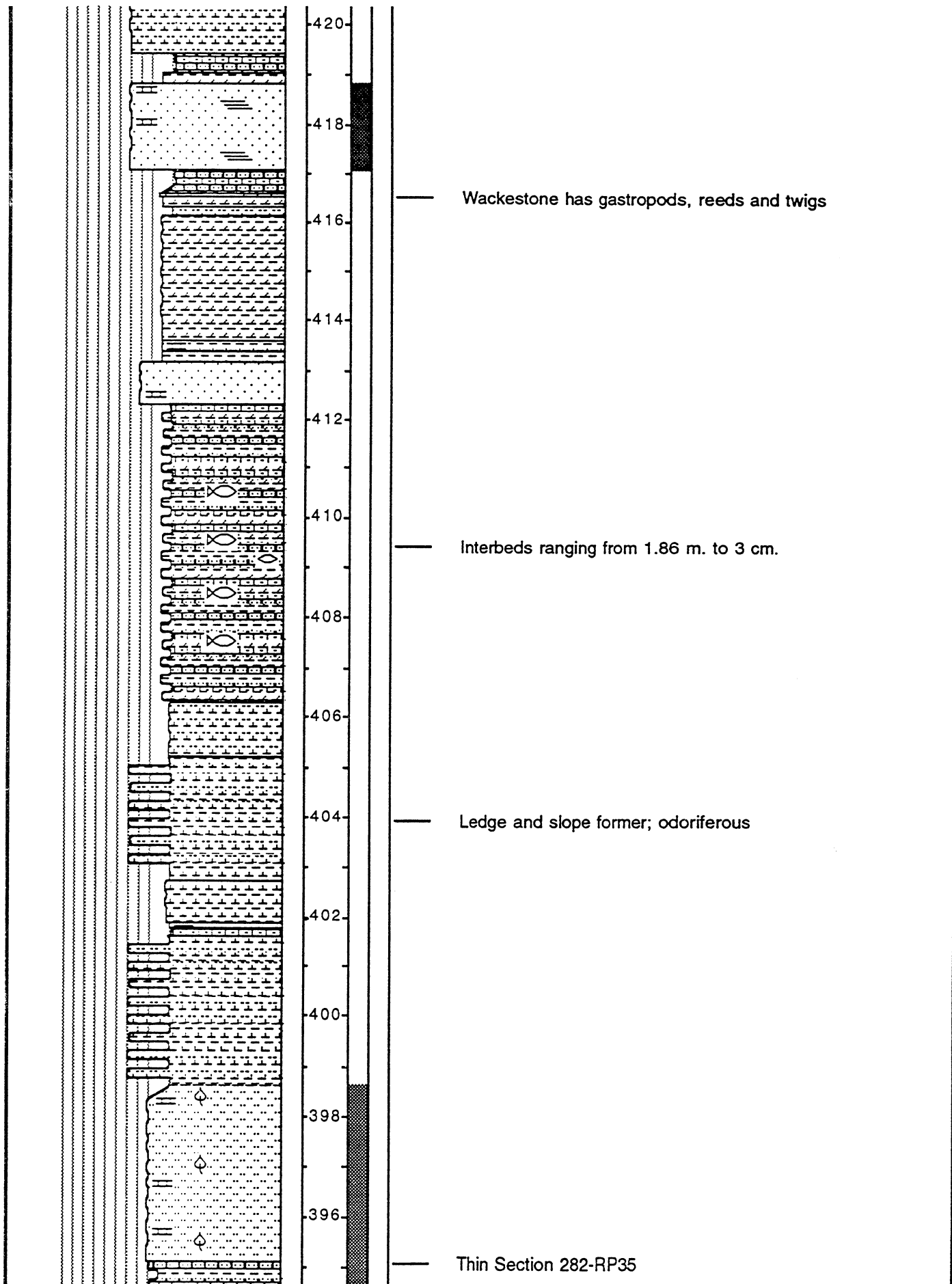


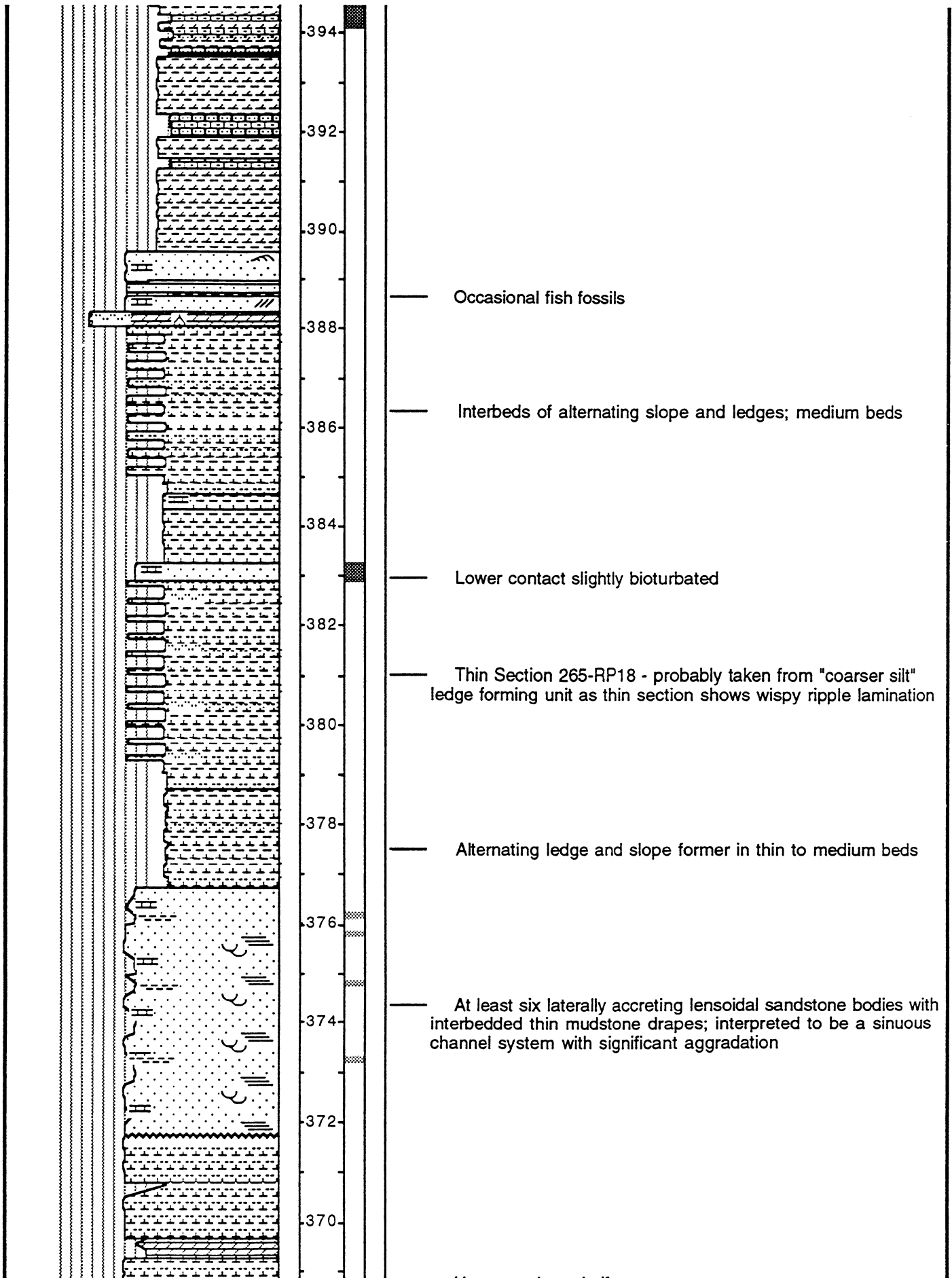




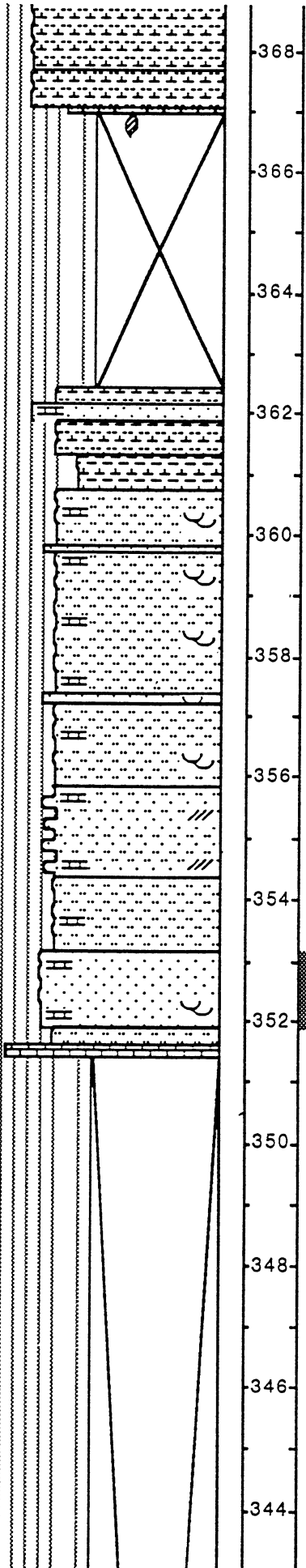
- Broad swaley beds of siltstone and discontinuous broad lenses of mudstone
- Individual units of sandstone swell and thin at low angles - one such bed can be traced laterally into a channel-form sandstone body; overbank or splay sandstones (?)
- Aggrading channel-form sandstones with mudstone drapes; porosity in drapes is poor while some sandstones have excellent porosity
- Ash (?)
- Three interbeds 1-3 cm. in thickness that are muddy; one 5 cm. bed 20 cm. from base has approximately 5% fish hash and is slightly odoriferous
- 2 cm. unit pinches out then reappears





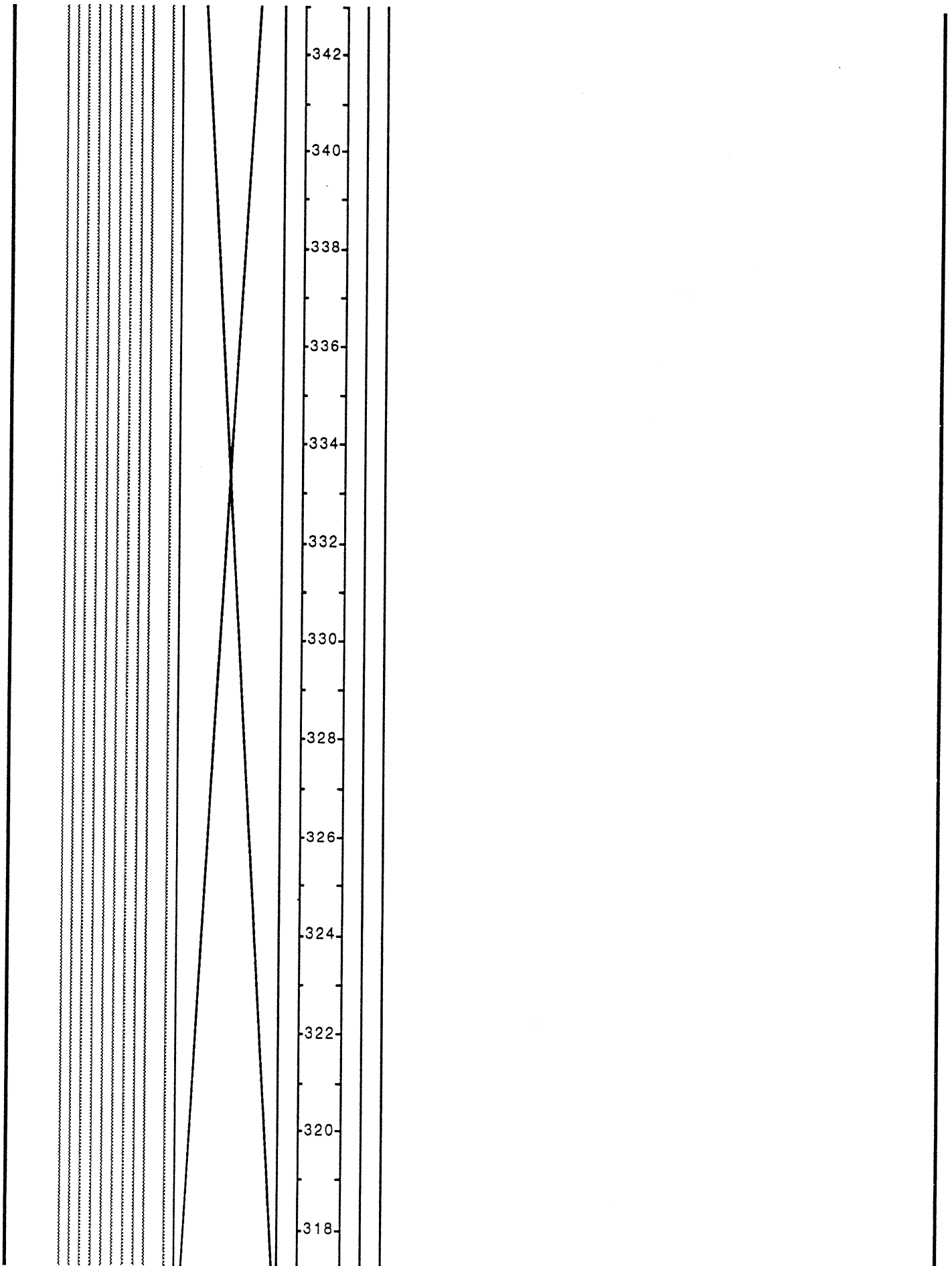


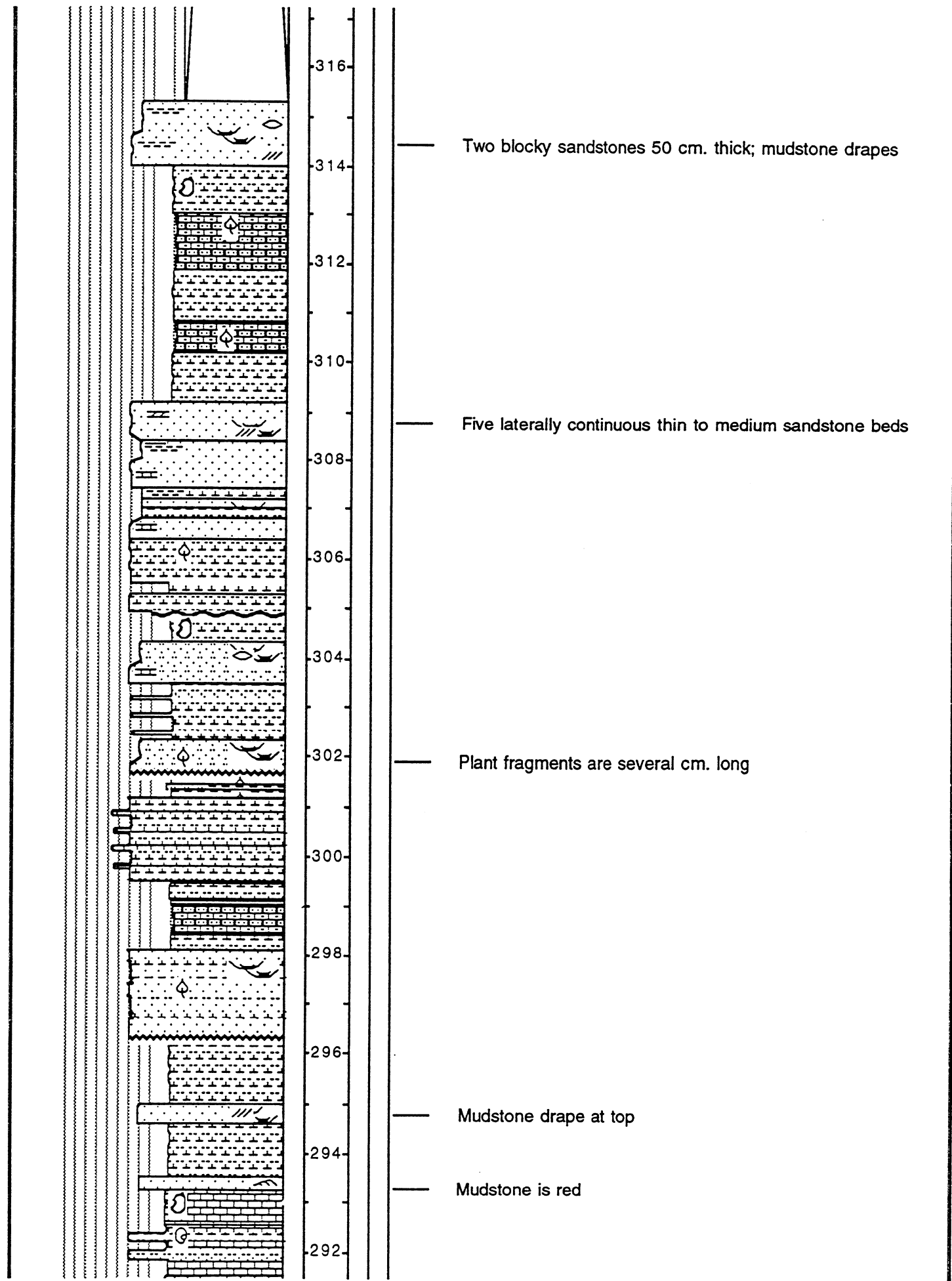
Upper portion oolitic

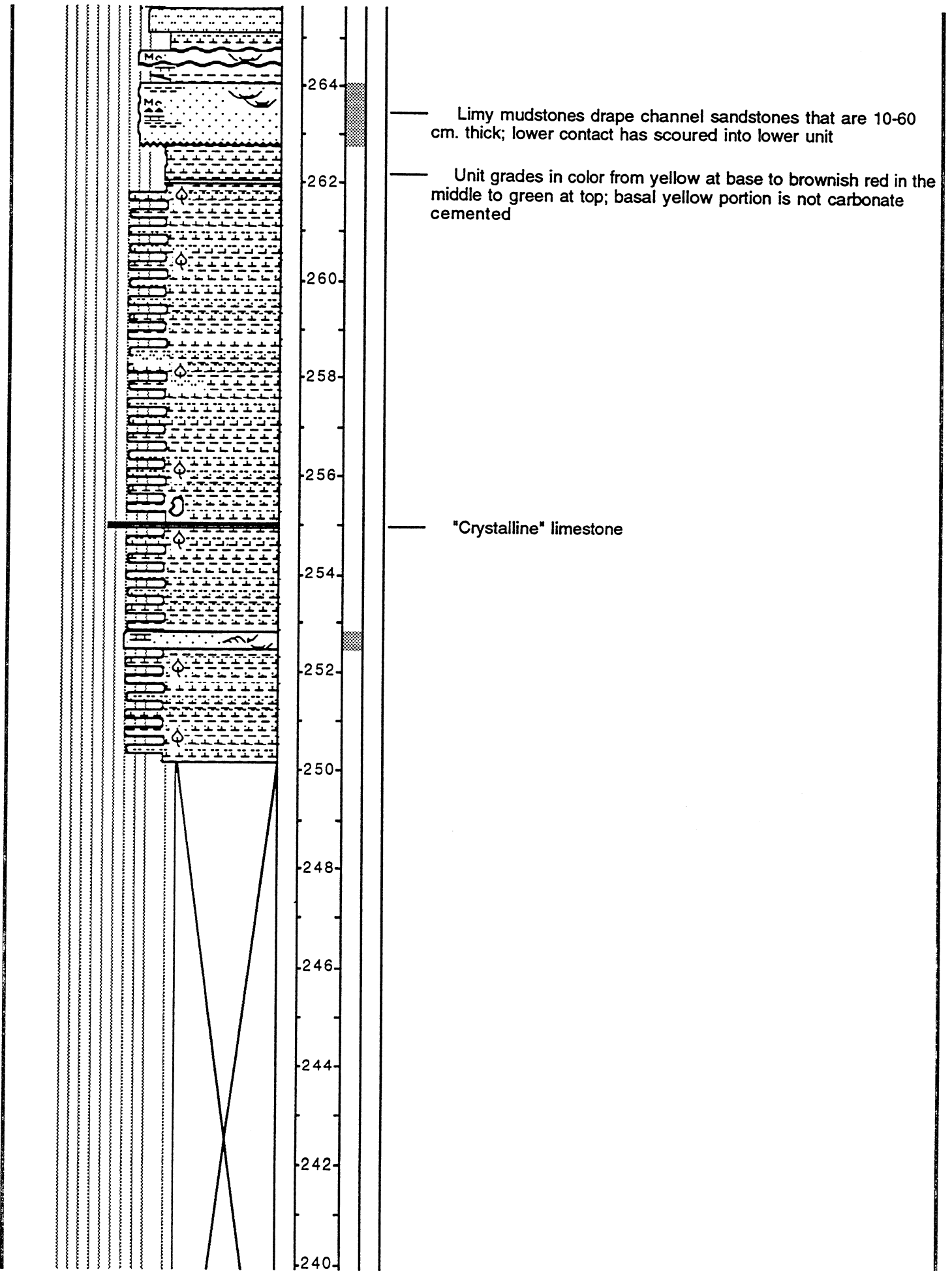


Sandstones have up to 10% biotite

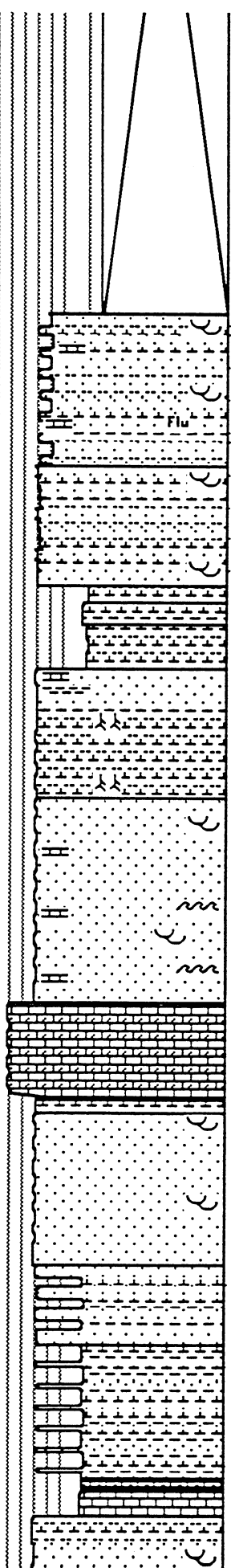
Recrystallized "sugar" limestone







238
 236
 234
 232
 230
 228
 226
 224
 222
 220
 218
 216

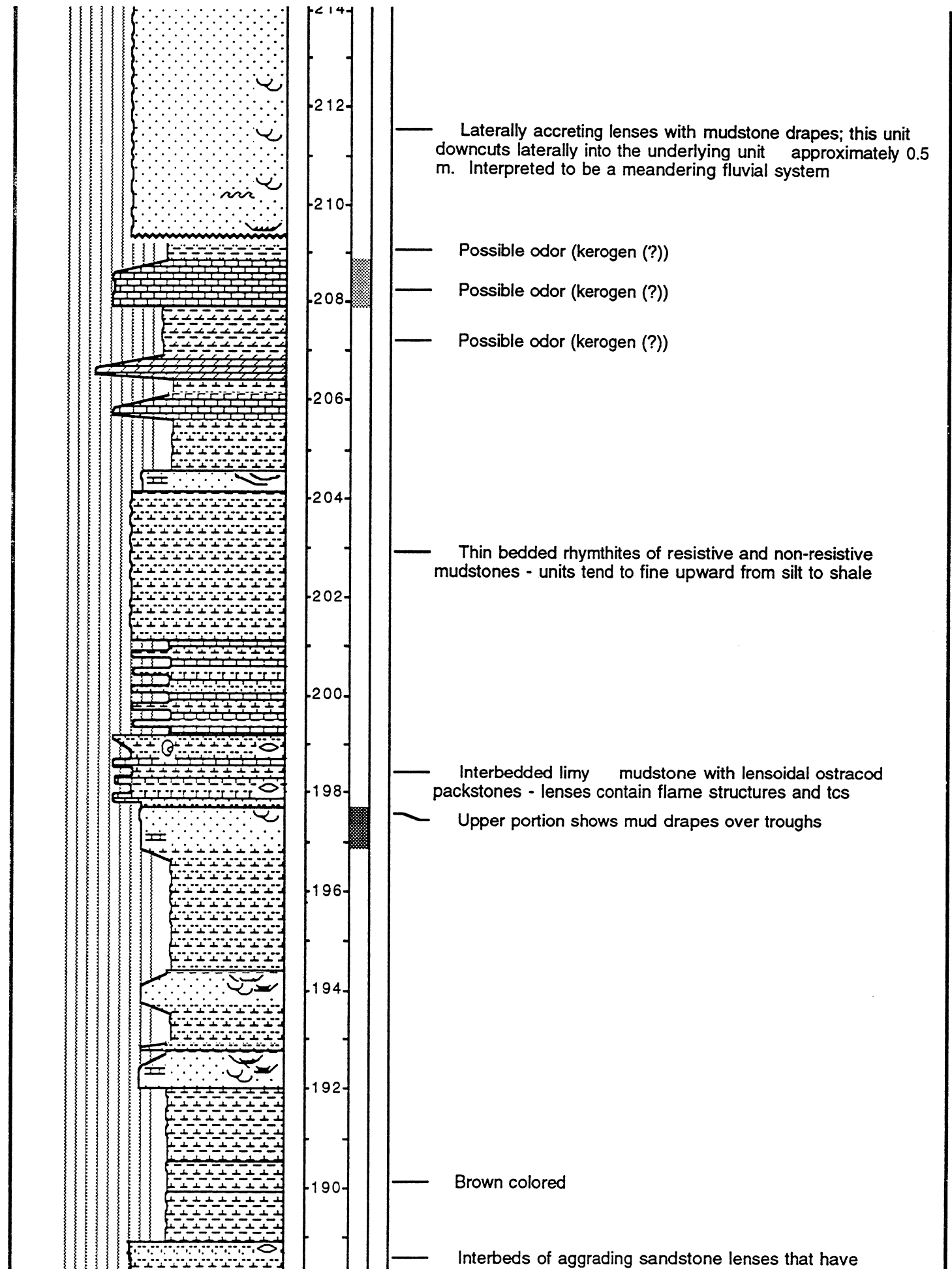


— Aggrading channel complex; contains siltstone lenses

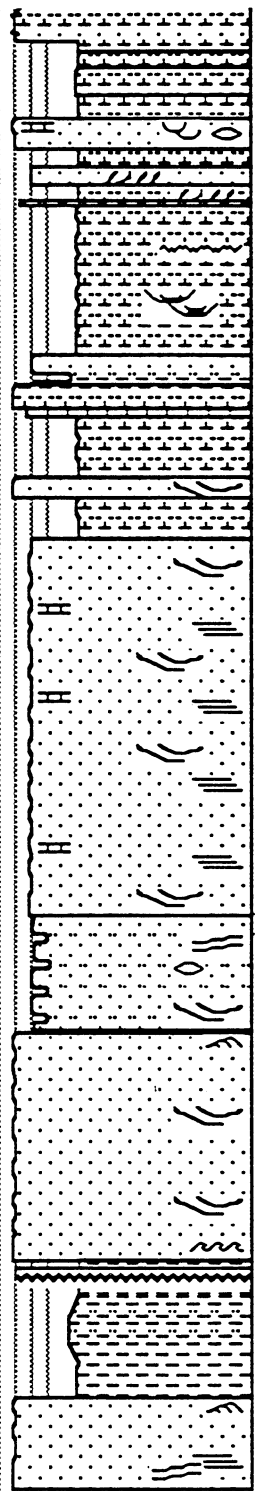
— Thin beds of sandstone have undulatory bottom contacts, small tcs, are well sorted and have high porosity

— Thin sandstone interbeds are well sorted, show small tcs, and have good to excellent porosity

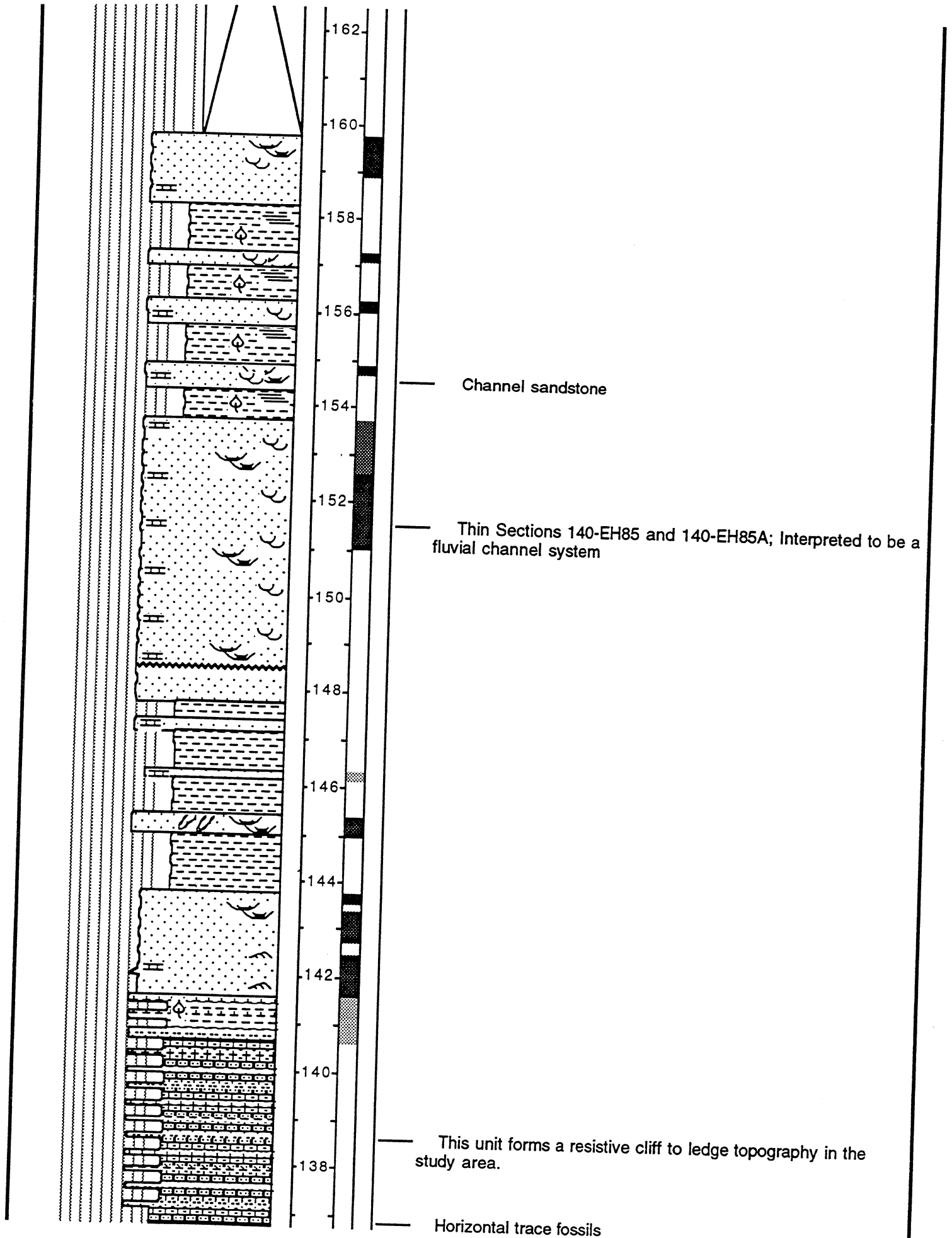
— Upper half of unit has varves (?)

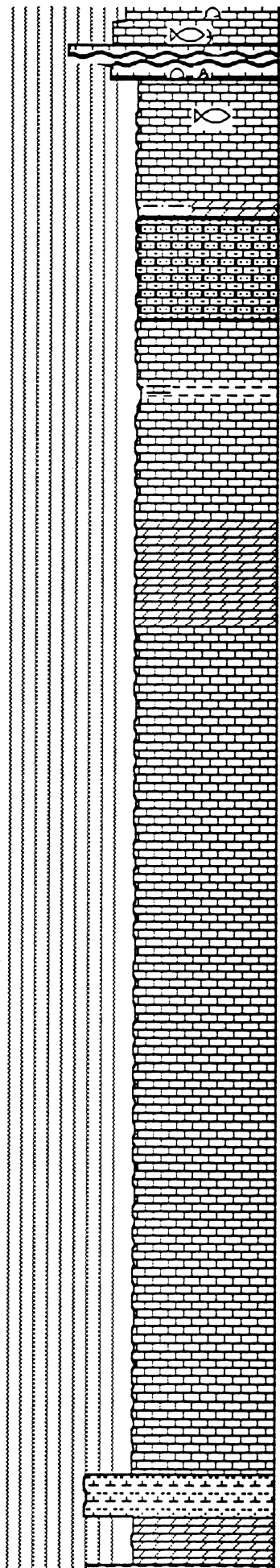


mudstone drapes - lenses are up to 18m long and 1.3m thick

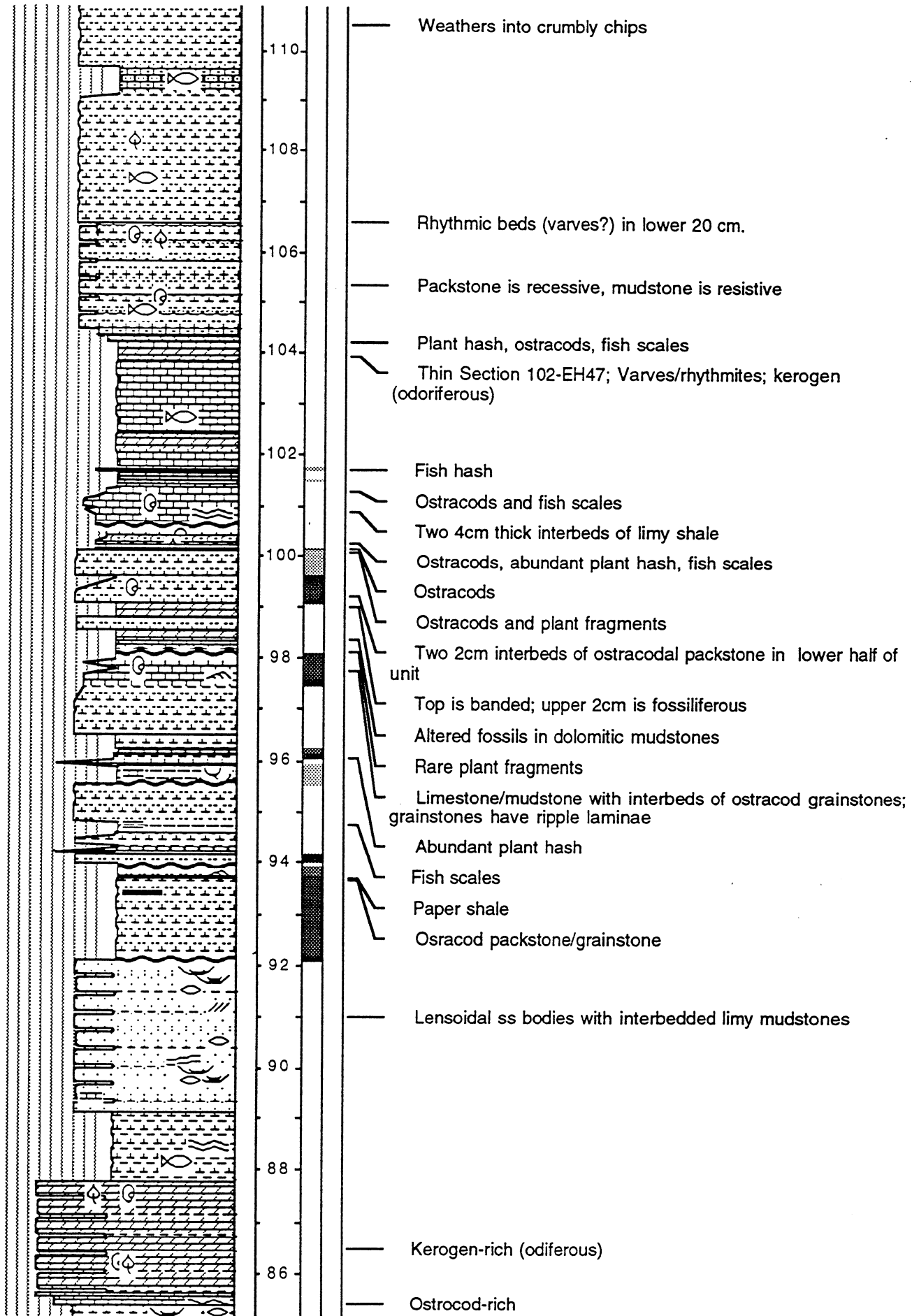


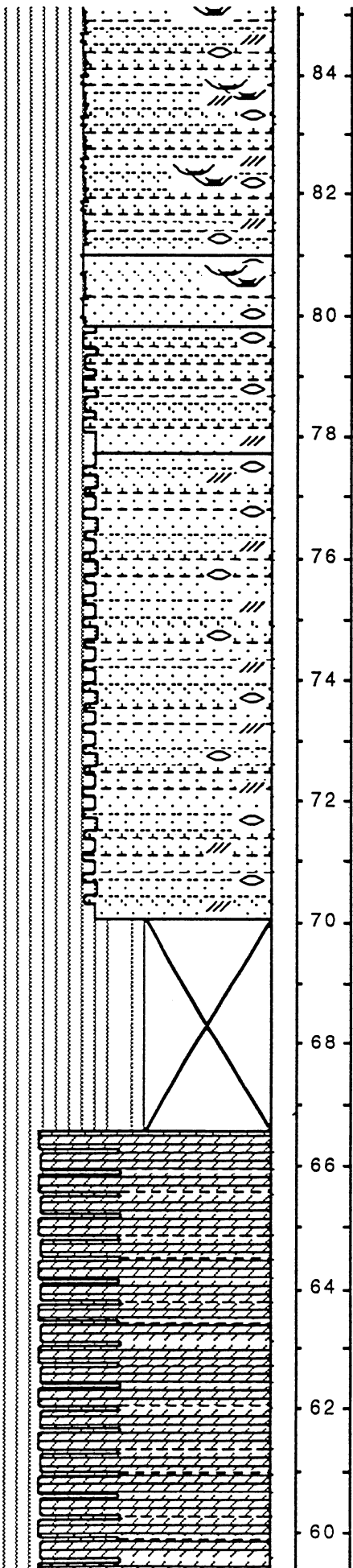
- Brown color
- Sandstone lens pinches out on both sides - 70cm. max thickness - high porosity
- Fossilized bone (mammal(?))
- Interbeds of sandstone up to 12 cm.
- Fish scales
- 8 cm sandstone with flaser lamination, tcs, and gar fish scales
- Two brown colored mudstones (red beds (?)) in bottom half of unit
- Sandstone lenses (near base) within crumbly limy mudstone
- Iron concretions; possible HCS (?)
- Siltstone lenses pinchout to the north; max. thickness of lenses = 26 cm.
- Shale break; mudcracks extend through shale and are filled with sandstone from above
- Sandstone thins to the south; iron concretions
- Also pinches out to the north
- Sandstone lens that pinches out to the north; maximum thickness in outcrop is 73 cm.
- Iron stained concretions





- 136 ——— Mud covered
- 2 mm "white" seam at top; mud covered
- Mud covered
- Mud covered
- 134 ———
- Odoriferous; This unit marks the top of a prominent cliff-forming outcrop section which is approximately 3.5 m. thick
- Mud covered
- Mud covered
- Mud covered
- 130 ——— Mud covered; very odoriferous
- Thin Sections 113-EH58 bag and block; Mud covered
- 128 ———
- Slightly odoriferous; outcrop covered with mud
- 126 ———
- 124 ———
- 122 ———
- 120 ———
- Poorly exposed outcrop - vertical face covered with mud
- 118 ———
- 116 ———
- 114 ———
- 112 ——— Slightly odoriferous





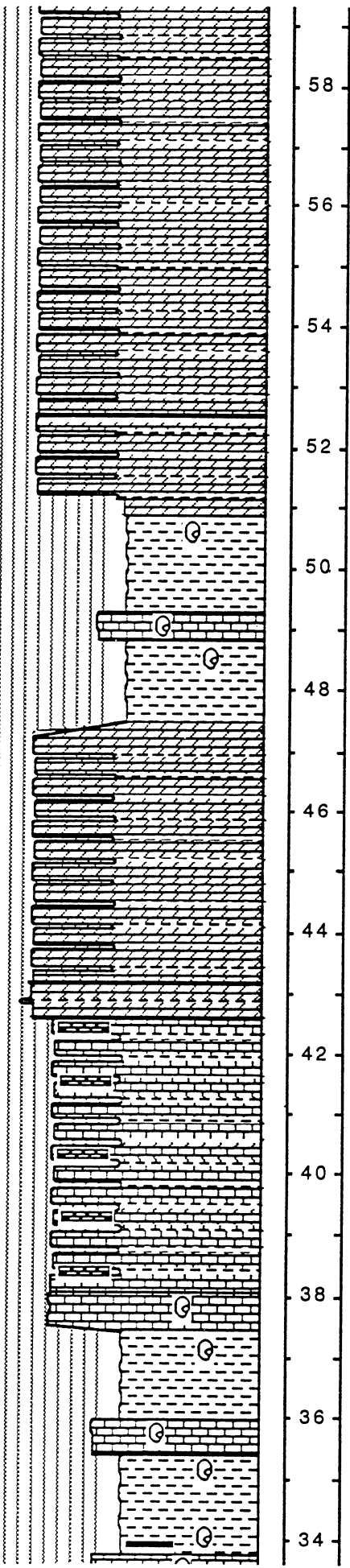
— Thin ss lenses with mudstone drapes; interbedded flat bottomed laterally continuous ss bodies (overbank splays (?))

— Lensoidal ss bodies that pinchout laterally; mudstone drapes over ss; interbeds of flat bottomed laterally continuous ss (overbank splay-type deposits(?))

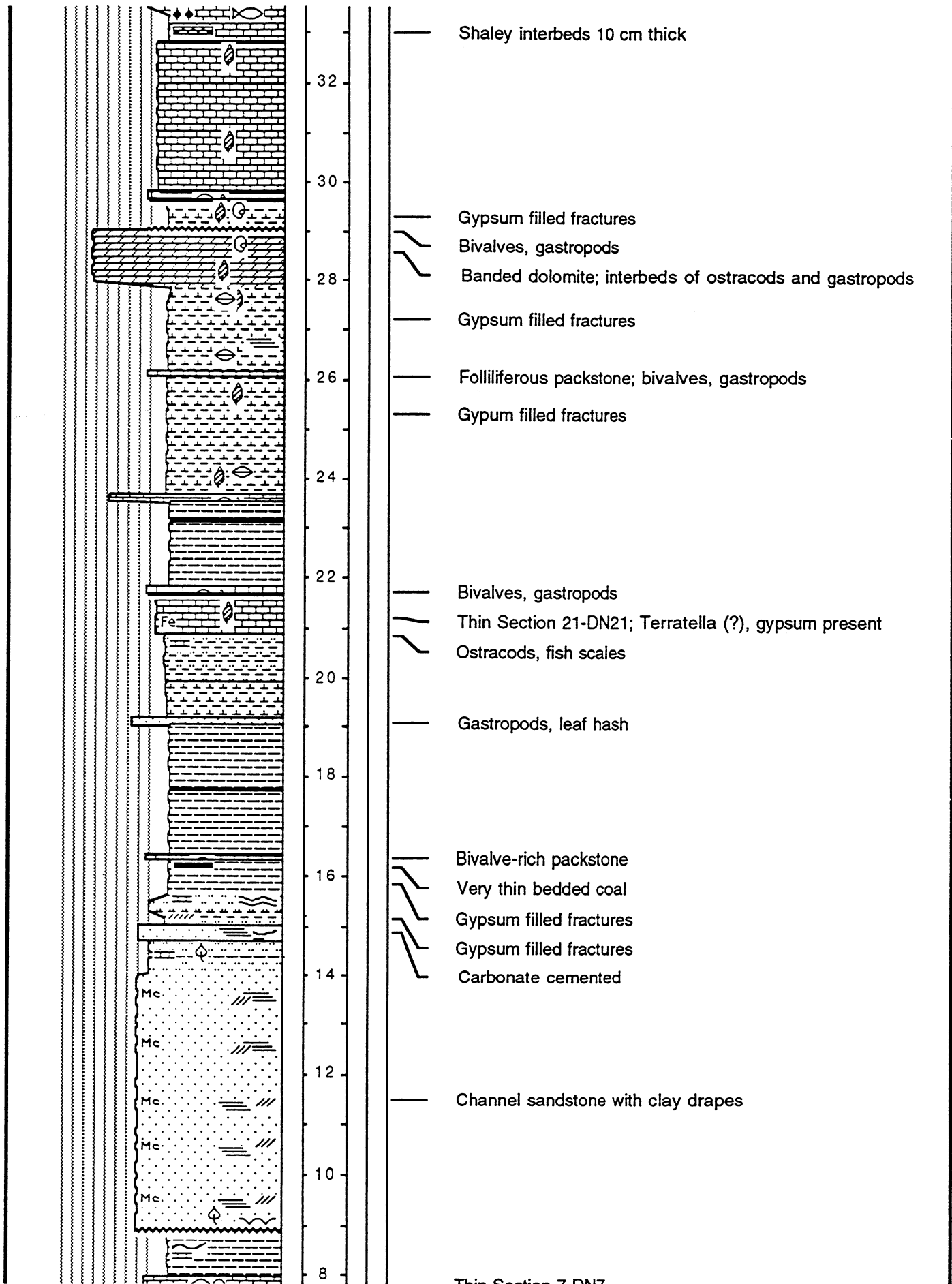
— Small channel-like lenses down to 3cm in thickness

— Lensoidal ss bodies pinch out laterally and are draped by mudstone; flaser bedding in mudstones; very fine sand

— Recessive, slope covered



- Kerogen-rich
- Thin Section 43; Kerogen-rich
- Lower portion "banded"; kerogen-rich
- Chert bands 5mm - 4cm thick; kerogen-rich (odiferous)
- Thin Section 37-DN37
- Thin Section 36-DN36



This Section 7 DN7

Thin Section 7-DN7

Thin Section 5-DN5

